CALIFORNIA
ENERGY COMMISSION

Energy Research and Development Division

**FINAL PROJECT REPORT**

# Nitrogen Oxide Sensor to Optimize Dispatchable Distributed Generation Systems

**Gavin Newsom, Governor**

**January 2021 | CEC-500-2021-006**

**PREPARED BY**:

**Primary Authors**:
Ryan Ehlig
Vince McDonell

University of California, Irvine
Irvine, CA 92697
Phone: 949-824-5950 | Fax: 949 824 7423

**Contract Number**: EPC-15-062

**PREPARED FOR**:
California Energy Commission

Yu Hou
**Project Manager**

Jonah Steinbuck, Ph.D
**Office Manager**
**ENERGY GENERATION RESEARCH OFFICE**

Laurie ten Hope
**Deputy Director**
**ENERGY RESEARCH AND DEVELOPMENT DIVISION**

Drew Bohan
**Executive Director**

# ACKNOWLEDGEMENTS

The authors of this report would like to acknowledge Capstone Turbine Corporation for providing Combustion Lab at the University of California, Irvine (UCICL) with technical support for the C-60 Engine and support for modifying the engine software to implement the control logic developed. The authors would also like to acknowledge EmiSense and parent company CoorsTek for providing UCICL with the necessary sensors to complete this project report. Lastly, the authors would also like to acknowledge HORIBA for all their help related to emissions measurements.

# PREFACE

The California Energy Commission's Energy Research and Development Division supports energy research and development programs to spur innovation in energy efficiency, renewable energy and advanced clean generation, energy-related environmental protection, energy transmission and distribution and transportation.

In 2012, the Electric Program Investment Charge (EPIC) was established by the California Public Utilities Commission to fund public investments in research to create and advance new energy solutions, foster regional innovation and bring ideas from the lab to the marketplace. The California Energy Commission and the state's three largest investor-owned utilities—Pacific Gas and Electric Company, San Diego Gas & Electric Company and Southern California Edison Company—were selected to administer the EPIC funds and advance novel technologies, tools, and strategies that provide benefits to their electric ratepayers.

The Energy Commission is committed to ensuring public participation in its research and development programs that promote greater reliability, lower costs, and increase safety for the California electric ratepayer and include:

- Providing societal benefits.
- Reducing greenhouse gas emission in the electricity sector at the lowest possible cost.
- Supporting California's loading order to meet energy needs first with energy efficiency and demand response, next with renewable energy (distributed generation and utility scale), and finally with clean, conventional electricity supply.
- Supporting low-emission vehicles and transportation.
- Providing economic development.
- Using ratepayer funds efficiently.

*Nitrogen Oxide Sensor to Optimize Dispatchable Distributed Generation Systems* is the final report for the *Nitrogen Oxide Sensor to Optimize Dispatchable Distributed Generation Systems* project (Contract Number EPC-15-062) conducted by University of California, Irvine. The information from this project contributes to the Energy Research and Development Division's EPIC Program.

For more information about the Energy Research and Development Division, please visit the Energy Commission's research website (www.energy.ca.gov/research/) or contact the Energy Commission at 916-327-1551.

# ABSTRACT

The increase in intermittent renewable sources has created a need for clean dispatchable generation sources that can quickly generate electricity to meet demand. Dispatchable generation devices include microturbines and reciprocating engines. They can be certified as low emission, but the certification process involves generating at full capacity. Often, only partial capacity generation is needed to meet demand, yet a means to ensure clean operation at partial capacity is needed. This project evaluated the viability of using low-cost automotive sensors for nitrogen oxides (criteria air pollutants typically generated from the combustion process) and oxygen to continuously monitor emissions performance of a 60-kilowatt microturbine generator. In this study, the generator operated over a programmed range of capacity for six months, during which sensors from UniNOx and NTK, two commercial manufacturers, were evaluated for durability and accuracy by comparing their readings to a referee instrument, Horiba PG-350. Results showed that both sensors were robust and did not exhibit significant errors. The NTK sensor proved to be more precise and was thus selected for integration into the 60-kilowatt engine operating system. The project team developed the necessary electronics and control algorithms and modified the engine control software to integrate both. Testing of active control of the engine operation using the sensor information led to a reduction of about 10 percent in nitrogen oxides compared to baseline emissions levels. The project demonstrated that using such sensors to attain performance to minimize emissions is feasible and relatively economical.

**Keywords**: solid state sensor, NOx emissions, active control, microturbine generator, experimental study, durability, accuracy, dispatchable generation

Please use the following citation for this report:

Ehlig, Ryan and Vincent McDonell. University of California, Irvine. 2021. *Nitrogen Oxide to Optimize Dispatchable Distributed Generation Systems*. California Energy Commission. Publication Number: CEC-500-2021-006.

# TABLE OF CONTENTS

# LIST OF FIGURES

# LIST OF TABLES

# EXECUTIVE SUMMARY

## Introduction

Within the past decade, California has experienced tremendous growth in renewable generation such as solar and wind as a result of the Renewables Portfolio Standard. Under Senate Bill (SB) 100, 60 percent of California's power must be derived from renewable sources by 2030. Because renewable generation is intermittent in nature — wind is not always prevalent, and sunlight peaks in the daytime — dispatchable generation — sources that can start and generate electricity in a very short period of time — is important to ensure reliable availability of electricity. Such generation will be more critical to California's energy system within the next several decades as the state adopts more intermittent renewable sources. Dispatchable generation devices such as microturbine generators and reciprocating engines represent a viable strategy for dealing with the intermittent nature of renewables. A certification procedure outlined by the California Air Resources Board facilitates timely deployment of "clean" (low polluting) distributed generation. These certification standards are developed for pollutant emissions produced when a generator operates at 100 percent capacity, also known as full load. But because these systems operate in a dispatchable manner, emissions performance at partial capacity also becomes important. Large, centralized generation units require equipment that uses highly specialized continuous emissions monitoring analyzers to monitor and report the emissions performance of those generating devices in real time. While appropriate for large-scale power generation systems, currently approved continuous emissions monitoring systems are not cost effective for distributed generation systems operating in a dispatchable manner. A potential cost-effective solution to real-time monitoring of distributed generation systems exists within the transportation industry. In particular, oxygen and nitric oxide sensors are commonly used in diesel vehicles. A question for the present work is whether those analyzers could monitor real-time distributed generation engine performance. Such sensors could also provide information enabling the engine to continually minimize emissions by monitoring load, fuel composition, and ambient conditions, as well as engine wear and tear. Ideally, the sensor information would be integrated directly into the engine control system.

## Project Purpose

The goals of this project are to (1) assess the viability of solid state nitric oxide sensors from the transportation industry for monitoring the emissions performance of a distributed generation device, and if viable, (2) develop and integrate an emission reduction algorithm into the engine control system using the sensor information to minimize nitric oxide emission in real time.

## Project Approach

This study used a Capstone C60 engine as the representative distributed generation device. The project team developed an exhaust duct test section to install and monitor the performance of two solid state nitric oxide sensors, from NTK and UniNOx®, over a six-month period. A referee instrument, HORIBA PG-350, provided true exhaust emission levels. The team also developed an extensive data acquisition network to capture and record data from all sensors and analyzers in a synchronized manner.

## Project Results

Both solid state sensors performed reliably over the six-month evaluation. Results indicated that the NTK sensor performed more comparably to the established referee instrument (PG-350) than the UniNOx sensor in measuring NOx concentrations. The team developed and integrated a control algorithm with the engine system to improve the emission performance. The control algorithm showed the ability to actively reduce nitric oxide emissions at part load by approximately 10 percent. In general, this study provided proof of concept that these solid-state sensors can be used reliably in distributed generation systems. Additional durability testing and evaluation of other brand sensors would provide further support for this technology.

## Technology Transfer

The results from this study were disseminated in a number of ways. The project team orally presented at two technical conferences and presented a poster at the 2018 EPIC Symposium. The team also provided final report briefings to Capstone Turbine Corporation, Solar Turbines, and Emisense, companies that, along with other engine manufacturers or packagers, are the primary targets for the outcomes of the research. Each has expressed interest in potentially adopting the technology for use in its products. The team also reported results to the U.S. Department of Energy and Southern California Gas Company, either of which may be in a position to fund further work on the development or evaluation of these sensors.

Because the tested sensors represent an inexpensive and viable approach to traditional continuous emissions monitoring analyzers for monitoring emissions from distributed generation devices, the current certification procedure for distributed generation systems could, ideally, be modified to include these sensors as monitoring tools. In terms of market potential, the specific system evaluated — microturbine generators — represents about 50 megawatts of generation. The market for other systems including reciprocating engines and larger gas turbines is considerably higher.

The cost to add the sensor system to a given engine is estimated to be about $2,000. This figure should decrease as the number of units with sensor systems increases. Because the sensor technology and control algorithm approach optimizes the engine parameters to reduce emissions and does not noticeably alter the performance or configuration of the device, the sensors represent a feasible and viable approach to improving the performance of distributed generation systems in California.

## Project Benefits

Considering the estimated current 50-megawatt fleet of microturbine generators in California, a 10 percent reduction in nitric oxide emissions for each device outfitted with this sensor technology and control algorithm could translate to the elimination of more than 30 tons of nitric oxide each year. If the research can be applied to other technologies such as reciprocating engines and small gas turbines, this benefit will increase proportionately. Although emissions reduction is the primary benefit, other potential benefits include maintenance schedule optimization based on information from the sensors, which could save operations and maintenance service costs.

Regarding further research, steps taken to reduce nitric oxide emissions often increase carbon monoxide emissions. Therefore, development of a similar sensor to measure carbon monoxide emissions, along with the NOx sensor,would provide a more comprehensive picture on emissions from dispatchable generation devices. The current study inferred carbon monoxide emissions from extensive measurements; however, having explicit carbon monoxide emission data would help simultaneously address both nitric oxide and carbon monoxide emissions.

Also notable is the fact that the estimated 50-megawatt fleet of microturbine generators is small compared to the fleet of reciprocating engines. Research evaluating the possibility of similar sensors in reciprocating engines to reduce nitrogen oxides would be worthwhile, particularly because reciprocating engine conditions are similar to those in automobiles.

# CHAPTER 1: Introduction

California is currently on track to have 60 percent of power generated from renewable sources by 2030. Because renewable generation is intermittent in nature — wind is not always prevalent, and sunlight peaks in the daytime — dispatchable generation — sources that can start and generate electricity in a very short period of time — is important to ensure reliable availability of electricity. Dispatchable generation devices such as microturbine generators and reciprocating engines represent a viable strategy for dealing with the intermittent nature of renewables. A certification procedure outlined by the California Air Resources Board facilitates timely deployment of "clean" (low polluting) distributed generation. These certification standards are developed for pollutant emissions produced when a generator operates at 100 percent capacity, also known as full load. But because these systems operate in a dispatchable manner, emissions performance at partial capacity also becomes important. Large, centralized generation units require equipment that uses highly specialized continuous emissions monitoring analyzers to monitor and report the emissions performance of those generating devices in real time. While appropriate for large-scale power generation systems, currently approved continuous emissions monitoring systems are not cost effective for distributed generation systems operating in a dispatchable manner. A potential cost effective solution to real-time monitoring of distributed generation systems exists within the transportation industry. In particular, oxygen and nitric oxide sensors are commonly used in diesel vehicles. A question for the present work is whether those analyzers could monitor real-time distributed generation engine performance. Such sensors could also provide information enabling the engine to continually minimize emissions by monitoring load, fuel composition, and ambient conditions, as well as engine wear and tear. Ideally, the sensor information would be integrated directly into the engine control system.

As part of a research project funded by the California Energy Commission Grant EPC-15-062, the Combustion Lab at the University of California, Irvine (UCICL) successfully completed three technical tasks to establish and demonstrate an inexpensive alternative to traditional continuous emissions monitoring systems (CEMS) capable of minimizing emissions in real-time for dispatchable generation devices. The objectives were to first establish the viability of using solid-state nitric oxide (NO) sensors commonly used in the diesel automotive industry as a robust and inexpensive alternative to traditional monitoring devices, and if viable, to develop a control strategy, coupled with the feedback of the solid-state sensor, capable of optimizing the emissions performance of the distributed generation (DG) device in real-time.

Figure 1 shows the "duck curve" chart first published by the California Independent System Operator (California ISO) in 2013.

**Figure 1: California Independent System Operator "Duck Curve" Chart**

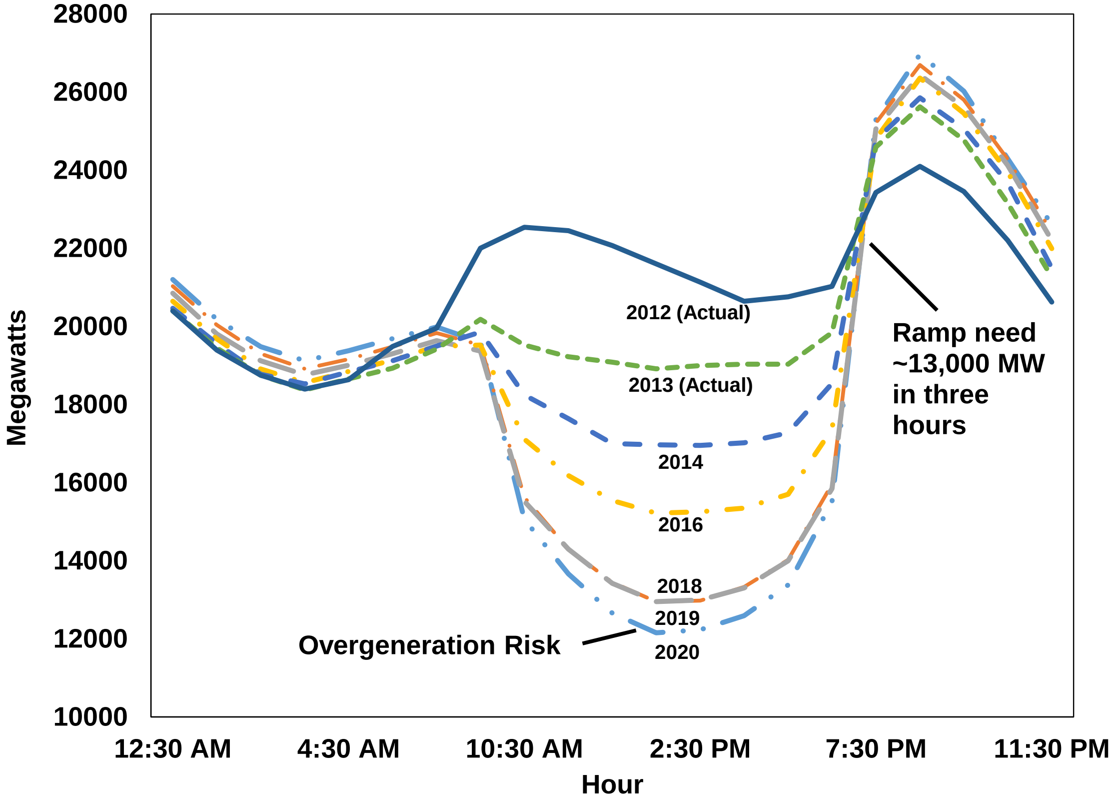


Source: California Independent System Operator

The figure clearly illustrates that as renewable energy penetration increases in California, the need for generating devices able to ramp up, ramp down, and perform quickly on command also will increase. By 2020, the risk of overgeneration will be high and increases in rotational speed and frequency beyond their capable limits could  damage generators. Thus local DG is necessary to alleviate pressure from increasing renewable penetration and to increase the flexibility of the grid.

Table 1 and Table 2 show the certification requirements a DG device must meet before it can be sold commercially in California. Distributed generation emissions limits were first adopted in 2003 and subsequently changed in 2007. To facilitate the deployment of clean distributed generation throughout California, emissions certification is conducted at 100 percent of full load for each device (Distributed Generation Certification Program, 2003)  Certification uses a traditional continuous emission monitoring analyzer to verify that emissions meet the established criteria. CEMS, defined by the Air Emissions Measurement Center, are "the total equipment necessary for the determination of a gas or particulate matter concentration or emission rate using pollutant analyzer measurements and a conversion equation, graph, or computer program to produce results in units of the applicable emission limitation or standard"(US EPA, 2018). Power generating devices with a nameplate capacity of 25 megawatts electric (MWe) or greater require a traditional CEMS configuration with the ability to minimize the emissions of the operating device in real time. Because the specifications in Table 1 and Table 2 are only for full-load conditions and emissions are not continuously monitored during operation of the device, an inexpensive alternative to traditional CEMS (analyzer and other necessary equipment for monitoring and tuning of the engine) that provides feedback to the engine to perform corrective action to reduce NO would be beneficial.

**Table 1: Emissions Standards for Distributed Generation 2003**

| Pollutant | DG Unit Not Integrated with Combined Heat and Power (a)(1) (lb/MW-hr) | DG Unit Integrated with Combined Heat and Power (a)(1) (lb/MW-hr) |
|---|---|---|
| Oxides of Nitrogen (NOx) | 0.5 | 0.7 |
| Carbon Monoxide (CO) | 6.0 | 6.0 |
| Volatile Organic Compounds (VOCs) | 1.0 | 1.0 |
| Particulate Matter (PM) | An emission limit corresponding to natural gas with fuel sulfur content of no more than 1 grain/100 scf (Standard Cubic Foot) | An emission limit corresponding to natural gas with fuel sulfur content of no more than 1 grain/100 scf |

Source: UC Irvine

**Table 2: Emissions Standards for Distributed Generation 2007**

| Pollutant | Emission Standard (lb/MW-hr) |
|---|---|
| NOx | 0.07 |
| CO | 0.10 |
| VOCs | 0.02 |

Source: California Air Resources Board, Adapted from Ref. [2]

Using inexpensive solid-state NO sensors to monitor emissions and mitigate nitric oxide offers appreciable benefits to support California's energy policy. The intermittent nature of renewables and their growing percentage in the share of generation devices in California's Renewable Portfolio Standard suggest the need to re-examine and amend the certification procedure to accommodate DG devices. The successful completion of the technical tasks outlined in this report represent a viable approach to improving these standards and would vastly improve the current capability of emissions monitoring for DG devices.

The following chapters encompass the three technical tasks conducted at UCICL to validate the use of solid-state NO sensors as an emissions control strategy and the calculated benefits for the California DG fleet from using the solid-state sensors.

# CHAPTER 2: Evaluating Sensor Robustness

## 2.1 Overview of Sensor Evaluation Testing

The goal of the second technical task, from the CEC EPC-15-062 project outline, is as follows: "to establish the characteristics and operability of different candidate sensors as a function of time to determine the response time of the sensors." This test will provide insight into how durable and reliable the candidate sensors are at accurately monitoring NOx levels in the exhaust. A "referee" analyzer will be used to document variation between the "actual" exhaust levels and those determined by the candidate sensors. Equipment with California Air Resources Board and/or South Coast Air Quality Management District (SCAQMD) approved measurement methods will be used. The University of California, Irvine Combustion Laboratory has such equipment available in the form of multi-gas analyzers, otherwise known as "reference" analyzers.

To complete this second technical task, two different brands of the latest commercially available solid-state nitric oxide (NO) sensors were obtained (NTK sensor from Ford and UniNOx® sensor from Continental) and installed in the exhaust of a C-60 Capstone microturbine generator (MTG) testbed, which was used as a representative for DG devices. To prevent bias associated with the location of emissions measurements, the sensors were installed at different radial locations around the exhaust duct: 120° apart from each respective sensor in the same brand and 15° apart from each respective brand of sensor. A traditional "CEM-like" referee instrument (HORIBA PG-350) was used as a reference device for the sensors to compare against a representative "true" measurement. Data were collected and analyzed over a period of six to eight months in accordance with the procedures set forth in the proposed test plan (see EPC-15-062 Technical Task 2 Test ) to determine the sensor that best matched the output and characteristics of the referee analyzer according to:

- Accuracy
- Precision
- Lower Detectable Limit
- Fall Time (Lag Time) and Rise Time
- Concentration Resolution

## 2.2 Overview of Data Acquisition Network

To initiate the testplan and to begin measuring nitric oxide concentration in the gas turbine testbed, four main components were needed:

- Sensor electrical installation on the part of CoorsTek Sensors (six sensors total, including three UniNOx® and three NTK sensors from Ford)
- Sensor test section for installing the sensors
- C-60 turbine engine running and preprogrammed with a daily load profile to follow
- DAQ (data acquisition) equipment working with PG-350 and sensors, LabVIEW VI working

The most difficult challenges that presented themselves were as follows:

- Controlled environment for PG
- -350 was located 150 feet from the test section, which presented a challenge with conventional USB signals. Bus-powered cables were not sufficient to transmit signals between sensors and DAQ computer at this length.
- Length to engine from DAQ computer also presented a problem. This was also another 150-foot length. Rainy season also presented challenges for C-60, which displayed faults on a regular basis.
- Length from PG-350 to DAQ compared with sensors to DAQ led to problems with frequency of sampling.

These were resolved in the following way:

- Conventional bus-powered USB cables were insufficient to transmit data from the sensor CAN-USB box. Signal loss accumulated over the length to the test section from the DAQ room; instead, 150-foot CAT 5e cable was used. This was then connected to an RJ45 to DB-9 pin converter on either end. This was then connected to the CAN-USB converter that connected the sensors to the DAQ computer.
- Resolved the same way problem 1 was resolved. Familiarity with C-60 rebooting process also helped fix this issue, especially during the rainy season.
- Frequency of sampling was fixed by reducing to 0.1 Hertz (Hz) for all sensors. This fixed any issues regarding time-drift.

Figure 2 shows the data acquisition network constructed to capture and record the sensor signals on a 24/7 basis. Refer to EPC-15-062 Technical Task 2 Test for specific details regarding the sensor test section and for information on specific equipment used. Figure 3 and Figure 4 are pictures of the sensors and test section in which the sensors were installed. Figure 5 shows the gas turbine testbed used for this study.

CoorsTek Sensors provided UCICL with the sensors as well as the proper equipment to power the solid-state sensors and send the signals to the DAQ computer in CAN-Bus protocol. This was converted to a USB signal using an NI-8473 CAN-to-USB converter. The sensor pinout (shown in Figure 6) was used to connect the sensor to the host PC as well as to power the sensors. This was achieved through the use of a sensor box with the PCB mounted inside. CoorsTek Sensors also provided UCICL with a LabVIEW 2015 VI, which served as a basis from which all data were received and stored. Data were collected at 0.1 Hz for most of the testing phase, and 1 Hz for Fall Time, Rise Time tests.

**Figure 2: Communication Diagram**

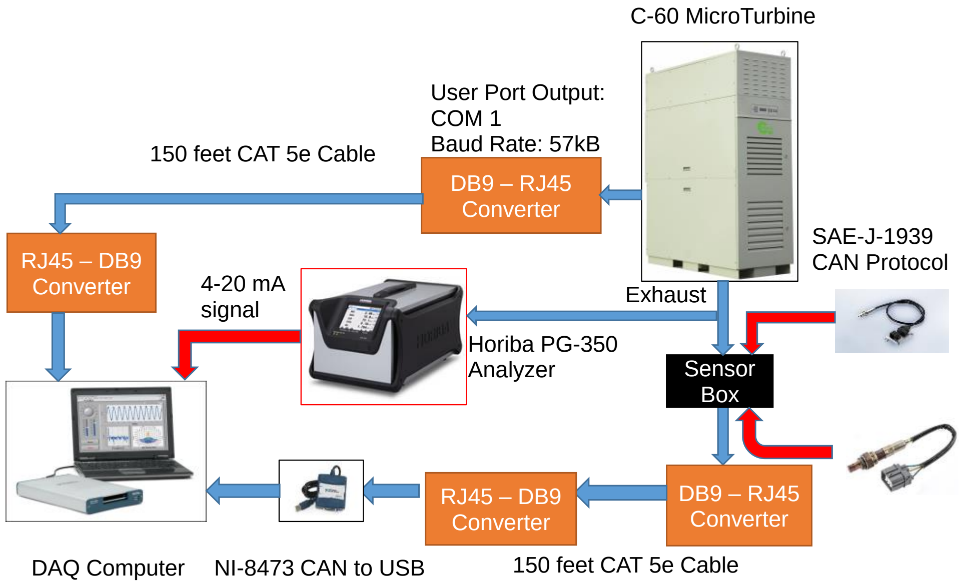


Source: UC Irvine

**Figure 3: Sensors (UniNOx® left, NTK right)**

Source: UC Irvine

## Figure 4: Sensor Section

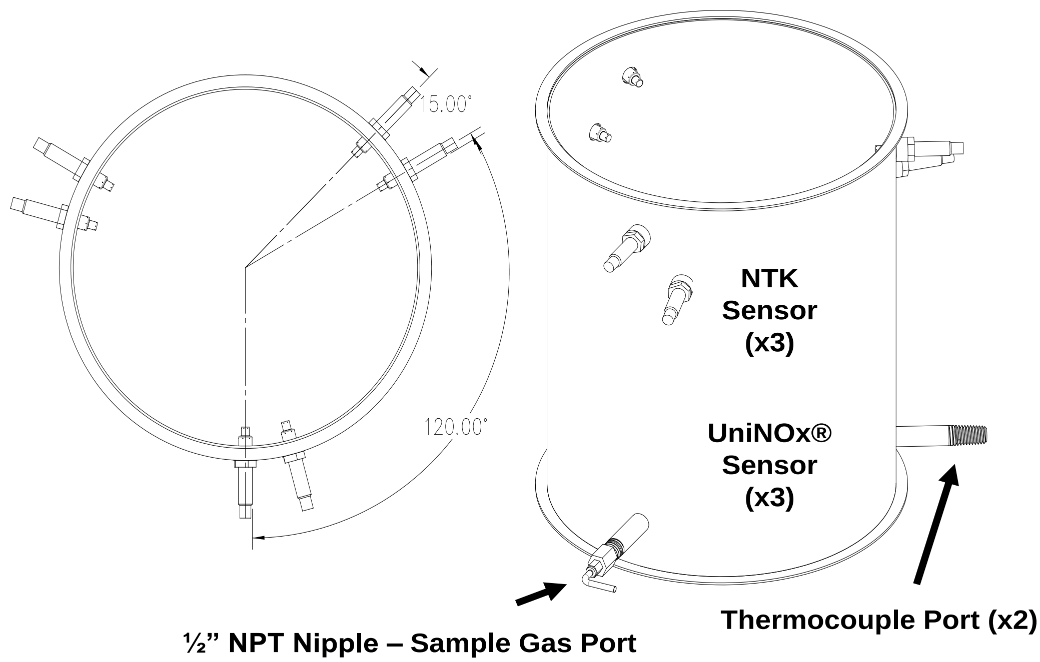


Source: UC Irvine

## Figure 5: Gas Turbine Testbed

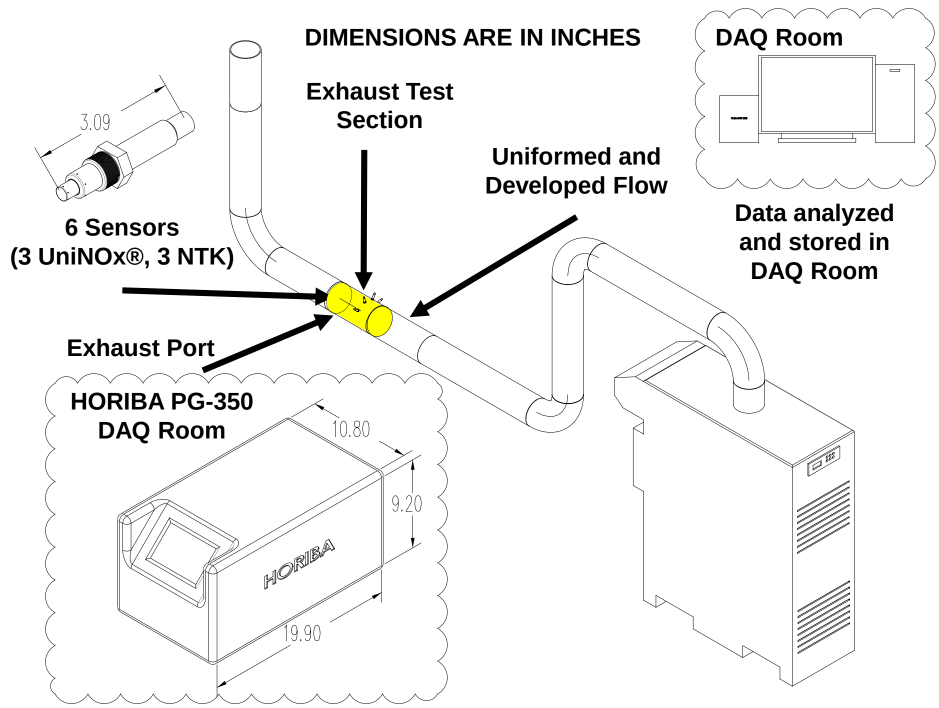


Source: UC Irvine

**Figure 6: CAN Box Pinout**

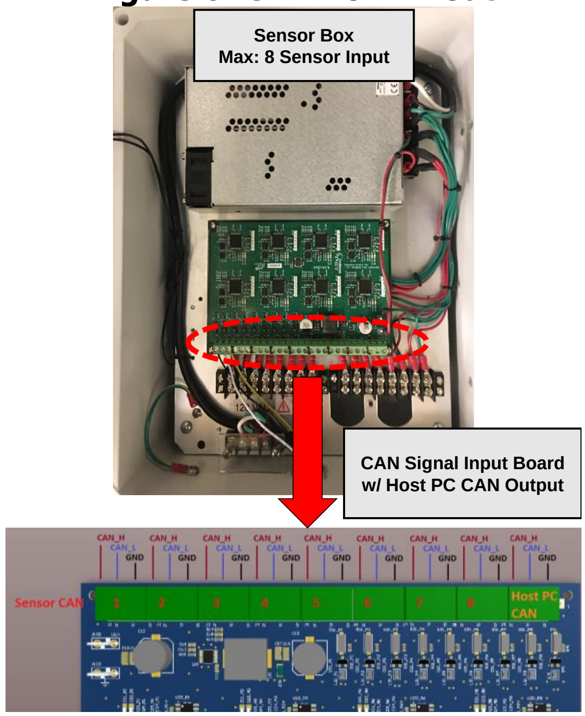


Source: UC Irvine

## 2.3 Engine Load

The engine was run on a modified load profile to allow different levels of NO exposure. The C60 is a lean-premix combustion system that operates using six injectors that simultaneously turn on/off depending on the load that is being demanded (from 0-60 kW); two injectors are continuously firing at every load, and at various programmed load points an additional injector will fire. By using the injector staging, sensor signals were able to report a wide range of nitric oxide concentrations (approximately 190 parts per million by volume, dry (ppmvd), 15 percent $O_2$), which were simultaneously compared against the reported PG-350 measurements. This enabled sensor characteristics to be measured across the entire operation regime of the Capstone C60 engine. Figure 7 shows the NO concentrations from the C60 as a function of load, and Figure 8 shows the modified load profile that was run on a daily basis. The load profile was programmed onto the engine software by using the Capstone Remote Monitoring Software (CRMS).

The proposed test plan incorporated a load profile in which each subsequent load was run for five-minute intervals, with 20 kilowatts (kW) being the lowest set load; however, this presented two problems.

- At 20 kW (three injectors firing in the combustor), a maximum of approximately 50 ppmvd of NO was read by each sensor, which is significantly lower than what can be measured at 10 kW.
- At five minutes for each load, only four minutes of available data was quantifiable as steady-state data that could be used for measuring sensor characteristics (20 points per load of available data and 323 points of available data at the lowest set load).

By changing the lowest set load to 10 kW and by extending each set load by 10 minutes, the range of nitric oxide levels that were able to be measured increased (up to approximately 190 ppmvd from 50 ppmvd) and the number of sampling points during each set load increased.

**Figure 7: Nitric Oxide/Nitrogen Dioxide (Uncorrected) vs. Load**

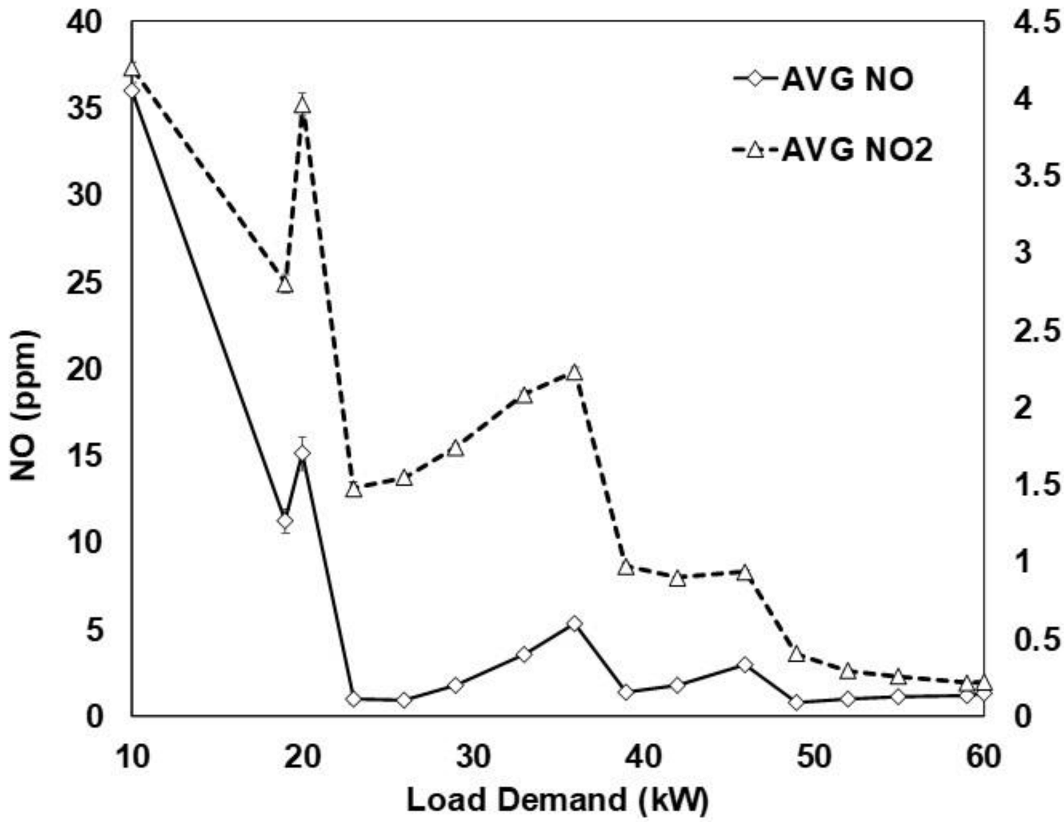


Source: UC Irvine

Graph showing nitric oxide/nitrogen dioxide emissions versus electric load.

**Figure 8: Capstone C-60 Load Profile**

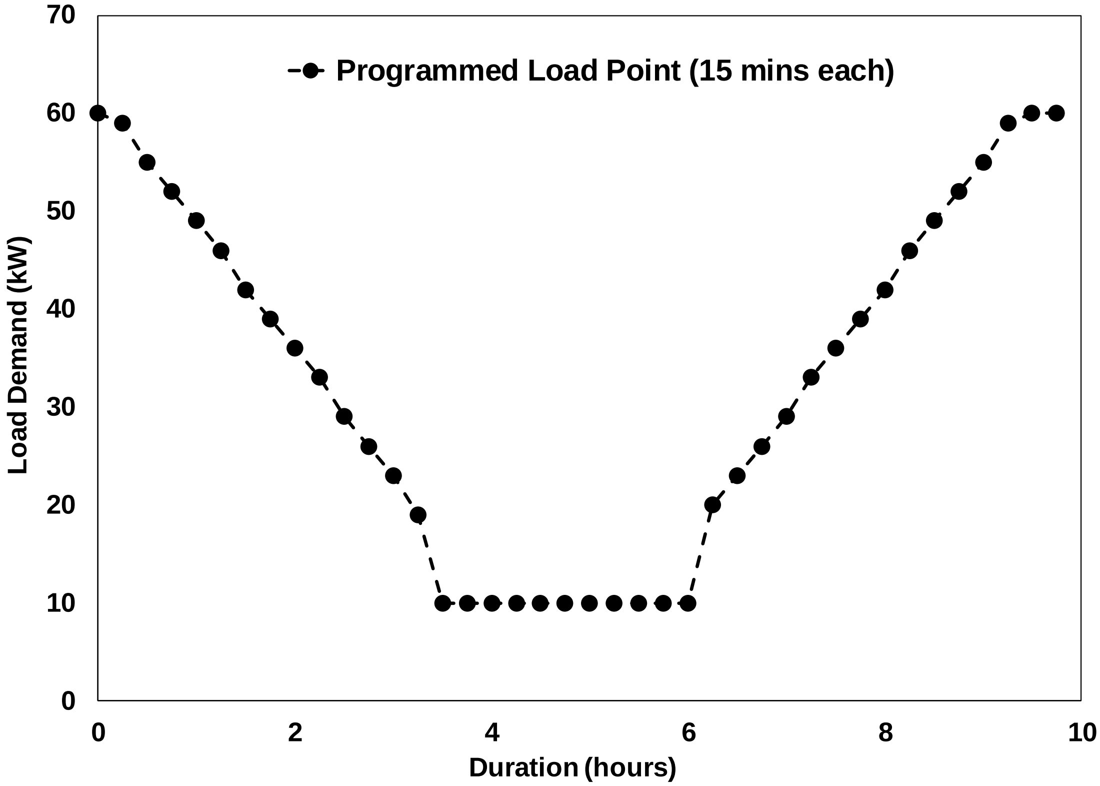


Source: UC Irvine

## 2.4 Data Analysis

To fairly compare the data from the solid-state sensors with respect to the established referee instrument (HORIBA PG-350), several steps were required to account for the different measurement basis of the two devices and for any referee instrument drift.

The PG-350 was calibrated once every four to five weeks (every one to two weeks later in the testing period) during the testing phase. The calibration results showed a maximum drift of 4 – 5 ppm of NO over a 250 ppm span range for the PG-350; whereas, it showed a maximum drift of .3 percent $O_2$ over a 25 percent span range. The drift that was found was then incorporated into a MATLAB[1] code that was written to analyze the data taken. Linear drift behavior was assumed over the period between calibrations.

Because the solid-state sensors measure on a wet basis compared to a dry-basis measured for the PG-350, fuel and air flow data were taken CRMS to find the theoretical water content in the exhaust of the gas turbine at any given load. The PG-350 requires sample conditioning so water condensate cannot harm the analyzer's internal components or interfere with sample measurements. The air-to-fuel ratio was used to correct the sensors to a dry-basis from a wet-basis. Appendix B shows the method of calculating water mole-fraction. The following equations were used to correct the $O_2$ and NO readings of the solid-state sensors:

$$NO_{ppmvd} = \frac{NO_{ppm}}{1-x_{H_2O}} \qquad \text{Equation 2.1}$$

[1] High performance language for technical computing.

$$O_{2\,ppmvd} = \frac{O_{2\,ppm}}{1 - x_{H_2O}} \qquad \text{Equation 2.2}$$

where $x_{H2O}$ is the mole fraction of water present in the exhaust

Once corrected from wet to dry, the readings from all sensors and the reference analyzer were corrected to a standard 15 percent $O_2$ concentration:

$$NO_{ppmvd,15\%\,O_2} = NO_{ppmvd}\left(\frac{20.9-15}{20.9-O_{2,ppmvd}}\right) \qquad \text{Equation 2.3}$$

By incorporating transient data in the results, the project team found significant hysteresis due to the lag in response between the sensors (best response time between 4 and 5 seconds, which are shown in the results section) and the referee instrument (response time of 10 seconds), the sample time delay due to the long sample train required to condition the sample for the PG-350 instrument, and the inherent differences between time averaging on the PG-350 (60 minutes moving time average) compared to the raw data coming from the sensors. To generate a fair comparison of steady-state data, the transient data had to be removed from the averaging process within the steady-state conditions. After some careful evaluation of the data, this filtering process was accomplished by taking out 10 points during each transitional period when the load changed. An example of this can be seen in Figure 9 when the load changes from 19 kW to 10 kW.

**Figure 9: Transient Data**

| Time | NTK 1 | NTK 2 | NTK 3 | UniNOx 1 | UniNOx 2 | UniNOx 3 | PG-350 |
|---|---|---|---|---|---|---|---|
| 4:09:01 PM | 11 | 15 | 14 | 18 | 15 | 17 | 6.72 |
| 4:09:11 PM | 12 | 18 | 16 | 20 | 16 | 17 | 11.13 |
| 4:09:20 PM | 13 | 20 | 19 | 21 | 17 | 18 | 12.65 |
| 4:09:31 PM | 5 | 9 | 8 | 9 | 6 | 7 | 11.53 |
| 4:09:41 PM | 8 | 14 | 13 | 23 | 20 | 27 | 7.31 |
| 4:09:51 PM | 16 | 27 | 24 | 26 | 16 | 23 | 17.36 |
| 4:10:01 PM | 10 | 19 | 17 | 20 | 12 | 18 | 19.15 |
| 4:10:10 PM | 10 | 17 | 17 | 25 | 21 | 28 | 15.62 |
| 4:10:21 PM | 37 | 56 | 53 | 62 | 44 | 61 | 24.42 |
| 4:10:31 PM | 43 | 63 | 59 | 65 | 44 | 62 | 43.42 |
| 4:10:41 PM | 43 | 63 | 59 | 65 | 44 | 62 | 48.65 |
| 4:10:51 PM | 44 | 64 | 60 | 66 | 45 | 63 | 50.36 |
| 4:11:01 PM | 42 | 62 | 57 | 61 | 39 | 55 | 50.46 |
| 4:11:11 PM | 32 | 48 | 45 | 49 | 34 | 46 | 45.21 |
| 4:11:21 PM | 32 | 46 | 43 | 47 | 31 | 44 | 38.55 |
| 4:11:31 PM | 29 | 45 | 42 | 46 | 31 | 43 | 36.17 |
| 4:11:41 PM | 34 | 49 | 48 | 58 | 45 | 60 | 34.91 |
| 4:11:50 PM | 48 | 71 | 67 | 75 | 54 | 72 | 44.74 |

19 kW Data

10 kW Transient Data

10 kW Steady-State Data

Source: UC Irvine

**Error! Not a valid bookmark self-reference.** shows the typical load profile used for a given day and the number of sample points available per load (minus the transient data). These data were used to find an average nitric oxide level per load, which was then used to calculate the sensor characteristics in the results section. For calculating all the sensor parameters, the data from each day for all instruments were sorted in ascending order based on the PG-350 NO readings. This step simplified the method in which calculations are done. Data were sorted in upscale direction (load going up), downscale direction (direction of load going down), and both (combined data). Once data were sorted, PG-350 data is rounded to the nearest hundredth decimal place for concentrations below 10 ppm, and to the nearest tenth decimal place for concentrations above 10 ppm. A MATLAB code was used to perform calculations and sort data.

**Table 3: Sampling Points for 0.1 Hertz Data**

| Load (kW) | Sampling Points | Load (kW) | Sampling Points |
|---|---|---|---|
| 10 | 983 | 39 | 160 |
| 19 | 80 | 42 | 160 |
| 20 | 80 | 46 | 160 |
| 23 | 160 | 49 | 160 |
| 26 | 160 | 52 | 160 |
| 29 | 160 | 55 | 160 |
| 33 | 160 | 59 | 160 |
| 36 | 160 | 60 | 5285 |

Source: UC Irvine

Table 4 displays a small segment of the daily measurements that were collected for the sensors as well as the PG-350. The following is an explanation of the four circles in the table and how the calculations were conducted for the measured sensor characteristics.

- Circle 1. are the PG-350 measurements that were recorded. At three times in the day (could be at different timestamps and at different conditions throughout the day), the PG-350 reported 5.06 ppmvd (15 percent O2).
- At the same time the PG-350 reported 5.06 ppmvd, the three NTK sensors also reported measurements. These are shown in circle 2 (the blue circle).
- At the same time the PG-350 reported 5.06 ppmvd, the three UniNOx® sensors also reported measurements. These are shown in circle 3 (the yellow circle).
- The purple circle (circle 4) represents the corresponding load (kW) at which the data were measured.

**Table 4: Sample Data**

| PG-350 | NTK 1 | NTK 2 | NTK 3 | UniNOx 1 | UniNOx 2 | UniNOx 3 | Load (kW) |
|---|---|---|---|---|---|---|---|
| 5 | 6.728508 | 5.833674 | 5.614943 | 0 | 1.821652 | 1.855635 | 33 |
| 5 | 0 | 1.788429 | 0 | 0 | 0 | 0 | 46 |
| 5.04 | 1.61355 | 0 | 0 | 0 | 0 | 0 | 46 |
| 5.06 | 3.082251 | 3.368874 | 1.690571 | 0 | 0 | 0 | 46 |
| 5.06 | 5.137812 | 4.179985 | 3.830412 | 0 | 0 | 0 | 29 |
| 5.06 | 3.464234 | 6.205357 | 3.873933 | 0 | 0 | 0 | 33 |
| 5.07 | 3.481312 | 4.222372 | 3.905154 | 0 | 1.876998 | 0 | 29 |
| 5.07 | 1.622051 | 1.775909 | 0 | 0 | 0 | 0 | 46 |
| 5.14 | 3.077597 | 3.366685 | 1.691808 | 0 | 0 | 0 | 46 |

Source: UC Irvine

Using these data, accuracy can be calculated using the following equation:

$$\text{Accuracy (\%)} = \frac{D_{Max}}{IN_{f.s.}} \cdot 100 \qquad \text{Equation 2.4}$$

To use this to calculate the percentage accuracy of each individual NTK and UniNOx® sensor, $D_{Max}$ must first be calculated. Since each individual sensor has three responses at the same input, these differences will be averaged. These results are shown in the following equations and Table 5:

$$D_{Max}\,NTK_1(\text{ppmvd}) = \frac{|3.08-5.06|+|5.14-5.06|+|3.46-5.06|}{3} = 1.22 \qquad \text{Equation 2.5}$$

$$D_{Max}\,NTK_2(\text{ppmvd}) = \frac{|3.37-5.06|+|5.14-5.06|+|3.46-5.06|}{3} = 1.24 \qquad \text{Equation 2.6}$$

$$D_{Max}\,NTK_2(\text{ppmvd}) = \frac{|1.69-5.06|+|3.83-5.06|+|3.87-5.06|}{3} = 1.93 \qquad \text{Equation 2.7}$$

$$D_{Max}\,UniNOx_1(\text{ppmvd}) = \frac{|0-5.06|+|0-5.06|+|0-5.06|}{3} = 5.06 \qquad \text{Equation 2.8}$$

$$D_{Max}\,UniNOx_2(\text{ppmvd}) = \frac{|0-5.06|+|0-5.06|+|0-5.06|}{3} = 5.06 \qquad \text{Equation 2.9}$$

$$D_{Max}\,UniNOx_3(\text{ppmvd}) = \frac{|0-5.06|+|0-5.06|+|0-5.06|}{3} = 5.06 \qquad \text{Equation 2.10}$$

**Table 5: Explanation of Accuracy**

| *PG-350* | *NTK 1* | *NTK 2* | *NTK 3* | *UniNOx 1* | *UniNOx 2* | *UniNOx 3* | *Load (kW)* |
|---|---|---|---|---|---|---|---|
| *5* | 6.728508 | 5.833674 | 5.614943 | 0 | 1.821652 | 1.855635 | 33 |
| *5* | 0 | 1.788429 | 0 | 0 | 0 | 0 | 46 |
| *5.04* | 1.61355 | 0 | 0 | 0 | 0 | 0 | 46 |
| *5.06* | 3.082251 | 3.368874 | 1.690571 | 0 | 0 | 0 | 46 |
| *5.06* | 5.137812 | 4.179985 | 3.830412 | 0 | 0 | 0 | 29 |
| *5.06* | 3.464234 | 6.205357 | 3.873933 | 0 | 0 | 0 | 33 |
| *5.07* | 3.481312 | 4.222372 | 3.905154 | 0 | 1.876998 | 0 | 29 |
| *5.07* | 1.622051 | 1.775909 | 0 | 0 | 0 | 0 | 46 |
| *5.14* | 3.077597 | 3.366685 | 1.691808 | 0 | 0 | 0 | 46 |

**Unique PG-350 value**

| *PG-350* | *NTK 1* | *NTK 2* | *NTK 3* | *UniNOx 1* | *UniNOx 2* | *UniNOx 3* |
|---|---|---|---|---|---|---|
| **5.06** | 1.22 | 1.24 | 1.93 | 5.06 | 5.06 | 5.06 |

**Averaged Differences between individual sensor and PG-350 (at 5.06 ppmvd)**

Source: UC Irvine

Once the averaged differences are computed, the maximum range of PG-350 data observed throughout the testing day are used to determine the accuracy.

Precision can be calculated using the following equation:

$$Precision\ (\%) = \frac{\Delta S_{Max}}{IN_{f.s.}} \cdot 100 \qquad \text{Equation 2.11}$$

To use this to calculate the percentage precision of each individual NTK and UniNOx® sensor, $\Delta S_{Max}$ must first be calculated. Since each individual sensor has three responses at the same input, these differences will be averaged. These results are shown in the following equations and Table 6.

$$\Delta S_{Max}\ \mathrm{NTK_1(ppmvd)} = \frac{|3.08-5.14|+|3.08-3.46|+|3.08-3.08|}{3} = .813 \qquad \text{Equation 2.12}$$

$$\Delta S_{Max}\mathrm{NTK_2(ppmvd)} = \frac{|3.37-3.37|+|3.37-4.18|+|3.37-6.21|}{3} = 1.22 \qquad \text{Equation 2.13}$$

$$\Delta S_{Max}\ \mathrm{NTK_2(ppmvd)} = \frac{|1.69-1.69|+|3.83-1.69|+|3.87-1.69|}{3} = 1.44 \qquad \text{Equation 2.14}$$

$$\Delta S_{Max}\ \mathrm{UniNOx_1(ppmvd)} = \frac{|5.06-5.06|+|5.06-5.06|+|5.06-5.06|}{3} = 0 \qquad \text{Equation 2.15}$$

$$\Delta S_{Max}\ \mathrm{UniNOx_2(ppmvd)} = \frac{|5.06-5.06|+|5.06-5.06|+|5.06-5.06|}{3} = 0 \qquad \text{Equation 2.16}$$

$$\Delta S_{Max}\ \mathrm{UniNOx_3(ppmvd)} = \frac{|5.06-5.06|+|5.06-5.06|+|5.06-5.06|}{3} = 0 \qquad \text{Equation 2.17}$$

**Table 6: Explanation of Precision**

| *PG-350* | *NTK 1* | *NTK 2* | *NTK 3* | *UniNOx 1* | *UniNOx 2* | *UniNOx 3* | *Load (kW)* |
|---|---|---|---|---|---|---|---|
| *5* | 6.728508 | 5.833674 | 5.614943 | 0 | 1.821652 | 1.855635 | 33 |
| *5* | 0 | 1.788429 | 0 | 0 | 0 | 0 | 46 |
| *5.04* | 1.61355 | 0 | 0 | 0 | 0 | 0 | 46 |
| *5.06* | 3.082251 | 3.368874 | 1.690571 | 0 | 0 | 0 | 46 |
| *5.06* | 5.137812 | 4.179985 | 3.830412 | 0 | 0 | 0 | 29 |
| *5.06* | 3.464234 | 6.205357 | 3.873933 | 0 | 0 | 0 | 33 |
| *5.07* | 3.481312 | 4.222372 | 3.905154 | 0 | 1.876998 | 0 | 29 |
| *5.07* | 1.622051 | 1.775909 | 0 | 0 | 0 | 0 | 46 |
| *5.14* | 3.077597 | 3.366685 | 1.691808 | 0 | 0 | 0 | 46 |

**Unique PG-350 value**

| *PG-350* | *NTK 1* | *NTK 2* | *NTK 3* | *UniNOx 1* | *UniNOx 2* | *UniNOx 3* |
|---|---|---|---|---|---|---|
| **5.06** | 0.812515 | 1.215864 | 1.441068 | 0 | 0 | 0 |

**Averaged Differences between individual sensor responses at same PG-350 measurement (at 5.06 ppmvd)**

With all the values reported at the same input (in this case the PG-350 value of 5.06 ppmvd is taken as the actual "true" NO concentration in the exhaust), the average difference either between the sensors themselves (for precision) or the difference between the sensor value and the PG-350 (for accuracy) is reported. When calculating precision, the first value each sensor reports is treated as the established measurement value at that input, of which a difference from this value is zero. This is established so only one unique output is reported for the same input (only one unique sensor measurement for each PG-350 measurement).

## 2.5 Results

### 2.5.1 Explanation of Accuracy and Precision

To gain a basic underlying understanding of the results that will be discussed, it is important to highlight the differences between accuracy and precision in greater detail. This can be best illustrated with the dartboard analogy. The two dartboards displayed in Figure 10 show the distinct differences. To be precise, each dart that lands on the board must land close to the dart that came before it; however, to be accurate, each dart must land within a certain distance of the middle of the board. If the average distance between each subsequent dart is closer to the middle (left board), the shooter is precise but not accurate. If the average distance between each dart is farther than the distance to the middle of the board, the shooter is accurate but not precise. By applying this analogy to the solid-state sensors, an accurate but imprecise sensor is one that measures close to the PG-350 response, but during repeated measurements fails to achieve a similar response to what it measured before. A precise but inaccurate sensor would fail to measure close to the PG-350 response, but during repeated measurements would achieve a similar response to previous measurements. Because three sensors for each brand are used (three NTK and three UniNOx® sensors), an average precision and average accuracy of the three will be found.

**Figure 10: Dartboard Analogy**

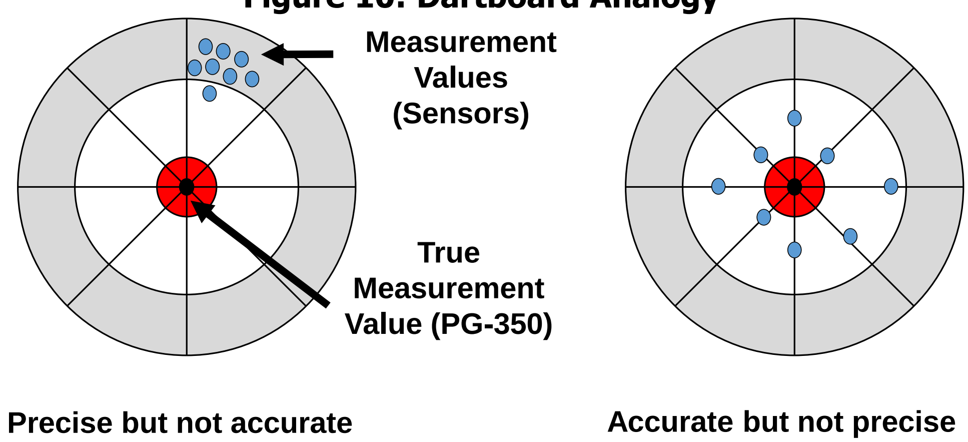


Source: UC Irvine

### 2.5.2 Accuracy

Accuracy was calculated by following the procedure outlined in Appendix A. The testplan included non-linearity instead of accuracy, but the equations for both are the same.

Accuracy represents the difference between the recorded output (sensor response) and the "ideal" linear input (PG-350 response). It is the closeness to which the output follows the input. In this case, the straight line would be a line of 1:1 correlation with the reported values of the PG-350, and the output would be the solid-state sensor values.

Running the C-60 gas turbine on the modified load profile (as explained in the previous sections), the project team was able to expose NTK and UniNOx© sensors to a significant range of nitric oxide levels (0 – approximately 190 ppmvd) over a six-month period. Testing was conducted between early March and late May and after a brief halt in the measurement period, was conducted between late September and mid-October. Over the PG-350's measured range of values, the accuracy of each sensor was calculated by:

- Filtering out transient data as the engine transitioned from one load to the next (10 points at the beginning of each load)
- Taking the average of steady-state measurements at each load. The number of sampling points per load is due to the preset load profile that is programmed into CRMS software.
- With this average value for each sensor per load, the average deviation was found at each load by subtracting the mean value of each sensor at each respective load from the ideal sensor value (PG-350 nitric oxide value), and then dividing by the total range over which the PG-350 reported for that day. This number was multiplied by 100 to present it in terms of a percentage.
- Each sensor brand was averaged to show the corresponding trend for one particular brand of sensor.

Initially, there were some concerns that the sensors reported total NOx measurements instead of NO measurements. These results are shown in Figure 11. The graph displays the one-one comparison of the PG-350 results with the sensor measurements while operating the PG-350 on the NOx setting during a week in late September. By looking at the graph, it is obvious that the PG-350 significantly over-reports compared to the sensor measurements, so the sensors did not measure total NOx. The comparison of PG-350 versus the sensor response while operating on the NO setting is shown in Figure 12, which is a much closer comparison. This testing was conducted during a week in late September to early October.

Following are the percentage accuracies for each sensor over the entire testing period. These percentage accuracies were computed from the following equation:

$$\text{Accuracy (\%)} = \frac{D_{Max}}{IN_{f.s.}} \cdot 100 \qquad \text{Equation 2.18}$$

where $\mathrm{D_{in(Max)}}$ is the maximum reported deviation (difference between averaged output and averaged input) between the sensors and the PG-350 and $\mathrm{IN_{f.s.}}$ is the maximum, full scale input range reported for each testing day.

The lower the calculated percentage, the more accurate is the response of the sensor.

Figure 13 shows the calculated percentage accuracy over the course of the testing period from March to May and subsequently from September to mid-October when testing was resumed. Seasonal variation affects the calculated accuracies, which can most likely be attributed to changes in humidity and ambient temperature from the different season in which testing occurred. This variation can be seen in Figure 14. Solid-state NO measurements are known to be directly affected by water vapor concentrations, which can interfere with the sensor signals(L. Woo and R Glass, 2012). This could explain the lower percentage accuracy (more accurate) found in the drier months compared to the wet, more humid months.

Each square- and diamond-shaped data point represents the average of three sensor percentage accuracies (three UniNOx® and three NTK sensors) for one day. Standard error represents the variation in individual accuracies calculated for each sensor. Table 7 shows the results of a t-test that was conducted that allows a statistical comparison of the reported accuracies for the two sensors. Given the differences between the mean variation of each sensor (comparing 12 percent versus 14.8 percent) compared to the variability among the three of each sensor (0.547 percent) over the entire testing period, the t-test, with 132 degrees of freedom for the data set, indicates that the NTK sensor achieves better accuracy (lower percentage accuracy) than the UniNOx® sensor with more than 99 percent confidence.

**Figure 11: PG-350 Nitrogen Oxide One-One Output (Week of 9/18/2017 – 9/24/2017)**

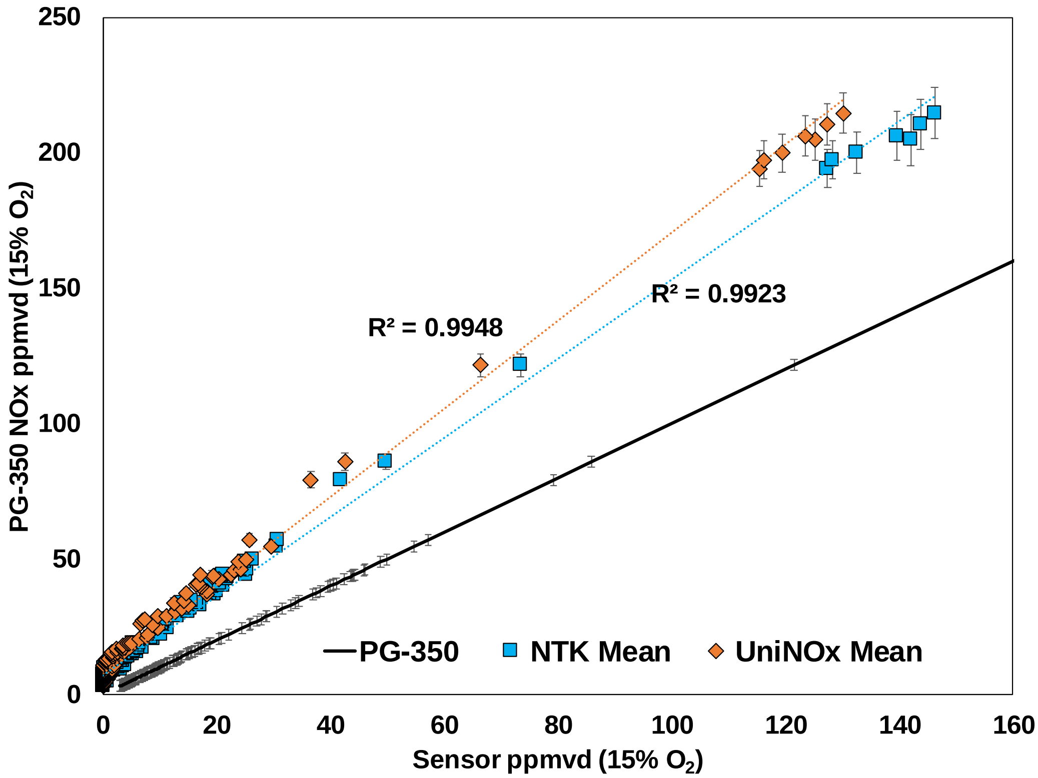


Source: UC Irvine

**Figure 12: PG-350 Nitric Oxide One-One Output (late September/ early October)**

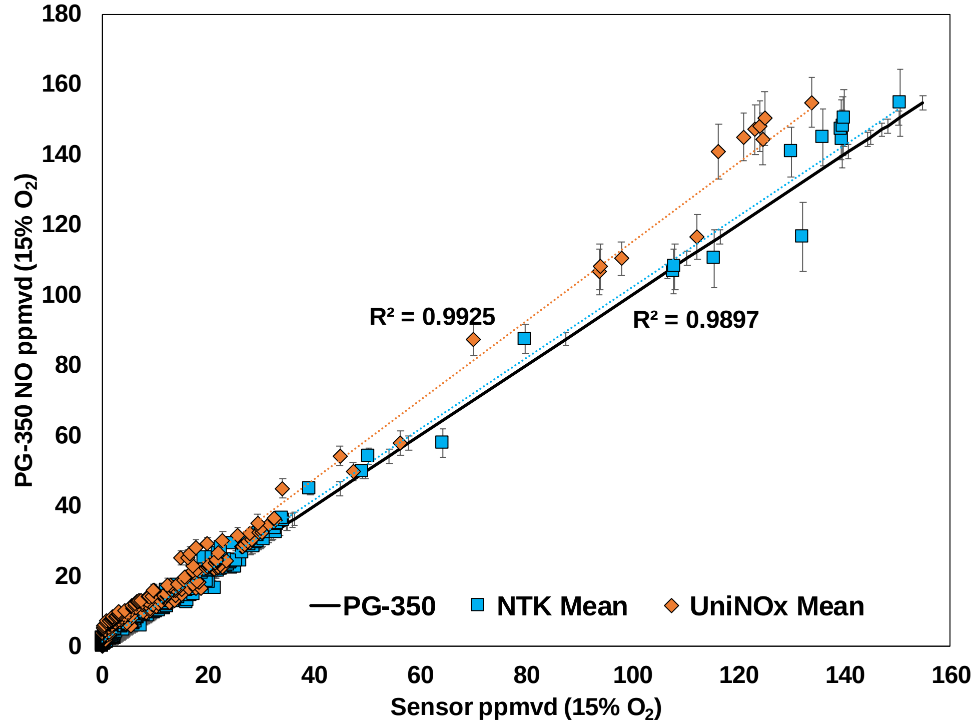


Source: UC Irvine

**Figure 13: Percentage Accuracy**

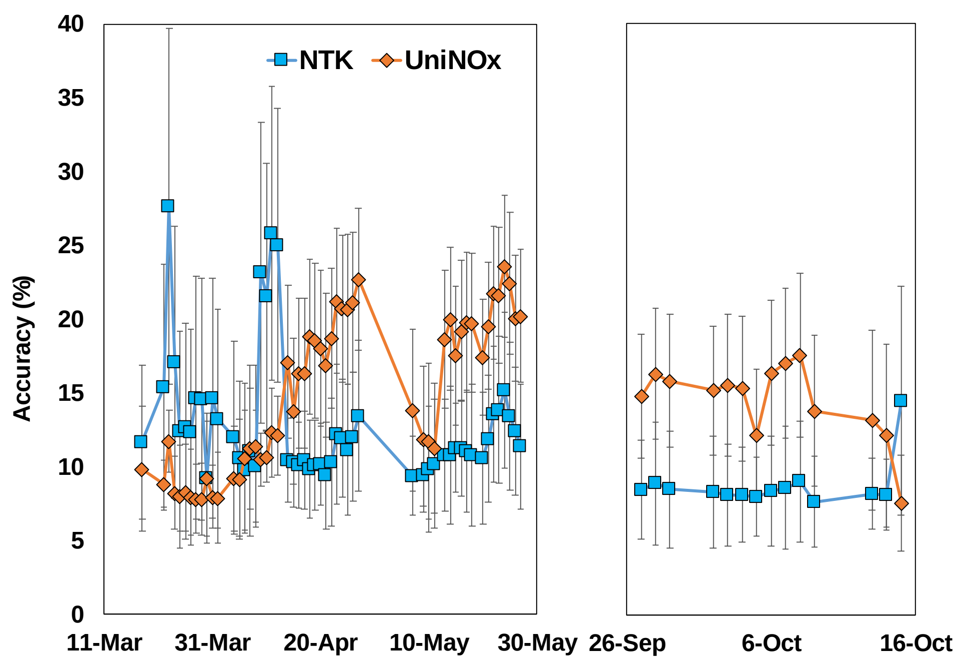


Source: UC Irvine

**Table 7: T-Test Accuracy Results**

| Sensor Brand | Est. Mean | Std Error | Treat-ment | Mean Diff. | df | Std Error | Prob > \|t\| |
|---|---|---|---|---|---|---|---|
| 1-NTK | 12.036 | 0.547 | 1 vs 2 | -2.81 | 132 | 0.773 | 0.00039 |
| 2-UniNOx® | 14.849 | 0.547 | | | | | |

Source: UC Irvine

**Figure 14: Ambient Temperature and Relative Humidity Over Testing Period**

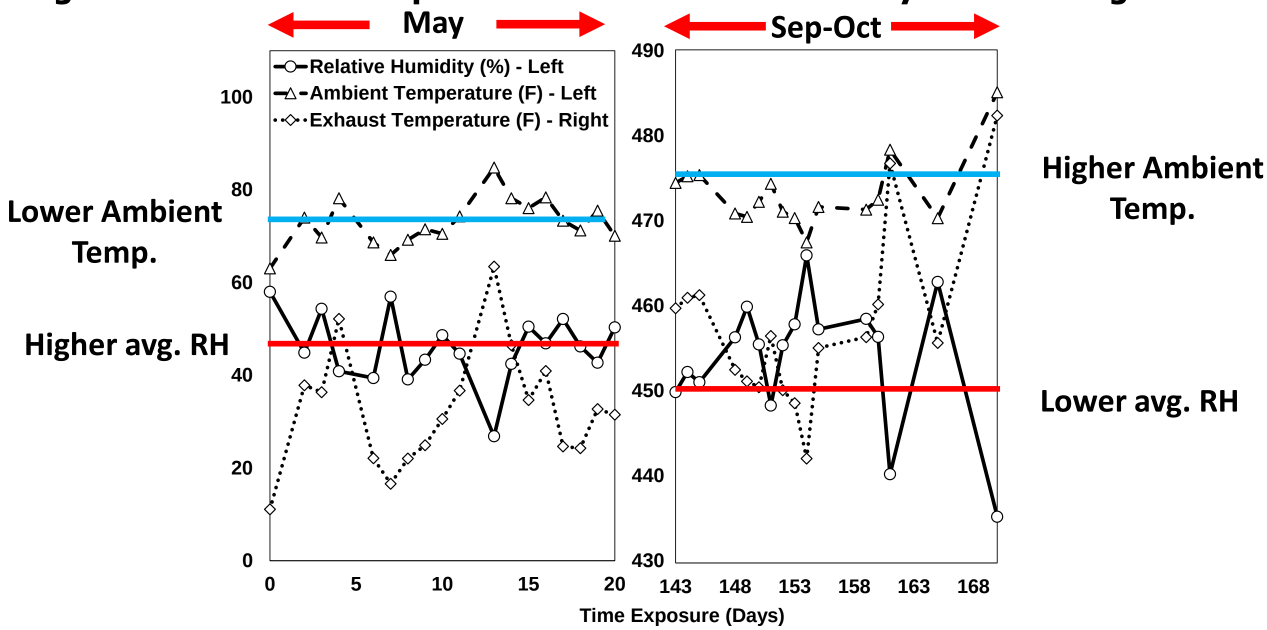


Source: UC Irvine

### 2.5.3 Precision

Sensor precision was calculated by following the procedure outlined in Appendix A. Precision represents the maximum difference between recorded output values over a single input. In terms of this project's sensors, it represents how close the readings of each sensor are with respect to other readings at the same input condition (which is represented by the PG-350 concentration reading).

To summarize, the steps were as follows:

- Filter out the transient data.
- Sort data from all sensors and PG-350 in ascending order, for both the upscale and downscale directions of load.
- Find the averaged difference between what one sensor reports at a given PG-350 measurement. If only one unique input is reported, the averaged difference will be zero (no other readings to compare against)
- Divide the maximum averaged difference seen over the upscale and downscale range for each sensor over the maximum PG-350 measurement range observed.
- Show the corresponding trend for each sensor brand.

Sensor precision can be expressed as:

$$Precision\ (\%) = \frac{\Delta S_{Max}}{IN_{f.s.}} \cdot 100 \qquad \text{Equation 2.19}$$

where $\Delta S_{Max}$ is the maximum difference in reported output values at the same input for a given sensor in the upscale and downscale direction of measurements, and $IN_{f.s.}$ is the full-scale range of NO values reported by the PG-350 for each day of testing.

Figure 15 shows the percentage precision for the NTK and UniNOx® sensors over the entire period of testing. Standard error represents the variation in reported values of percentage precision for different sensors within the same brand. Each square- and diamond-shaped point represents the average of three sensor precision percentages (three UniNOx® and three NTK sensors) for one day. Over the course of the testing period, the general trend indicates that precision is decreasing slightly for both sensor brands (increasing percentage). Because the sensors are installed directly into the exhaust environment, the exposure of different exhaust species to the electrodes could affect precision loss over time. The challenge with taking repeated measurements for these sensors is that input conditions are never truly identical; when individual sensor measurements are compared at the same input (same PG-350 measurement reported), the exhaust temperatures, ambient conditions, and other external factors may be dissimilar (all of which affect the sensor), which will lead to a larger standard deviation and subsequently larger differences between signals than may actually be the case. To truly assess the precision of the device, a controlled environment with close monitoring of input factors would be required; nonetheless, the large amount of data available from testing and the averaging of the three sensor signals are suitable to account for this fact.

Table 8 shows the results from the t-test, which indicate that, with a confidence interval greater than 99 percent, the UniNOx® sensor is more precise than the NTK sensor for the duration of the testing period. This means that a measurement taken with the UniNOx® sensor is more likely to be the same at a given condition (given PG-350 measurement) than the NTK sensor.

The upscale direction was not used in the measurements of precision for the sensors. This is because the sensors perform worse in the downscale direction than in the upscale direction (due to their performance at 10 kW being considered in the downscale direction).

**Figure 15: Precision (Downscale Direction)**

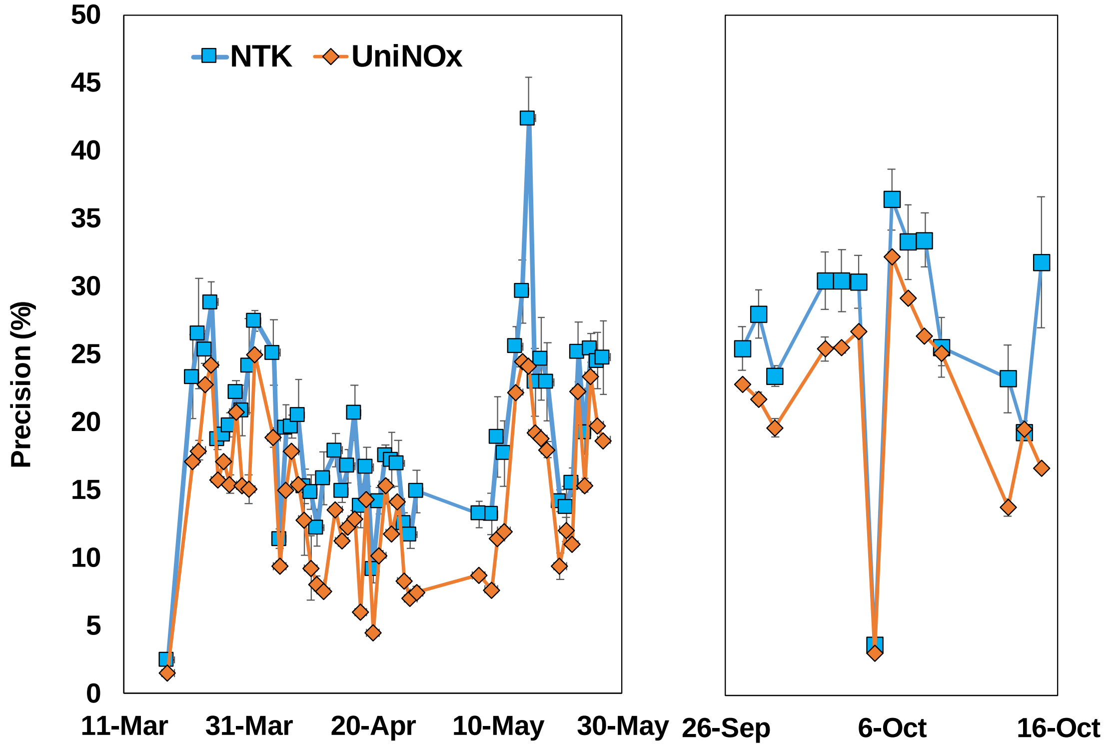


Source: UC Irvine

**Table 8: T-Test Precision Results**

| Sensor Brand | Est. Mean | Std. Error | Treat-ment | Mean Diff. | df | Std. Error | Prob > \|t\| |
|---|---|---|---|---|---|---|---|
| 1-NTK | 19.74 | 0.75 | 1 vs 2 | 4.56 | 132 | 1.06 | 0.0001 |
| 2-UniNOx® | 15.19 | 0.75 | | | | | |

Source: UC Irvine

### 2.5.4 Lower Detectable Limit

The lower detectable limit (LDL) is defined as the smallest concentration level that can be statistically differentiated from a zero concentration level by a 99 percent confidence interval (D. MacDougall et al, 1980). In terms of the sensors, it is the reported NO concentration that can be differentiated from a zero ppm concentration with 99 percent confidence, determined with the following equation:

$$\text{LDL (ppmvd)} = \overline{NO}_{0,ppmvd} + 3\sigma_{0,ppmvd} \qquad \text{Equation 2.20}$$

where $\overline{NO}_{0,ppmvd}$ is the average first non-zero concentrations reported by each sensor and $3\sigma_{0,ppmvd}$ is three times the standard deviation of the reported non-zero concentrations

To calculate LDL, steps were taken similar to those outlined in EPC-15-062 Technical Task 2 Test . To summarize, the steps were as follows:

- Filter out the transient data as described in the previous sections.
- Sort data from all sensors and PG-350 in ascending order for the combined upscale and downscale direction.
- Find the first non-zero concentration the sensors report and the corresponding PG-350 concentration associated with the sensor measurement.
- Find the average PG-350 concentration reported for the sensors in a particular brand for the first non-zero value.
- Find the standard deviation across the three averages for each sensor brand.
- Calculate the LDL.

At high loads, low moisture content present in the exhaust will lead the UniNOx® sensors to report erroneously high levels of NO (greater than 3000 ppm). These data were filtered out by replacing these values with a concentration of zero ppm.

Figure 16 shows the average reported LDL for each sensor type over the entire testing period.

**Figure 16: Lower Detectable Limit**

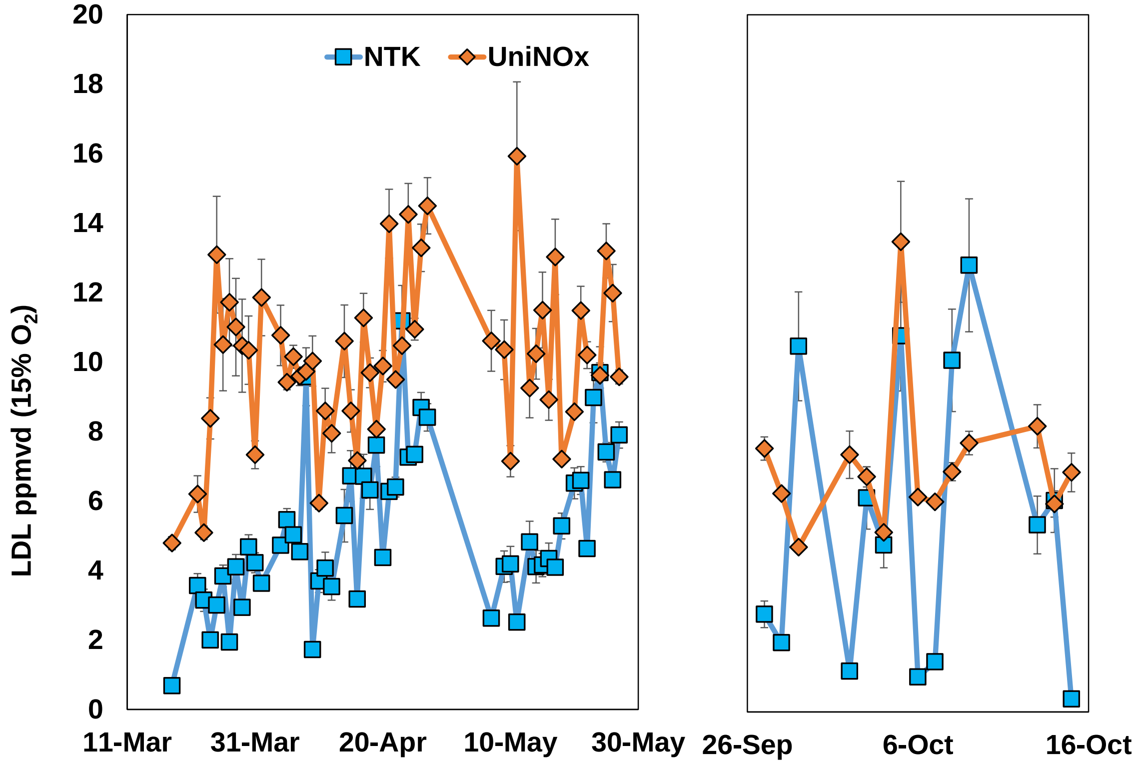


Source: UC Irvine

Standard error represents the variation in the first non-zero concentrations that are reported. To measure LDL, a MATLAB code was to find the first non-zero values of each sensor and subsequently use the reported measurement of the PG-350 at those values as the LDL for that individual sensor. This was done for each device and subsequently averaged with two other measurements, along with the calculated standard deviation of all three devices, to calculate the LDL of the particular brand. Each square- and diamond-shaped point represents the calculated LDL for each day in the testing period. Table 9 reports the results of the t-test that was conducted for the average reported LDL of each brand. With greater than 99 percent confidence, the results indicate that the LDL of the NTK sensor (5.22 ppmvd) is lower than the LDL of the UniNOx® sensor (9.44 ppmvd). These results were shown to agree with results directly given by EmiSense for both of these sensors.

**Table 9: Estimated Mean and Standard Error — Lower Detectable Limit**

| Sensor Brand | Est. Mean | Std. Error | Treat-ment | Mean Diff. | df | Std. Error | Prob > \|t\| |
|---|---|---|---|---|---|---|---|
| 1-NTK | 5.22 | 0.33 | 1 vs 2 | -4.22 | 131 | 0.46 | < 0.0001 |
| 2-UniNOx® | 9.44 | 0.33 | | | | | |

Source: UC Irvine

### 2.5.5 Rise Time and Fall Time

Fall time and rise time are important indicators of how fast the sensor can respond to changes in input parameters. Rise time is the time sensor takes to rise from 10 percent to 90 percent of the output signal step height (in the direction of increasing output). Fall time is the time it takes to fall from 10 percent to 90 percent of the initial starting value. Appendix A details the test procedure and proposed test approach.

Because precise care was needed to measure fall time and rise time, a 10 percent nitric oxide concentration bottle was used to inject nitric oxide into the exhaust at a preset load (60 kW). A pounds per square inch (psi) pressure setting on the regulator was found to the extent that a 0 – 100 ppm resulting step change could be induced in the exhaust and subsequently measured on the PG-350. This was done with a number 35 sonic orifice.

Sampling at 1 Hz was done to ensure a better time resolution of data (1-second increments compared to 10-second increments). The secure digital (SD) card feature on the PG-350 was used to collect the data, instead of using the USB DAQ.

To summarize, the steps to collect data were as follows:

- Set the engine to a load of 60 kW, ensuring a low nitric oxide starting point.
- With the sonic orifice attached to the regulator valve and then leading into a shutoff valve, inject nitric oxide. Read the reported values of the PG-350 on the monitor screen until approximately 100 ppm is reached.
- Once approximately 100 ppm is reached, turn the shutoff valve off. Proceed to record values any time after this point. Make sure 1 Hz data is collected.
- Proceed to mark a significant point in time. At this point, turn the shut-off valve in such a way that the flow is unrestricted. These sensor values recorded will be for the rise time calculations. Take into account any differences in the sampling delay time present in the PG-350.
- After another significant point in time, when the sensor values have remained consistently within a difference of 1 – 2 ppm over a 15-second time frame, proceed to turn the shutoff valve in such a way that the flow is restricted. These subsequent values

will be used for the fall time calculations. Take into account any differences in the sampling delay time present in the PG-350.

- After data has been sufficiently collected and the PG-350 has reported a final steady-state value, proceed to stop recording data.

To analyze the data, the steps were as follows:

- Proceed to split the data into two segments in time: the upward direction and the downward direction.
- For both, take the initial steady-state value to be where the sensors report a difference of the previous and initial value of zero for three or more consecutive seconds. This will be the initial starting point from which the time will be measured.
- For both, take the final steady-state value to be where the sensors report a difference of the previous and initial value of zero for three or more consecutive seconds. This will be the final steady-state value.
- Compute fall time and rise time by using a linear interpolation by following the sub-steps listed:
    - Compute 0.9xF.V. (Final Value) and 0.1xF.V. (rise time) and 0.9xI.V. (Initial Value) and 0.1xI.V. (fall time)
    - Interpolate between the next available point after these values and the previous available point before these values. Find the time it takes to get to both.
    - Report these values for both directions (0.9xF.V. to 0.1xF.V. going up, 0.9xI.V. to 0.1xI.V. going down).

Figure 17 shows the results of the rise time and fall time tests and indicates that the NTK sensor responds more quickly than the UniNOx® sensor in both the rising and falling directions. The inherent 10-second sample delay for the PG-350 (configurable by the user for both a 10-second and 30-second response time) is the reason the instrument's initial response time is longer relative to the solid-state sensors. The PG-350 also uses a time-averaging feature, which was preselected to 60 seconds. This has the ability to allow for an even faster, smoother, and more stabilized response by the PG-350 than if it were measuring raw values, which is particularly useful for the instrument since it is used mostly in applications where steady-state data are taken; nonetheless, the results agree with the configurable 10-second response time.

Table 10 shows the results of the test. The difference in the fall time and rise time of the NTK and UniNOx® sensors is significant.

The fall and rise times were determined using the following equations:

$$t_{rise} = t_{.9F.V.} - t_{.1F.V.} \qquad \text{Equation 2.21}$$

$$t_{fall} = t_{.1I.V.} - t_{.9I.V.} \qquad \text{Equation 2.22}$$

where $t_{rise}$ represents rise time and $t_{fall}$ represents fall time.

To find the approximate fall time and rise time, linear interpolation is needed:

$$\frac{NO_i - NO_{i-1}}{NO_{i+1} - NO_{i-1}} = \frac{t_i - t_{i-1}}{t_{i+1} - t_{i-1}} \qquad \text{Equation 2.23}$$

**Figure 17: Rise Time and Fall Time Tests**

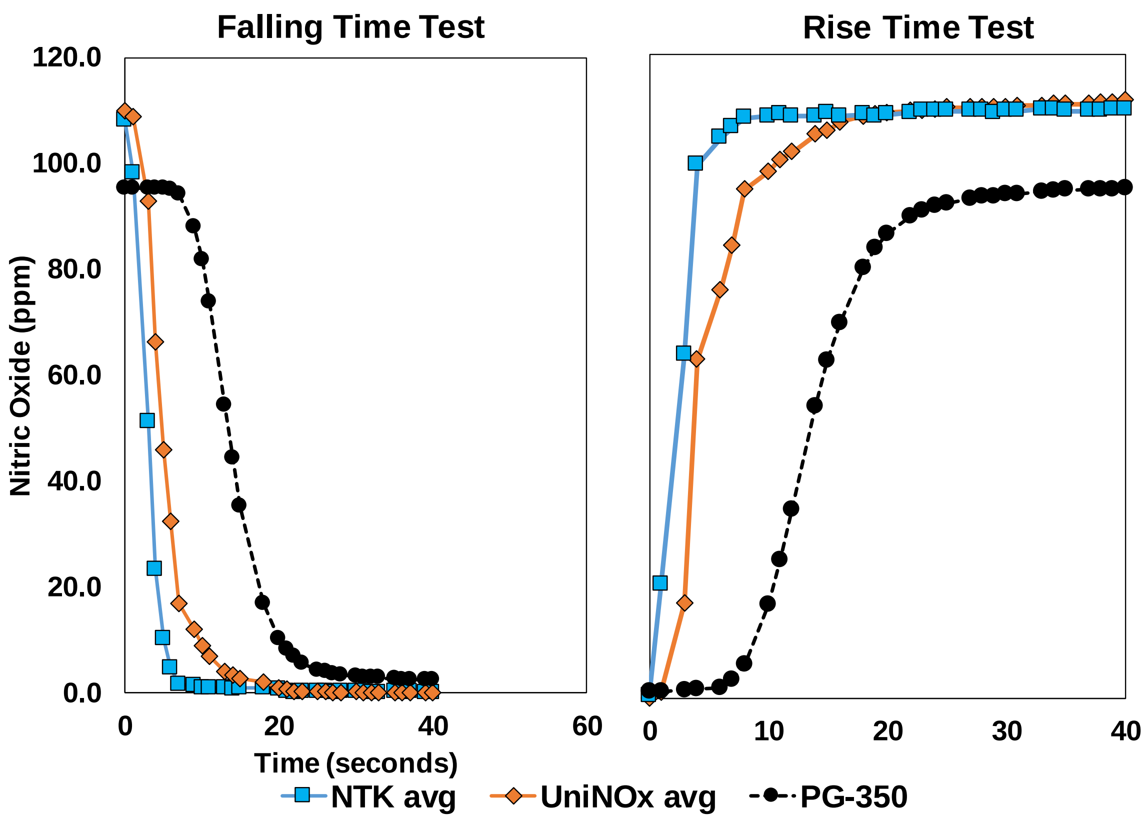


Source: UC Irvine

**Table 10: Rise Time and Fall Time Results**

| Test (5/19/17) | UniNOx Mean +/- Std Dev | NTK Mean +/- Std Dev | PG-350 |
|---|---|---|---|
| Rise Time (sec) | 8.26 +/- 0.60 | 3.70 +/- 0.38 | 11.02 |
| Falling Time (sec) | 6.83 +/- 0.74 | 4.02 +/1 0.36 | 10.41 |

Source: UC Irvine

### 2.5.6 Concentration Resolution

Concentration resolution is the smallest incremental change in nitric oxide that can be detected by the sensors. In the case of the UniNOx® and NTK sensors, both sensors can detect an incremental change of 1 ppm.

## 2.6 Summary of Sensor Evaluation Testing

Table 11 shows the results from each of the comparisons. A value of 1 represents the better performance of one sensor than another. The NTK sensor was found to perform more accurately on a 99 percent confidence interval. The UniNOx® sensor was found to perform better with regard to precision in the downscale direction with 99 percent confidence. The NTK was found to perform better with regard to LDL with a 99 percent confidence interval. The NTK sensor was found to perform faster with regard to fall time and rise time. Both sensors achieve a 1 ppm concentration resolution. In total, three sensor characteristics measured out of the six favor the NTK sensor over the UniNOx® sensor. This was the reason the NTK sensor was suggested for the control algorithm development.

**Table 11: Downselection Table**

| Performance | Accuracy | Precision | LDL | Lag Time/ Rise Time | Concentration Resolution | Total |
|---|---|---|---|---|---|---|
| UniNOx | 0 | 1 | 0 | 0 | 0 | 1 |
| NTK | 1 | 0 | 1 | 1 | 0 | 3 |

Source: UC Irvine

# CHAPTER 3: Integrate Sensor Information Into Engine

## 3.1 Overview of Control Algorithm Development

The goal of the technical task 3.0, from the CEC EPC-15-062 project outline, is as follows: "to integrate the signals from the NOx/Air-to-Fuel ratio sensor(s) that demonstrated promising performance in Task 2 with the engine control system. Initially, open loop concepts will be demonstrated and various algorithms for optimizing emissions performance evaluated."

After the successful completion of well over 3000 hours of testing, it was determined that the Ford NTK sensor performed better in most measured sensor characteristics (accuracy, LDL, and lag time and rise time) by a confidence interval of at least 99 percent or greater compared with the UniNOx® sensor. To implement the Ford NTK sensor within the control system of the engine, a total of four possible control algorithms were developed and an emissions map of CO and NO (ppmvd) at all possible operating conditions was generated. To generate the emissions map, open loop testing was performed using a Design of Experiments (DOEx) approach. Design Expert® was used and a response surface user-defined design was constructed. Using three factors (turbine exit temperature, injector staging, and load ), the resulting design was used to build the four distinct control algorithms that could be used to minimize emissions upon integration of the Ford NTK sensor within control system of the C-60 microturbine. The most feasible approach from the four resulting control strategies was chosen as the algorithm of choice for the technical task 4, (demonstrating the integrated control system) .

## 3.2 Open Loop Commands

### 3.2.1 Capstone Remote Monitoring Software

The Capstone C-60 microturbine uses the staging of six lean-premix injectors to keep emissions low; two injectors are constantly fired at start and four injectors are consecutively turned on as load increases until all six injectors are firing simultaneously from 50 kW to 60 kW. Turbine exit temperature (TET), measured in degrees Fahrenheit, is also a parameter used to trade off durability versus an increase in the efficiency of the system. Higher TET set points will result in more power output but also result in higher nitric oxide emissions and possible reduced durability of the engine. Table 12 shows the default staging settings. The last character in the injector notation (e.g., "0" in IJ30F"0") indicates a minimum ambient temperature for which the indicated load in Table 12 corresponds. "0" indicates 2 deg F, "1" indicates 65 deg F, and "2" indicates 128 deg F. The turbine exit temperature was permitted to vary between 1100 and 1175 deg F.

Using the CRMS, open loop commands were issued to the engine. Nitric oxide and carbon monoxide emissions were measured using the reference "CEM-like" analyzer (Horiba PG-350) that abides by established United States Environmental Protection Agency (USEPA) protocols for emissions measurements. Appendix A offers details about this analyzer.

**Table 12: Open Loop Commands — Default Staging and Turbine Exit Temperature**

| Staging | Turbine Exit Temperature | | |
|---|---|---|---|
| **3 Injectors** | | | |
| OFF (kW) | IJ3OF0<br>30 | IJ3OF1<br>21 | IJ3OF2<br>18 |
| Steady State (kW) | IJ3SS0<br>13.5 | IJ3SS1<br>13.5 | IJ3SS2<br>13.5 |
| ON (kW) | IJ3ON0<br>15 | IJ3ON1<br>15 | IJ3ON2<br>15 |
| **4 Injectors** | | | |
| OFF (kW) | IJ4OF0<br>35 | IJ4OF1<br>29 | IJ4OF2<br>29 |
| Steady State (kW) | IJ4SS0<br>26 | IJ4SS1<br>26 | IJ4SS2<br>26 |
| ON (kW) | IJ4ON0<br>23 | IJ4ON1<br>23 | IJ4ON2<br>23 |
| **5 Injectors** | | | |
| OFF (kW) | IJ5OF0<br>46 | IJ5OF1<br>46 | IJ5OF2<br>46 |
| Steady State (kW) | IJ5SS0<br>43 | IJ5SS1<br>43 | IJ5SS2<br>43 |
| ON (kW) | IJ5ON0<br>40 | IJ5ON1<br>40 | IJ5ON2<br>40 |
| **6 Injectors** | | | |
| OFF (kW) | IJ6OF0<br>56 | IJ6OF1<br>56 | IJ6OF2<br>56 |
| Steady State (kW) | IJ6SS0<br>53 | IJ6SS1<br>53 | IJ6SS2<br>53 |
| ON (kW) | IJ6ON0<br>50 | IJ6ON1<br>50 | IJ6ON2<br>50 |

Source: UC Irvine

### 3.2.2 Design of Experiments

To create the emissions map of the C-60 at all operating conditions, a statistically designed experiment was developed. To aide in this, a software package, Design Expert® version 10 was used. A three-factor, multi-level design was constructed with Load (kW), TET (°F), and Injector Staging as the factors. Load and TET are continuous; whereas, the number of injectors is discrete. Because the number of injectors readily available to be fired is dependent upon the load at which the engine is being operated ($\pm$ 1 injector can reasonably be fired at any given load from the default number of injectors before the engine encounters stability issues), the design was split into four smaller studies; a low range (12 – 22 kW), a medium range (22 – 38 kW), a high range (38 – 50kW), and 50 – 60 kW were modeled. A total of 27 points for each design was tested, with four vertices, four centers of edges, and one overall centroid (Figure 18). Table 13 through Table 16 show details for each of the experimental designs.

**Figure 18: Design of Experiments Design Points**

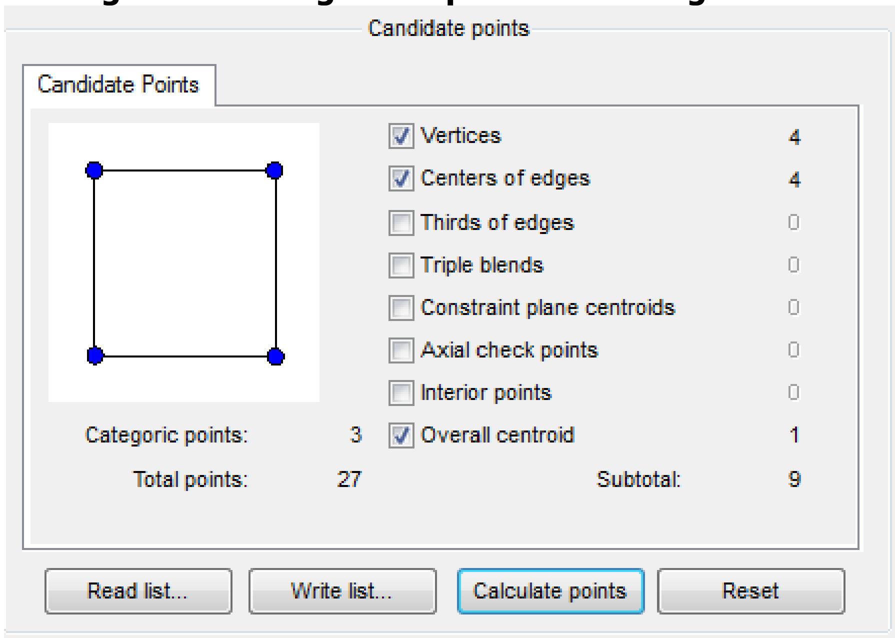


Source: UC Irvine

**Table 13: 12 – 22 Kilowatt Design**

| | Load | TET | # of Injectors |
|---|---|---|---|
| Units | kW | F | |
| Type | Continuous | Continuous | Discrete |
| Levels | N/A | N/A | 3 |
| L[1] | 12 | 1100 | 2 |
| L[2] | 22 | 1175 | 3 |
| L[3] | | | 4 |

Source: UC Irvine

**Table 14: 22 – 38 Kilowatt Design**

| | Load | TET | # of Injectors |
|---|---|---|---|
| Units | kW | F | |
| Type | Continuous | Continuous | Discrete |
| Levels | N/A | N/A | 3 |
| L[1] | 22 | 1100 | 3 |
| L[2] | 38 | 1175 | 4 |
| L[3] | | | 5 |

Source: UC Irvine

**Table 15: 38 – 50 Kilowatt Design**

| | Load | TET | # of Injectors |
|---|---|---|---|
| Units | kW | F | |
| Type | Continuous | Continuous | Discrete |
| Levels | N/A | N/A | 3 |
| L[1] | 38 | 1100 | 4 |
| L[2] | 50 | 1175 | 5 |
| L[3] | | | 6 |

Source: UC Irvine

**Table 16: 50 – 60 Kilowatt Factor Levels**

| | Load | TET | # of Injectors |
|---|---|---|---|
| Units | kW | F | |
| Type | Continuous | Continuous | Discrete |
| Levels | N/A | N/A | 2 |
| L[1] | 50 | 1100 | 5 |
| L[2] | 60 | 1175 | 6 |

Source: UC Irvine

### 3.2.3 Design Expert Results: Analysis of Variance

This section shows the results of the model from Design Expert® 10 (DX10). For Table 17 through Table 24, the analysis of variance (ANOVA) results are shown in table "a" and the equation for the model is displayed in table "b". Each equation is presented as a function of load, TET, and the number of injectors.

A quadratic model was recommended for analyzing each load range, with the exception of 50 – 60 kW. In all cases, the number of injectors was found to be the most significant factor for the model within a 99 percent confidence interval or greater, followed by TET.

**Table 17a: Analysis of Variance – 12 – 22 Kilowatt Range Nitric Oxide ANOVA Results**

| Result | Value |
|---|---|
| Std. Dev. | 0.98 |
| Mean | 5.56 |
| C.V. % | 17.61 |
| PRESS | 47.47 |
| -2 Log Likelihood | 62.95 |
| R-Squared | 0.9709 |
| Adj R-Squared | 0.9555 |
| Pred R-Squared | 0.9151 |
| Adeq Precision | 21.708 |
| BIC | 95.90 |
| AICc | 96.70 |

**Table 17b: Analysis of Variance – 12 – 22 Kilowatt Range Nitric Oxide Model Equation**

| Value | Equation |
|---|---|
| Sqrt(NO + 0.50) | = |
| +285.09390 | |
| -0.27307 | * Load |
| -0.45631 | * TET |
| -13.12938 | * # of Injectors |
| -3.93550E-005 | * Load * TET |
| -0.18184 | * Load * # of Injectors |
| -8.29246E-003 | * TET * # of Injectors |
| +0.023623 | * Load$^2$ |
| +2.17329E-004 | * TET$^2$ |
| +3.44009 | * # of Injectors$^2$ |

Source: UC Irvine

**Table 18a: Analysis of Variance – 12 – 22 Kilowatt Range Carbon Monoxide ANOVA Results**

| Result | Value |
|---|---|
| Std. Dev. | 2.94 |
| Mean | 21.50 |
| C.V. % | 13.70 |
| PRESS | 396.82 |
| -2 Log Likelihood | 117.32 |
| R-Squared | 0.9736 |
| Adj R-Squared | 0.9587 |
| Pred R-Squared | 0.9244 |
| Adeq Precision | 23.615 |
| BIC | 149.90 |
| AICc | 151.99 |

**Table 18b: Analysis of Variance – 12 – 22 Kilowatt Range Carbon Monoxide Model Equation**

| Value | Equation |
|---|---|
| Sqrt(CO + 0.50) | = |
| -1066.91380 | |
| +0.98280 | * Load |
| +1.76296 | * TET |
| +65.60712 | * # of Injectors |
| -8.91904E-004 | * Load * TET |
| -0.37298 | * Load * # of Injectors |
| -0.040235 | * TET * # of Injectors |
| +0.023617 | * Load$^2$ |
| -7.48197E-004 | * TET$^2$ |
| +0.53945 | * # of Injectors$^2$ |

Source: UC Irvine

**Table 19a: Analysis of Variance – 22 – 38 Kilowatt Range Nitric Oxide ANOVA Results**

| Result | Value |
|---|---|
| Std. Dev. | 0.17 |
| Mean | 0.56 |
| C.V. % | 29.89 |
| PRESS | 1.28 |
| -2 Log Likelihood | -31.64 |
| R-Squared | 0.9818 |
| Adj R-Squared | 0.9715 |
| Pred R-Squared | 0.9484 |
| Adeq Precision | 27.023 |
| BIC | 0.94 |
| AICc | 3.03 |

**Table 19b: Analysis of Variance – 22 – 38 Kilowatt Range Nitric Oxide Model Equation**

| Value | Equation |
|---|---|
| $Log_{10(NO)}$ | = |
| -26.01879 | |
| -0.64938 | * Load |
| +0.089138 | * TET |
| -6.57475 | * # of Injectors |
| +6.39060E-004 | * Load * TET |
| -7.96986E-003 | * Load * # of Injectors |
| +2.62221E-003 | * TET * # of Injectors |
| -3.42687E-004 | * $Load^2$ |
| -5.18733E-005 | * $TET^2$ |
| +0.33984 | * # of $Injectors^2$ |

Source: UC Irvine

**Table 20a: Analysis of Variance – 22 – 38 Kilowatt Range Carbon Monoxide ANOVA Results**

| Result | Value |
|---|---|
| Std. Dev. | 1.94 |
| Mean | 20.49 |
| C.V. % | 9.45 |
| PRESS | 176.15 |
| -2 Log Likelihood | 91.20 |
| R-Squared | 0.9795 |
| Adj R-Squared | 0.9673 |
| Pred R-Squared | 0.9359 |
| Adeq Precision | 28.393 |
| BIC | 123.39 |
| AICc | 126.91 |

**Table 20b: Analysis of Variance – 22 – 38 Kilowatt Range Carbon Monoxide Model Equation**

| Value | Equation |
|---|---|
| Sqrt(CO + 0.50) | = |
| -531.78661 | |
| +3.65427 | * Load |
| +0.45154 | * TET |
| +136.66794 | * # of Injectors |
| -4.77444E-003 | * Load * TET |
| -0.11545 | * Load * # of Injectors |
| -0.073718 | * TET * # of Injectors |
| +0.029328 | * $Load^2$ |
| -4.01916E-005 | * $TET^2$ |
| -4.84083 | * # of $Injectors^2$ |

Source: UC Irvine

**Table 21a: Analysis of Variance – 38 – 50 Kilowatt Range Nitric Oxide ANOVA Results**

| Result | Value |
|---|---|
| Std. Dev. | 0.17 |
| Mean | 0.32 |
| C.V. % | 53.42 |
| PRESS | 1.18 |
| -2 Log Likelihood | -29.89 |
| R-Squared | 0.9499 |
| Adj R-Squared | 0.9198 |
| Pred R-Squared | 0.8661 |
| Adeq Precision | 17.788 |
| BIC | 2.30 |
| AICc | 5.83 |

**Table21b: Analysis of Variance – 38 – 50 Kilowatt Range Nitric Oxide Model Equation**

| Value | Equation |
|---|---|
| $Log_{10(NO)}$ | = |
| +51.46796 | |
| -0.78093 | * Load |
| -0.026791 | * TET |
| -8.19065 | * # of Injectors |
| +3.72860E-004 | * Load * TET |
| +0.019215 | * Load * # of Injectors |
| +2.98810E-003 | * TET * # of Injectors |
| +2.94432E-003 | * $Load^2$ |
| +5.19224E-007 | * $TET^2$ |
| +0.32684 | * # of $Injectors^2$ |

Source: UC Irvine

**Table 22a: Analysis of Variance – 38 – 50 Kilowatt Range Carbon Monoxide ANOVA Results**

| Result | Value |
|---|---|
| Std. Dev. | 3.24 |
| Mean | 20.01 |
| C.V. % | 16.17 |
| PRESS | 377.97 |
| -2 Log Likelihood | 128.03 |
| R-Squared | .8915 |
| Adj R-Squared | .8643 |
| Pred R-Squared | 0.8041 |
| Adeq Precision | 19.820 |
| BIC | 147.58 |
| AICc | 144.45 |

**Table 22b: Analysis of Variance – 38 – 50 Kilowatt Range Carbon Monoxide Model Equation**

| Value | Equation |
|---|---|
| Sqrt(CO) | = |
| -438.26240 | |
| +1.95155 | * Load |
| +0.29510 | * TET |
| +127.37185 | * # of Injectors |
| -0.47941 | * Load * # of Injectors |
| -0.087034 | * TET * # of Injectors |

Source: UC Irvine

**Table 23a: Analysis of Variance – 50 – 60 Kilowatt Range Nitric Oxide ANOVA Results**

| Result | Value |
|---|---|
| Std. Dev. | 0.37 |
| Mean | 2.69 |
| C.V. % | 13.91 |
| PRESS | 2.83 |
| -2 Log Likelihood | 7.47 |
| R-Squared | 0.9642 |
| Adj R-Squared | 0.9534 |
| Pred R-Squared | 0.9276 |
| Adeq Precision | 25.549 |
| BIC | 18.03 |
| AICc | 19.92 |

**Table23b: Analysis of Variance – 50 – 60 Kilowatt Range Nitric Oxide Model Equation**

| Value | Equation |
|---|---|
| NO | = |
| -17.01774 | |
| +0.077764 | * Load |
| +0.026865 | * TET |
| -2.70199 | * # of Injectors |

Source: UC Irvine

**Table 24a: Analysis of Variance – 50 – 60 Kilowatt Range Carbon Monoxide ANOVA Results**

| Result | Value |
|---|---|
| Std. Dev. | 0.086 |
| Mean | 2.18 |
| C.V. % | 3.94 |
| PRESS | 0.22 |
| -2 Log Likelihood | -40.52 |

**Table 24b: Analysis of Variance – 50 – 60 Kilowatt Range Carbon Monoxide Model Equation**

| Value | Equation |
|---|---|
| $Log_{10(CO)}$ | = |
| -94.73527 | |
| +1.09357 | * Load |
| +0.078401 | * TET |
| +10.53181 | * # of Injectors |
| -8.42787E-004 | * Load * TET |
| -0.029820 | * Load * # of Injectors |
| -7.76025E-003 | * TET * # of Injectors |

Source: UC Irvine

## Control Algorithms

With the statistical analysis completed, algorithms that could be implemented are now presented. Four possible algorithms were developed and each is described in this section. While nearly unlimited approaches could be considered, the current situation is constrained by practicality associated with implementation into the Capstone engine control software. Essentially, new information (NO from sensor) can be brought in and used to make decisions regarding manipulation of parameters that can currently be controlled. This ensures the algorithms presented can actually be implemented into the current software without major restructuring of the current engine control software.

### 3.3.1 Control Algorithm #1: Nitric Oxide and Carbon Monoxide Optimization — Adjust Turbine Exit Temperature and Staging

Control Algorithm #1 is designed to achieve lower nitric oxide (NO) and carbon monoxide (CO) emissions by changing the number of injectors and the TET setpoint (°F). The models presented in the previous section show that an increase in the number of injectors lowers NO and increases CO; whereas, an increase in TET lowers CO and increases NO. Design Expert® 10 (DX10) was used to optimize the factors so that minimum emissions could be achieved at every load (1 kW – 60 kW).

The major features of the control algorithm include the following:

- Split into five different ranges: 49 – 60 kW, 39 – 48 kW, 30 – 38 kW, 11 – 29 kW, and less than 10 kw
- Emissions ranges expected (ppmvd, 15 percent O2)
- 49 – 60 kW: 1.9 – 2.4 ppmvd NO, 98 – 160 ppmvd CO
- 39 – 48 kW: 1.9 – 2.4 ppmvd, 160 – 280 ppmvd CO
- 30 – 38 kW: 7 – 9.2 ppmvd, 220 – 250 ppmvd CO
- 11 – 29 kW: 10 – 27 ppmvd, 220 – 400 ppmvd CO
- Less than 11 KW: 30 – 100 ppmvd, 400 – 1000 ppmvd CO
- TET setpoint (°F) and the number of injectors desired are determined using the Design Expert® software. This was used to find the optimal settings that minimized emissions at every load.
- Real-time emissions 1 is a variable for the time-averaged emissions before the engine parameters are changed. Real-time emissions 2 is a variable for the time-averaged emissions after engine parameters are changed. The difference between the two gauges whether the changes in TET and injector staging were effective. If they were, the engine will continue to operate in said condition.
- If changes in TET and injector staging are not effective, a general strategy will be used; decrease TET and increase the number of injectors by one, if possible.
- If changes in TET and injector staging are not effective after five attempts, an error will be issued and will signal the operator to monitor emissions for a possible issue with the Capstone engine.

An additional option for the algorithm includes:

- Error occurs when emissions fall outside of expected ranges for longer than two to three minutes in steady-state operation.

### 3.3.2 Control Algorithm #2: Nitric Oxide Optimization — Adjust Turbine Exit Temperature and Staging

Control Algorithm #2 is designed to achieve lower nitric oxide (NO) by changing the number of injectors and the TET setpoint. This presents an alternative to Control Algorithm #1 by minimizing NO alone (as opposed to minimizing both NO and CO).

Major features of the control algorithm include the following:

- Split into five different ranges: 49 – 60 kW, 39 – 48 kW, 30 – 38 kW, 11 – 29 kW, and less than 10 kW
- Emissions ranges expected (ppmvd, 15 percent O2)
- 49 – 60 kW: 1– 2 ppmvd NO, 100 – 340 ppmvd CO
- 39 – 48 kW: .2 – .4 ppmvd, greater than 1000 ppmvd CO
- 30 – 38 kW: .2 – .4 ppmvd, greater than 1000 ppmvd CO
- 11 – 29 kW: .2 – 8 ppmvd, greater than 1000 ppmvd CO
- < 11 KW: 10 – 90 ppmvd, greater than 1000 ppmvd CO

- TET setpoint and the number of injectors desired are determined using the Design Expert® software. This was used to find the optimal settings that minimized emissions at every load.
- Real-time emissions 1 is a variable for the time-averaged emissions before the engine parameters are changed. Real-time emissions 2 is a variable for the time-averaged emissions after engine parameters are changed. The difference between the two gauges whether the changes in TET and injector staging were effective. If they were, the engine will continue to operate in said condition.
- If changes in TET and injector staging are not effective, a general strategy will be used; decrease TET and increase the number of injectors, if possible.
- If changes in TET and injector staging are not effective after five attempts, an error will be issued and will signal the operator to monitor emissions for a possible issue with the Capstone engine.

An additional option for the algorithm includes:

- Error occurs when emissions fall outside of expected ranges for longer than two to three minutes in steady-state operation.

### 3.3.3 Control Algorithm #3: Adjust Turbine Exit Temperature

Control Algorithm #3 is designed to achieve lower nitric oxide (NO) and carbon monoxide (CO) by changing the TET setpoint (the injector staging is kept at the default settings). The models presented in the previous section show that an increase in the number of injectors lowers NO and increases CO; whereas, an increase in TET lowers CO and increases NO.

Major features of the control algorithm include the following:

- Split into six different ranges: 49 – 60 kW, 40 – 48 kW, 29 – 39 kW, 23 – 28 kW, 12 – 22 kW, and less than 12 kW
- Emissions ranges expected (ppmvd, 15 percent O2)
- 49 – 60 kW: .3 – 1 ppmvd NO, 500 – 1000 ppmvd CO
- 40 – 48 kW: .8 – 1 ppmvd, 500 – 730 ppmvd CO
- 29 – 39 kW: approximately 2 ppmvd, approximately 650 ppmvd CO
- 23 – 28 kW: 1 – 2 ppmvd, 450 – greater than 1000 ppmvd CO
- 12 – 22 kW: 0 – 12 ppmvd, greater than 1000 ppmvd CO
- Less than 12 kW: 100 – 160 ppmvd, 50 – 90 ppmvd CO
- The TET setpoint for every load range is determined using the Design Expert® software. This was used to find the optimal settings that minimized emissions at every load.
- Real-time emissions 1 is a variable for the time-averaged emissions before the engine parameters are changed. Real-time emissions 2 is a variable for the time-averaged emissions after engine parameters are changed. The difference between the two gauges whether the changes in TET were effective. If they were, the engine will continue to operate in said condition.
- If changes in TET and injector staging are not effective, a general strategy will be used; decrease TET from the desired setpoint if possible.

- If changes in TET are not effective after 5 attempts, an error will be issued and will signal the operator to monitor emissions for a possible issue with the Capstone engine.

An additional option for the algorithm includes:

- Error occurs when emissions fall outside of expected ranges for longer than two to three minutes in steady-state operation.

### 3.3.4 Control Algorithm #4: Adjust Staging

Control Algorithm #4 is designed to achieve lower nitric oxide (NO) and carbon monoxide (CO) by changing the injector staging (the TET setpoint is left at the default value).

Major features of the control algorithm include the following:

- Split into four different ranges: 39 – 60 kW, 22 – 38 kW, 6 – 21 kW, and 1 – 5 kW
- Emissions Ranges Expected (ppmvd, 15% O2)
- 39 – 60 kW: 1 – 3 ppmvd NO, 20 – 550 ppmvd CO
- 22 – 38 kW: .2 – 1 ppmvd, 350 – 1000 ppmvd CO
- 6 – 21 kW: 2 ppmvd – 40 , greater than 1000 ppmvd CO
- 0 – 5 kW: 50 – 100 ppmvd, greater than 1000 ppmvd CO
- The TET setpoint for every load range is determined using the Design Expert® software. This was used to find the optimal settings that minimized emissions at every load.
- Real-time emissions 1 is a variable for the time-averaged emissions before the engine parameters are changed. Real-time emissions 2 is a variable for the time-averaged emissions after engine parameters are changed. The difference between the two gauges whether the changes in TET were effective. If they were, the engine will continue to operate in said condition.
- If changes in TET and injector staging are not effective, a general strategy will be used; decrease TET from the desired setpoint if possible.
- If changes in TET are not effective after five attempts, an error will be issued and will signal the operator to monitor emissions for a possible issue with the Capstone engine.

## 3.4 Summary of Control Algorithm Development

After previous work by the University of California, Irvine's Combustion Laboratory (UCICL) showed that the Ford NTK commercial nitric oxide (NO) sensor showed promising results regarding reliability and accuracy when measuring emissions in-situ in the exhaust of the Capstone C-60 engine, a total of four control loop algorithms were developed that involved different strategies to minimize emissions using closed-loop control; all of them involve incorporating the feedback of the Ford NTK within the closed-loop control logic of the 60 kW Capstone gas turbine. Design Expert® 10 (DX10) was used to develop models for different load ranges, including: 12 – 22 kW, 22 – 38 kW, 38 – 50 kW, and 50 – 60 kW. Results from ANOVA are presented for each model in previous sections.

Results from each of the four load ranges show that the number of injectors is the most significant factor for each model, within a 99 percent or greater confidence interval. All models show that an increase in TET increases nitric oxide (NO) and lowers carbon monoxide (CO) due to the higher firing temperatures; whereas, an increase in the number of injectors increases CO and lowers NO due to the lower local equivalence ratios in each individual injector (same amount of fuel split to an additional injector). Using DX10, the factors for each model (TET setpoint and injector staging) were optimized at every load to minimize emissions. These optimal levels for each factor were subsequently used in each of the four control algorithms: Control Algorithm 1 is designed to minimize both NO and CO by adjusting TET setpoint and injector staging, Control Algorithm 2 is designed to minimize only NO by adjusting TET setpoint and staging, Control Algorithm 3 is designed to minimize NO by adjusting the TET setpoint and keeping the default staging, and Control Algorithm 4 is designed to minimize NO by keeping the default TET setpoint and altering injector staging.

Of the four control algorithms, Control Algorithm #1 is suggested. Because NO and CO are both minimized, it is a practical approach to achieving acceptable emissions levels. For the current application, maps of CO emissions as a function of the parameters studied will be needed until a similarly robust sensor for exhaust CO is identified/developed.

# CHAPTER 4: Demonstrate Control Performance

## 4.1 Overview of Control Algorithm Demonstration

The third technical task (Task 4) from the CEC EPC-15-062 project outline is: "to implement the recommended control algorithm from Task 3 into a demonstration study in which emissions levels are changed and the control algorithm demonstrates the ability to minimize them."

After the development of the initial control logic for Control Algorithm #1, the Combustion Laboratory at the University of California, Irvine (UCICL) successfully worked with Capstone Turbine Corporation and EmiSense to develop control algorithm software and an analog-output package capable of sending the NTK sensor signal to the engine communications bay (see Figure 19) in the form of two output signals: an NO (ppm) signal (uncorrected and wet) from 4-20 mA (milliampere) and 0 mA during the initial warm-up period, and a $O_2$ (percent) signal (wet) from 4-20 mA and 0 mA during the initial warm-up period.

**Figure 19: Capstone Communications Bay**

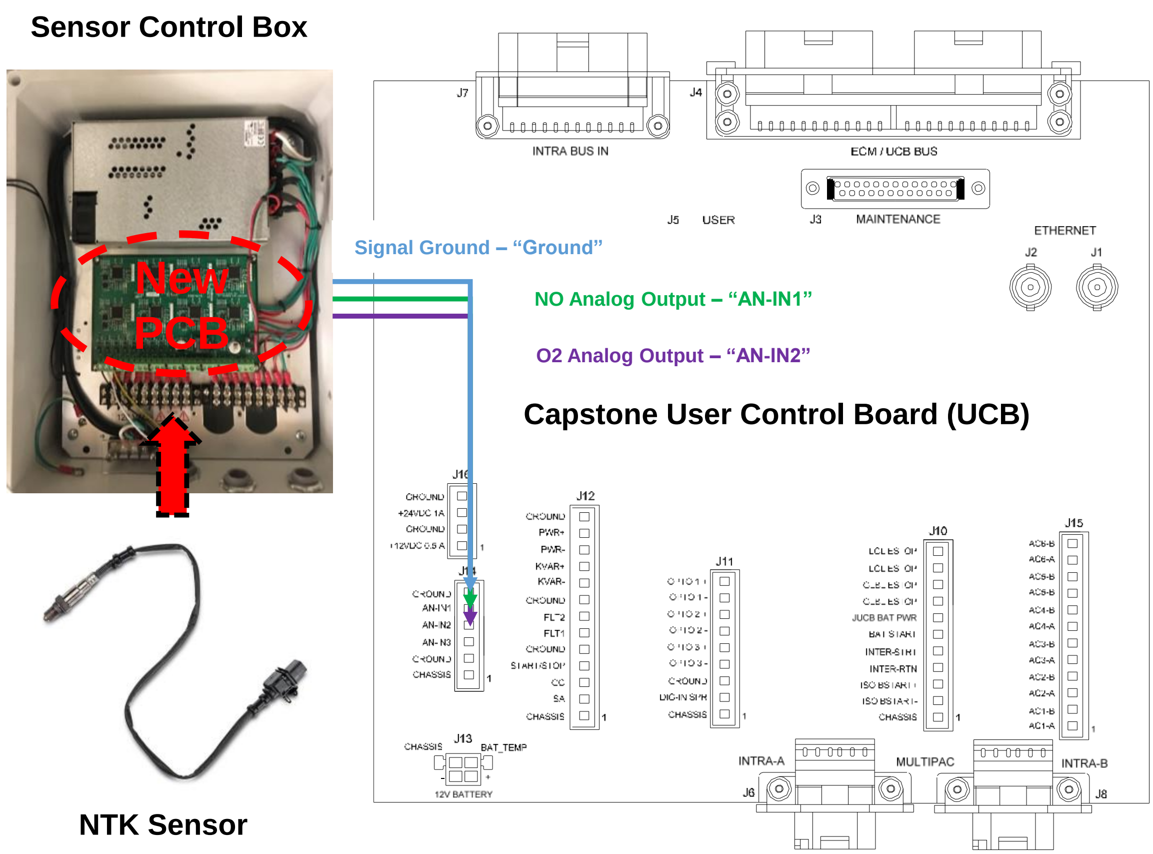


Source: UC Irvine

Once the control logic was programmed onto the engine in the form of a software update, a total of four tests were conducted across different load ranges (16 kW, 29 kW, 44 kW, and 55 kW) to test the algorithm across a wide range of operating conditions. Measurements were taken and recorded using the PG-350 referee instrument as well as the solid-state devices. The results of the tests are outlined in the following sections.

## 4.2 Testing Results

Upon loading the latest Capstone codeset (Codeset_C65_v5.40rc) and upgrading the fuel system with a Woodward control valve, the engine was able to use the NTK sensor feedback (measured in the software as combined heat and power [CHP] water flow [gallons per minute] and CHP temperature feedback for NO and $O_2$, respectively; see Figure 20). Software was built into the latest codeset to allow for configurable scaling for both outputs. The digital conversion device on the NTK board is 8-bit, and the user control board (UCB) in the communications bay of the MTG allows for up to 10-bit precision. The NTK analog board outputs information (actively averaging the 10 ms (millisecond) signals from the NTK sensor) at a 1 Hz rate, and CRMS outputs information every 5 seconds. See Figure 21 for the analog output board.

**Figure 20: Capstone Remote Monitoring Software Screen**

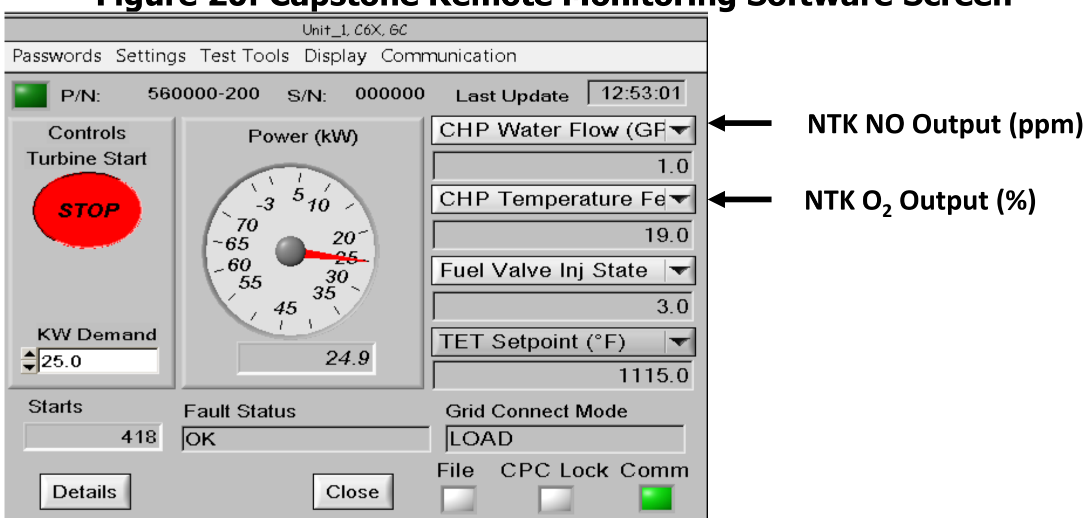


Source: UC Irvine

**Figure 21: NTK Analog Output Printed Circuit Board**

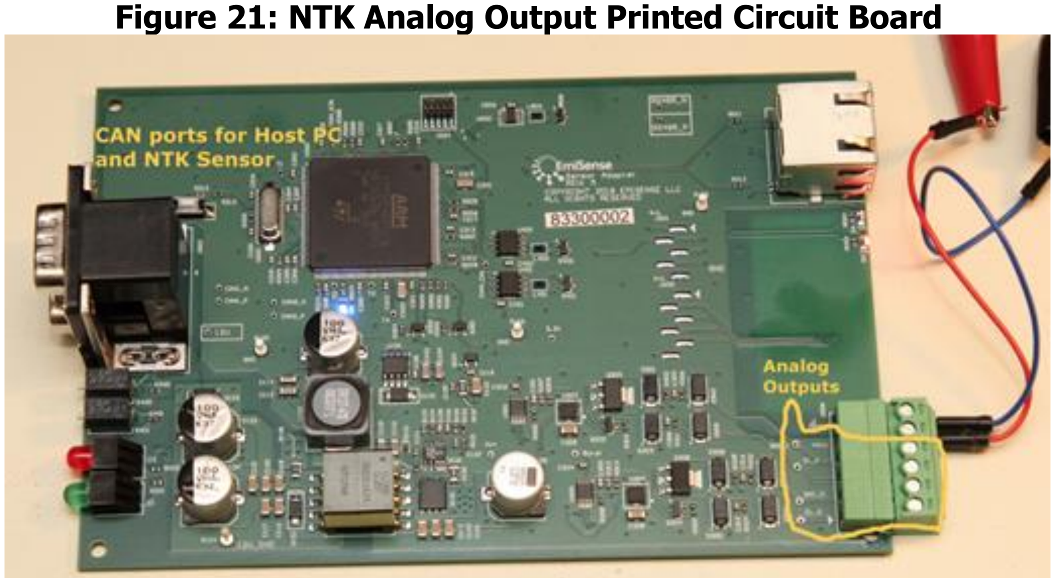


Source: UC Irvine

For higher loads (20 kW and up) it was found that the best performance was obtained with a scaling of 0 – 30 ppm for NO and 0 – 21 percent for $O_2$. The wet, uncorrected readings of the NTK sensors were already quite low at loads higher than 30 kW (0 – 2 ppm reported from the PG-350). This presented a challenge for the algorithm to distinctly identify if the emissions had been lowered once the control logic took effect; however, at the 16 kW load setting, a range of 0 – 100 ppm was employed for the NO output scaling as well as a 0 – 21 percent scaling for $O_2$. The injector staging also remained the same below 20 kW, but was adjusted above 20 kW to allow for higher NO output before the onset of the initial control logic. This was done so the algorithm could more easily identify if a reduction in emissions had occurred.

The algorithm results for 16 kW and 29 kW are displayed in Figures 22 through 29 for NO, $O_2$, and CO. The PG-350 10 second sample delay was taken into account, and the data were shifted by 10 seconds. The longer response time of the PG-350 results in a slightly delayed response compared to the NTK sensor. Note that there are no figures for any loads higher than 30 kW, as the algorithm was unable to resolve changes in NO at these points. Because the control board in the engine is unable to perform complex calculations, emissions could not be corrected in real time.

### 4.2.1 16 Kilowatt Results

The initial spike observed in Figure 22 – Figure 24 for the 16 kW results represents the transient emissions during the change from a previous load to the current load condition (21 kW to 16 kW). If a 5 kW difference from the previous load is demanded, the control algorithm will take that difference into effect for that load.

For Figure 22, the algorithm first measures the emissions (RT Emissions 1) when the desired load is achieved. This occurs after a predetermined time has elapsed to achieve steady-state conditions. This predetermined time is governed by the variable DBTIME in CRMS, which is set to a maximum of 1 minute. The default settings (TET and default staging already preset in CRMS) are still used during this first period. Note the 1 ppm resolution of the NTK sensor, which results in the small spikes observed.

The algorithm's first attempt to lower emissions is around the 16:49:26 mark. This is where the optimized settings from Control Algorithm #1 come into effect; however, there is no visible reduction in emissions because the optimized settings are nearly the same as the default settings programmed onto the engine. The TET is the same (1175°F [635°C]) and the injector staging is similar as well. Note that the emissions are measured for a second time at 16 kW right before the 16:50:53 mark (RT Emissions 2). This drop in TET is the algorithm's attempt to lower NO emissions, which is successful. The NO after the first drop (after 16:50:53) is visibly lower than before. The algorithm observes that after another steady-state period the second emissions measurements are lower than before, so it continues to operate with the optimized settings.

In Figure 23 and Figure 24, the CO and $O_2$ results are displayed. Note the 1 percent resolution of the NTK sensor, which results in two large spikes in Figure 23. The CO results in the figure also show that the algorithm is working. By decreasing the TET, the local equivalence ratios of each injector decrease, so NO decreases but CO increases.

**Figure 22: 16 Kilowatt Nitric Oxide Results**

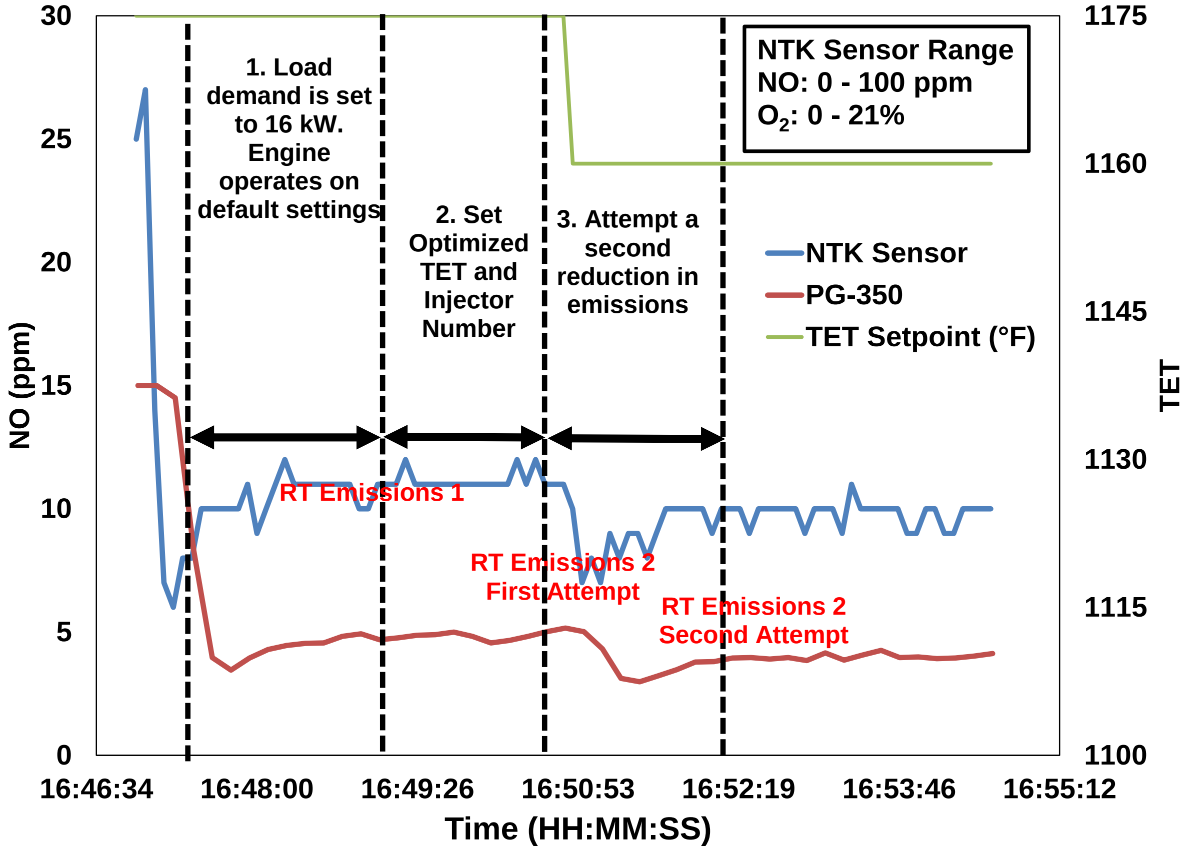


Source: UC Irvine

**Figure 23: 16 kilowatt Oxygen Results**

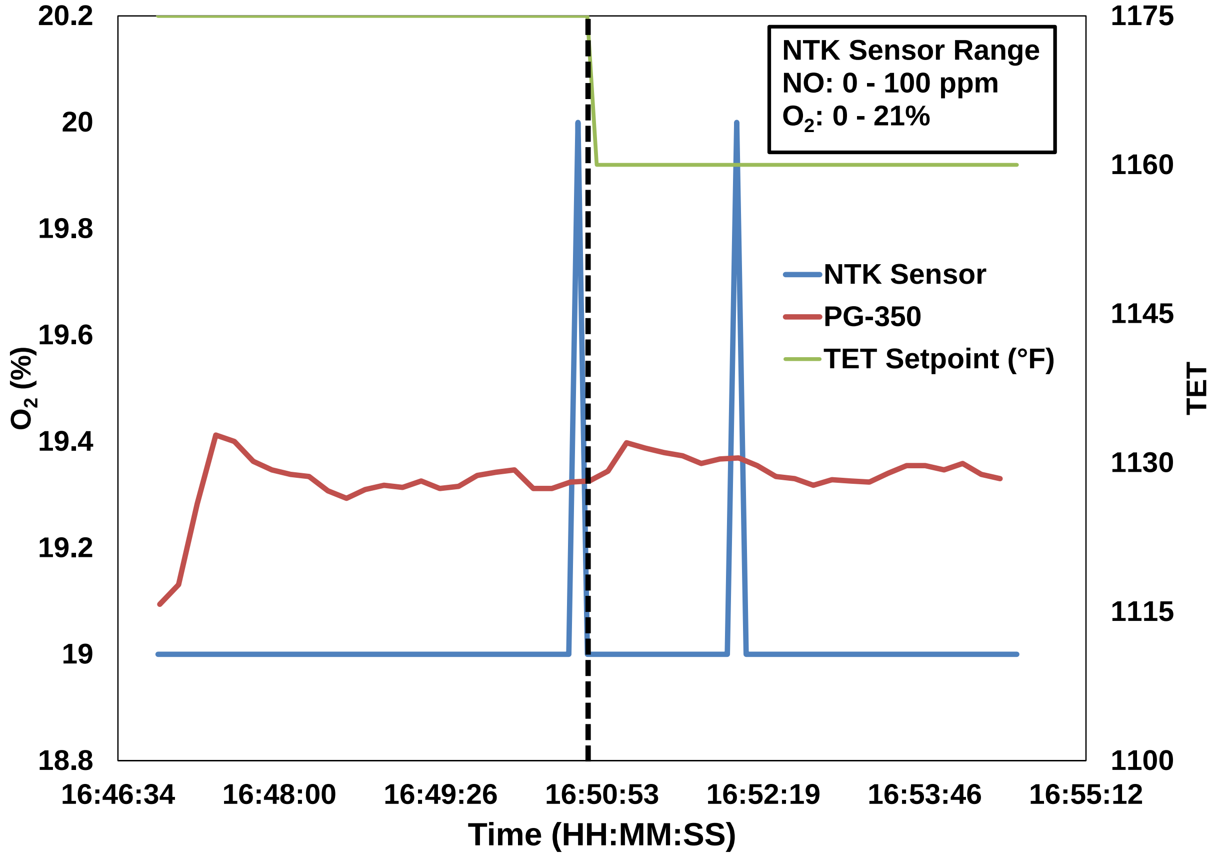


Source: UC Irvine

Figure 24: 16 Kilowatt Carbon Monoxide Results

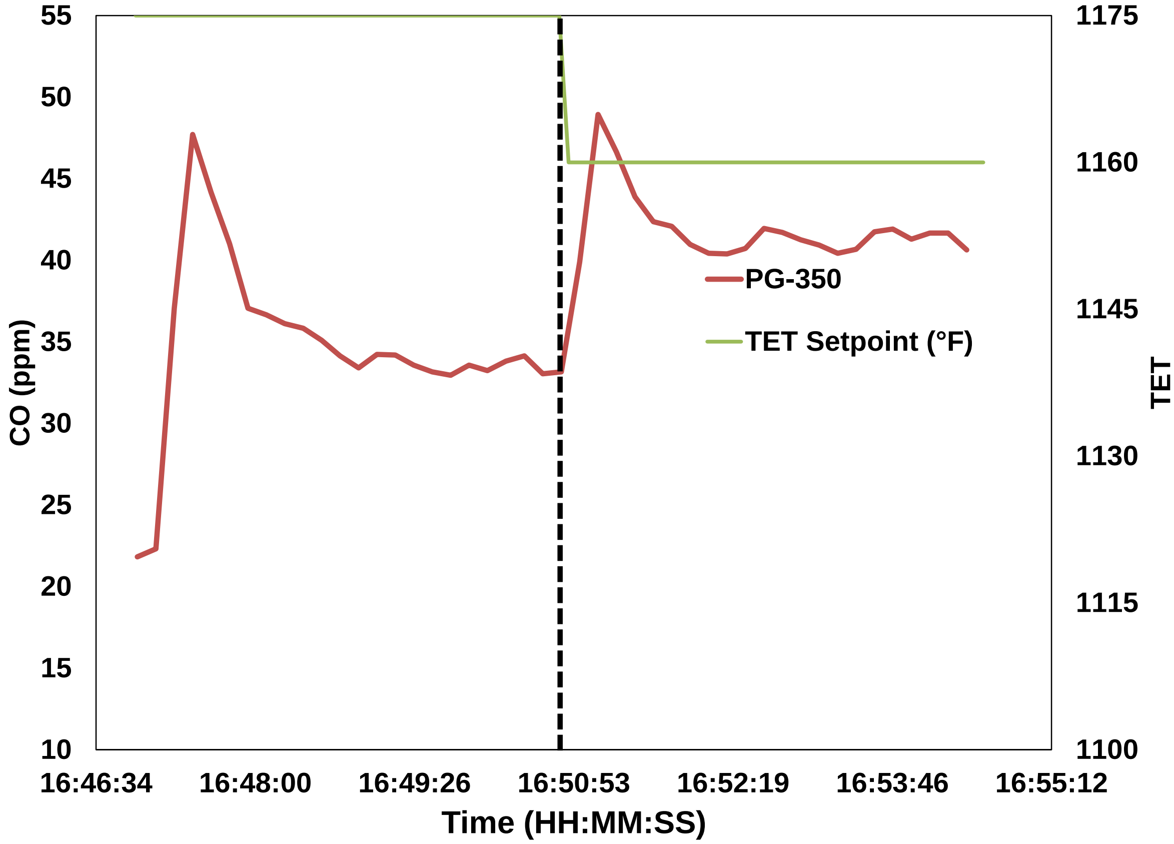


Source: UC Irvine

### 4.2.2 29 Kilowatt Results

Figure 25 – Figure 27 display the results for the 29 kW case. Note that from 14:54:14 – 14:57:07 the load had changed from 32 kW to 29 kW, so the algorithm had not reset to the initial logic. A minimum change of 5 kW is needed for control algorithm logic to start from the beginning. The first emissions measurements (RT Emissions 1) were taken sometime between 14:54:14 and 14:57:07.

Right before the 14:57:07 mark, a large spike is observed, which is measured as RT Emissions 2. Because the algorithm sees a large increase in NO, it attempts to correct it by lowering the TET by 15 degrees. A second and a third attempt also occur but eventually after the third attempt a reduction is seen and the algorithm continues to operate with the optimized settings.

The results for $O_2$ and CO are also displayed in Figure 26 and Figure 27. The sensor reports higher $O_2$ percentages than the PG-350 for this case. The CO results are also indicative of a change of TET as the emissions rise from approximately 140 – 160 ppm.

**Figure 25: 29 Kilowatt Nitric Oxide Results**

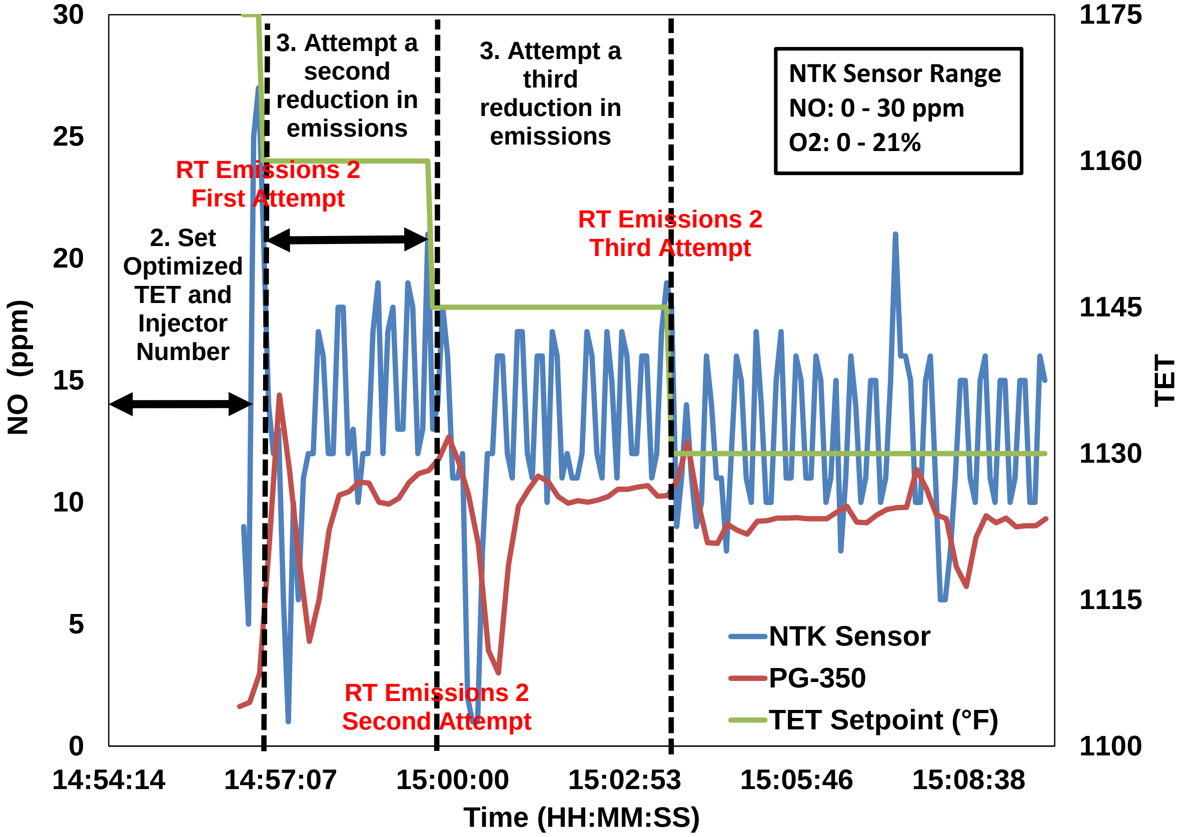


Source: UC Irvine

Figure 26: 29 Kilowatt Oxygen Results

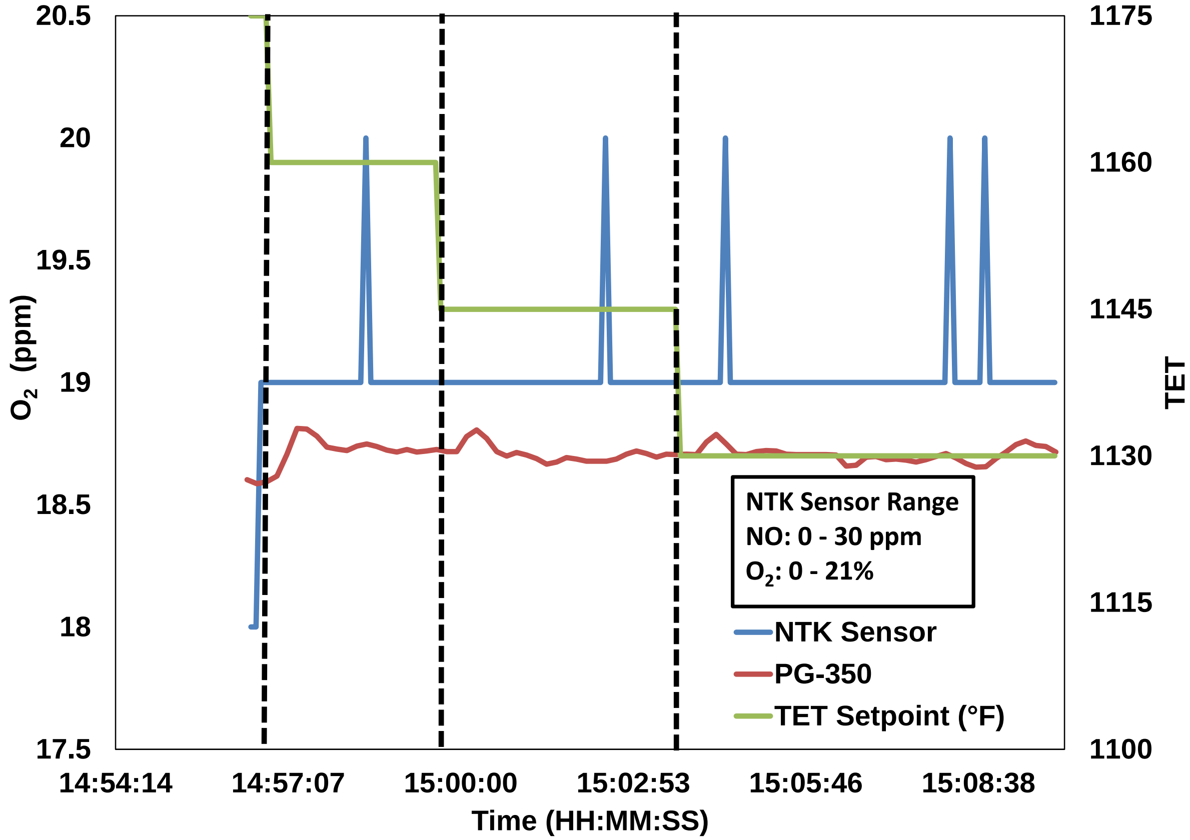


Source: UC Irvine

**Figure 27: 29 Kilowatt Carbon Monoxide Results**

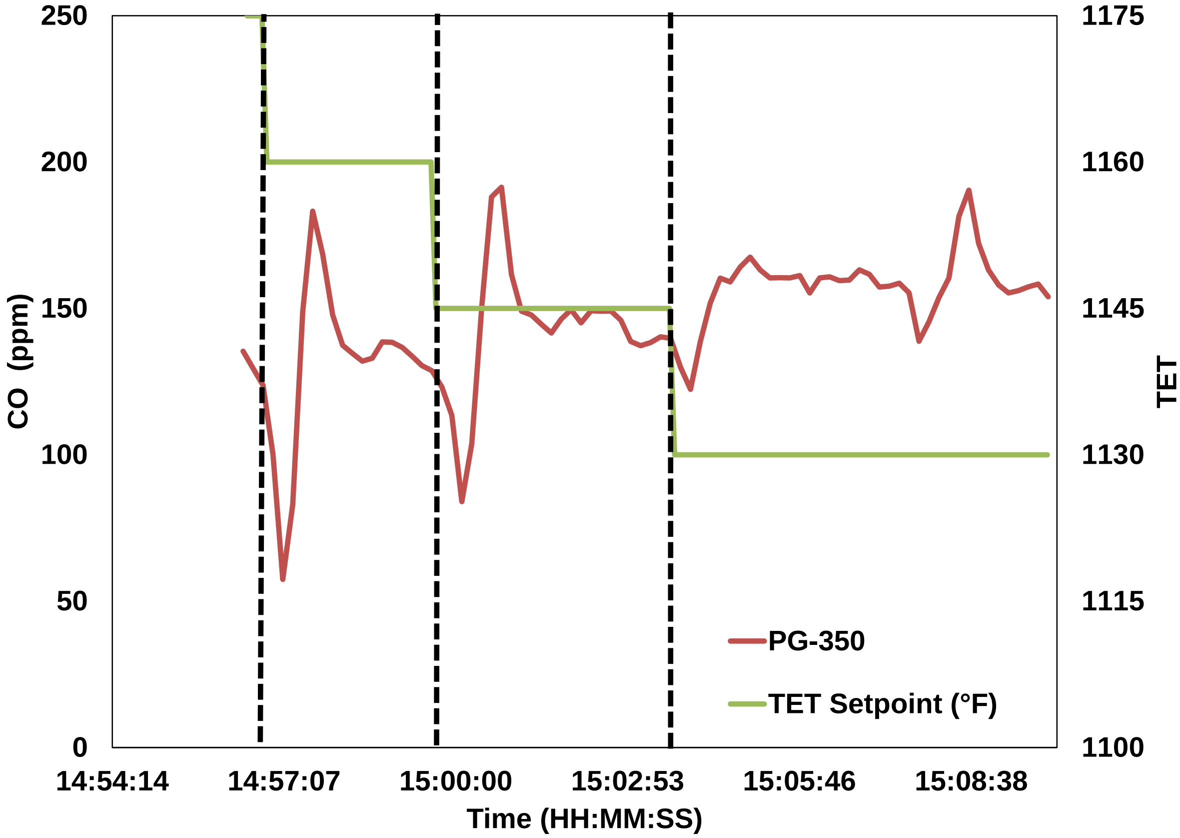


Source: UC Irvine

## 4.3 Summary of Control Algorithm Demonstration

Using the control algorithm logic developed in Technical Task 3 (Control Algorithm #1), a Capstone engine software codeset and hardware package were developed with the assistance of Capstone Turbine Corporation and EmiSense to demonstrate the ability of Control Algorithm #1 to successfully use the feedback of the NTK sensor to lower NO emissions in real time. After loading the codeset and sending the analog output of the sensor to the engine communications bay, the algorithm was able to successfully demonstrate that it could effectively lower NO emissions by lowering the TET and injector staging and subsequently use the feedback from the sensor to determine if further corrections were needed.

Because of the successful completion of the final Technical Task, the NTK sensor and control logic developed in Technical Task 3 represent a viable alternative to traditional CEMS for monitoring and certifying emissions performance for DG in California. The coupling of the sensor with the control algorithm represents an inexpensive and viable approach to helping improve the existing certification procedure.

# CHAPTER 5: Discussion of Benefits

## 5.1 Overview of Benefits

This section details the findings from the midterm benefits project questionnaire. Because the NTK sensor (coupled with the control algorithm logic and associated feedback from the sensor) represents a viable approach to traditional CEMS, it is important to highlight the benefits and associated cost of using this technology versus employing traditionally expensive, albeit ARB certified, equipment for monitoring and emissions certification. The scenario presented in this case is one of many possible scenarios in which this technology can be used as a NO reduction strategy for DG devices.

## 5.2 "Business as Usual"

If "business as usual" were to be conducted for DG devices in California, dispatchable generation (that is, microturbines and rotary engines) would continue to generate power without any control technology to minimize emissions — specifically nitric oxide — at most, if not all, operating conditions. As was discussed in the introduction section of this report, DG sold in California undergoes a certification procedure (as outlined by the California Air Resources Board) to facilitate the deployment of clean (low polluting) devices in the state. The current standards were first established in 2003, with further amendments passed in 2007. Since 2007, fossil-fueled distributed generation has been certified to an emissions standard of .07 pounds per Megawatt-hour (lb/MW-hr) for NOx, .10 lb/MW-hr for CO, and .02 lb/MW-hr for VOCs. In 2013, the 2007 standards were also adopted for DG operating on renewable fuels (digester gas, landfill gas, and oil-field waste gas) to help meet the state's goal of mitigating greenhouse gas (GHG) emissions while also lowering criteria pollutants.

Figure 28 (first shown in Chapter 2), shows the NOx emissions as a function of load for the Capstone microturbine generator (MTG) employed as the representative DG device in this project. This microturbine represents one in the fleet of California MTGs that collectively generate 50 MW. The device (certified under the 2003 ARB requirements) was operated at the UCI Combustion Laboratory and emissions were collected with the HORIBA PG-350 analyzer. For more information on this, please refer to Chapter 2 and Appendix A with the associated testplan. To estimate the total criteria pollutant emissions reduction for the 50-MW fleet using inexpensive solid-state NO sensors as monitoring devices and as corrective tools for reducing NO emissions, it is pertinent to establish a baseline scenario.

Figure 29 shows the California ISO "duck curve" chart (previously shown in Chapter 2) that illustrates the current situation regarding growing renewable penetration in California. In a baseline scenario with high renewable penetration throughout the state (as it is now in 2018), it is likely the MTG will have to be operated at full load part of the day when renewable generation is low, such as at night or in the early morning (4:30 A.M. – 10:00 A.M. and 11:30 P.M. – 4:30 A.M.); at part-load when renewable penetration just starts to increase in the late morning (10:00 A.M. – 12:00 P.M.), and when it decreases during the early evening (7:30 P.M. – 11:30 P.M.); and at the lowest loads when renewable penetration peaks (12:00 P.M. – 7:30 P.M.). Assuming the MTG spends a third of its time in a typical day operating in each of the established cases, the device would operate at full load (60 kW) for eight hours, at the lowest loads (10kW – 22 kW) for eight hours, and at part load (22 kW – 38 kW) for eight hours.

**Figure 28: Nitric Oxide/Nitrogen Dioxide vs. Load for Capstone C-60 Microturbine Generator**

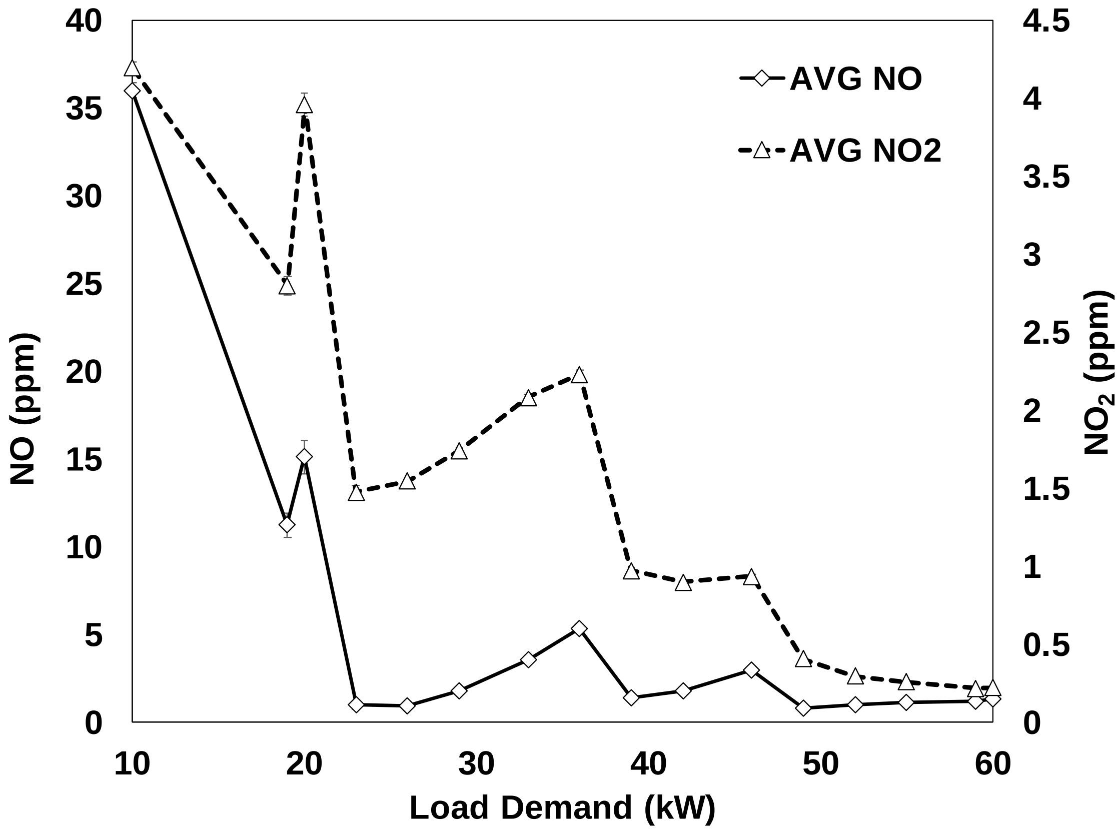


Source: UC Irvine

**Figure 29: California Independent System Operator "Duck Curve" Chart**

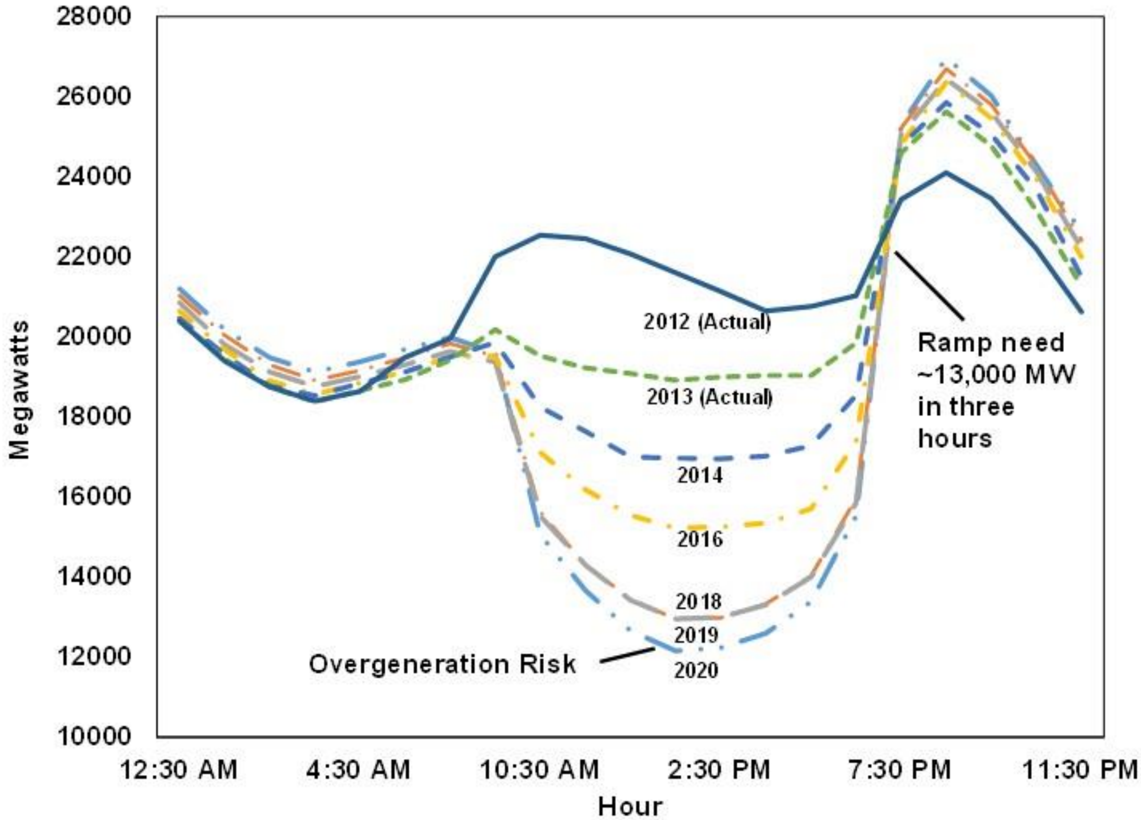


Source: UC Irvine, adapted from California Independent System Operator.

Using Figure 28 to estimate the total emissions from the 50-MW fleet, at full load it would be expected that the MTG would emit between 0 – 2 ppmvd NO (1 ppmvd average), at part load 0 – 5 ppmvd NO (2.5 ppmvd average), and at the lowest loads between 35 ppmvd to 15 ppmvd (25 ppmvd average) while operating on natural gas. Using the recorded air and fuel flow rates of the Capstone C-60 MTG at 60 kW (3905 lb/hr of air and 17 lb/hr fuel), at 29 kW (3000 lb/hr of air and 20 lb/hr of fuel), and at 16 kW (2308 lb/hr air and 13 lb/hr fuel), it is estimated that one-half ton of NO would be produced per year per turbine (mostly from operation at 16 kW) if operating 365 days a year in the way previously described (eight hours at each load condition): .028 tons/year are produced at 60 kW, .054 tons/year are produced at 29 kW, and .42 tons/year are produced at 16 kW. This corresponds to 415 tons of NO per year emitted in California from the 50-MW MTG fleet, assuming the entire fleet is composed of Capstone C-60 engines.

## 5.3 NO Reduction with Solid-State Sensors Strategy

Figure 30 and Figure 31, shown previously in Chapter 4, show the emission reductions that were observed when using the solid-state NO sensor as a feedback device for the Capstone C-60 MTG. These reductions were observed at 29 kW and 16 kW, since the emissions at full-load were already minimized. For the 16-kW case, a 10 percent reduction of NO was observed when comparing RT Emissions 1 (approximately 10 ppm) with RT Emissions 2 on the second attempt (approximately 9 ppm). For the 29-kW case, a 10 percent reduction was similarly observed when comparing RT Emissions 2 (approximately 15 ppm) with RT Emissions 2 on the third attempt (approximately 13 ppm). Assuming a 10 percent reduction in emissions would remain fixed for 29 kW and 16 kW at all times, this corresponds to .45 tons of NO per year per engine. The reduction for one engine would be .05 tons per year. For all the target adopters (California's fleet of MTGs collectively generating 50 MW), this corresponds to roughly 376 tons per year, a reduction in 39 tons per year of NO if a 10 percent improvement in performance was achieved. Appendix C details the calculations used to arrive at these numbers.

This strategy represents an effective approach to minimizing emissions at part load where emissions performance is typically poor and where it is not monitored under the current certification procedure. About 85 percent of the total emissions in this strategy comes from the NO that is produced at part load. With renewable penetration increasing each year, the need for dispatchable devices to operate at part load will increase, and the effective tons of NO that are mitigated will continue to increase. This strategy will only become more viable and practical with time.

**Figure 30: 16 Kilowatt Emissions Reduction**

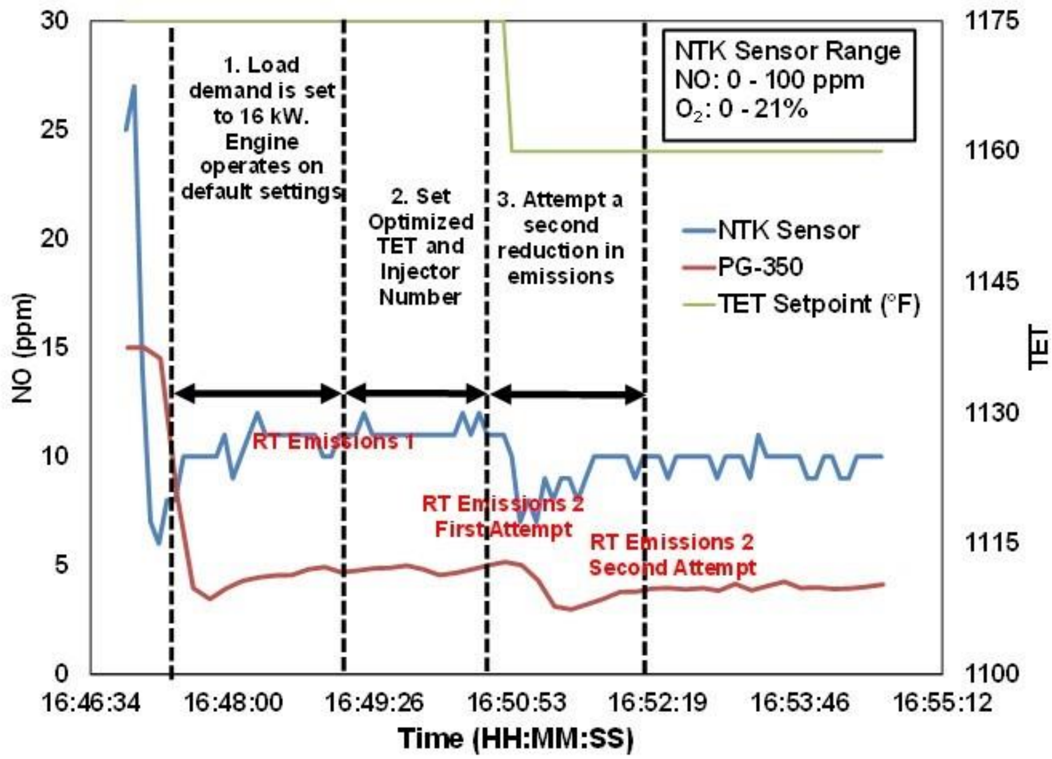


Source: UC Irvine

**Figure 31: 29 Kilowatt Emissions Reduction**

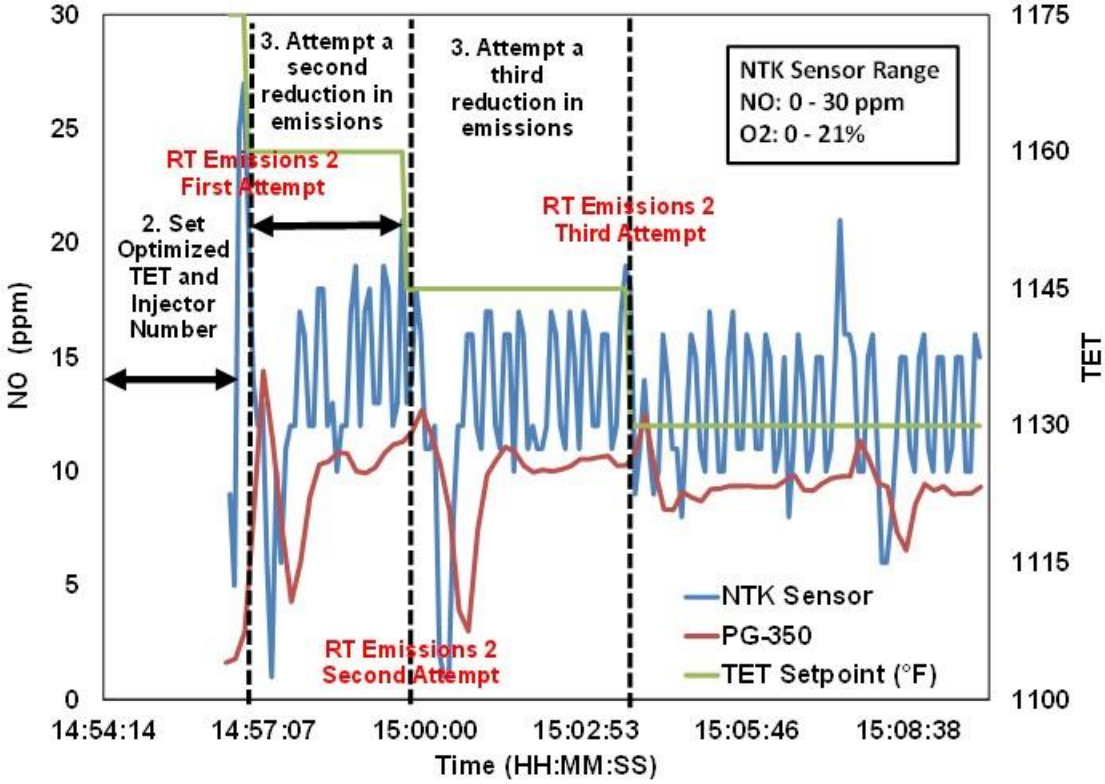


Source: UC Irvine

## 5.4 Cost of Strategy

The cost of using this strategy represents a one-time fixed capital cost as well as an annual operation cost to replace the sensor. Woo and Glass (2012) established that the ideal solid-state sensor technology would last for 150,000 miles (in an automotive vehicle) or a 10-year period. For UCICL, the one-time incremental cost to develop the solid-state sensor package (sensor box, analog-output PCB, and sensor integration with engine) amounted to approximately $2,000. Assuming a discount rate of 5 percent and an economic life of 10 years for each sensor, the present value of the one-time incremental cost amounts to $9,722. This also amounts to a one-time annualized cost of $1,259 every 10 years.

When comparing these combined costs to the cost of traditional CEMS analyzers and equipment, the savings is significant. Table 25 displays the one-time incremental costs associated with traditional emission monitoring analyzers. These are commonly used within the power generation industry as monitoring devices for systems with a nameplate capacity of 25 MWe or greater. Note that these are solely upfront capital costs that do not take into account the annualized cost, maintenance cost of installing the equipment, or the other equipment needed to complete the CEMS package. For a typical CEMS NOx extractive analyzer (capable of only measuring NO/$NO_2$) that adheres to established U.S. EPA and ARB sampling methods, the cost is $10,440 (greater than $15,000 accounting for inflation between 2000 and 2018). Note that this analyzer is also extractive and not in-situ, so it also requires additional equipment for proper sample conditioning and extraction.

Note that this closed-loop control strategy uses parameters in which the engine operates to minimize the NO emissions. It does not employ the use of other control strategies such as selective catalytic reduction found in diesel vehicles. This allows for significant cost savings and does not alter the configuration or performance of the engine in a significant manner compared to the current setup.

**Table 25: Default Analyzer and Monitor Equipment Costs for Continuous Emission Monitoring Systems ($)**

| Pollutant or Parameter | Extractive | In-situ | FTIR |
|---|---|---|---|
| Gaseous Compound Analyzers | | | |
| $NO_x$ | 10,440 | N/A | N/A |
| $SO_2$ | 12,500 | 35,000 | N/A |
| CO | 8,490 | 28,000 | N/A |
| $CO_2$ | 7,890 | N/A | N/A |
| $O_2$ | 5,860 | 6,600 | N/A |
| THC | 10,200 | N/A | N/A |
| HCl | 12,390 | N/A | N/A |
| $SO_2/NO_x$ | N/A | 37,000 | N/A |

Source: EPA [7]

# CHAPTER 6: Conclusions and Recommendations

The University of California, Irvine Combustion Laboratory successfully completed three technical tasks as part of a CEC-funded project (EPC-15-062) to demonstrate the viability of using inexpensive solid-state nitric oxide sensors (commonly used in the automotive industry as an integral part of selective catalytic reduction systems), coupled with closed-loop control logic, to monitor and minimize the NO emissions from dispatchable generation. Several conclusions were drawn from the technical tasks:

- The solid-state sensors represent a viable approach to traditional continuous emissions monitoring instruments for monitoring the emissions performance of dispatchable generation devices. Although the NTK sensor performed more comparably to the established referee instrument (PG-350) with a 99 percent confidence interval or greater for three of the five measured sensor characteristics, both devices followed similar measurement trends compared to the PG-350 analyzer. Both sensors achieved faster response times and proved to be robust and accurate over the entire testing period.
- The successful demonstration of the closed-loop algorithm control and the 10 percent reduction in NO observed across two different test cases (16 kW and 29 kW) show that the sensor, coupled with the control logic, represents a viable approach to using traditional CEMS to monitor and correct the emissions performance of DG systems in real time.
- Using the sensors and associated logic of the control strategy is an inexpensive solution to amending the current certification procedure for DG systems. Because the current certification procedure does not account for emissions performance at part load, using the solid-state devices and control logic strategy will benefit the health of Californians by reducing NO emissions at part load where emissions are typically poor. Using current CEMS equipment and analyzers would not be a cost-effective strategy to improve the current standards.

The research team recommends use of the NTK sensor and associated control algorithm developed for this project in California’s MTG fleet. A similarly robust, accurate, high-temperature CO sensor capable of providing feedback to the control algorithm (CO ppm) is also recommended, thus enabling real-time adjustments to reduce both CO and NO.

# REFERENCES


[1]California Independent System Operator, "California ISO : What the Duck Curve Tells us About Managing a Green Grid," p. https://www.caiso.com/Documents/FlexibleResourcesH, 2016.

[2]"Distributed Generation Certification Program," 2003.

[3]O. US EPA, "EMC: Continuous Emission Monitoring Systems." [Online]. Available: https://www.epa.gov/emc/emc-continuous-emission-monitoring-systems. [Accessed: 23-Jan-2018].

[4]L. Y. Woo and R. S. Glass, "NOx Sensor Development LLNL-TR-461511," 2010.

[5]D. MacDougall *et al.*, "Guidelines for Data Acquisition and Data Quality Evaluation in Environmental Chemistry," *Anal. Chem*, vol. 52, pp. 2242–2249, 1980.

[6]L. Woo and R. Glass, "NOx sensor development LLNL-PRES-536931," 2012.

[7]D. C. Mussatti, M. Groeber, D. Maloney, W. Koucky, and P. M. Hemmer, "EPA - Section 2: Generic Equipment and Devices, Chapter 4: Monitors," 2000.

# LIST OF ACRONYMS

| Term | Definition |
|---|---|
| ANOVA | Analysis of variance |
| California ISO | California Independent System Operator |
| CEMS | Continuous emissions monitoring system |
| CO | Carbon monoxide |
| CRMS | Capstone Remote Monitoring Software |
| DAQ | Data acquisition equipment |
| DG | Distributed generation |
| DOEx | Design of experiments |
| GPM | Gallons per minute |
| Hz | Hertz |
| kW | Kilowatts |
| lb/MW-hr | Pounds per megawatt-hour |
| LDL | Lower detectable limit |
| MTG | Microturbine generator |
| MW | megawatt |
| mWe | Megawatts electric |
| NO | Nitric oxide |
| Nox | Oxides of nitrogen |
| O2 | Oxygen |
| PM | Particulate matter |
| Ppm | Parts per million |
| Ppmvd | Parts per million by volume, dry |
| Psi | Pounds per square inch |
| scf | Standard cubic feet |
| SCAQMD | South Coast Air Quality Management District |
| TET | Turbine exit temperature |
| UCICL | Combustion Lab at the University of California, Irvine |
| VOCs | Volatile organic compounds |

# APPENDIX A
# Technical Task 2 Test plan

## EPC-15-062 Technical Task 2 Test Plan

### Introduction

As part of a research project funded by the California Energy Commission Grant EPC-15-062, the Combustion Lab at the University of California, Irvine will be installing solid state NO sensors in the exhaust of a C-65 Capstone Microturbine to measure NOx levels. The University of California, Irvine will be responsible for performing a robustness test on each of the candidate sensors as well as monitoring the output over an extended period of testing. These solid-state sensors will be measured against a CEMS instrument (continuous emission monitoring system), such as the Horiba PG-350. Data will be collected and analyzed to determine the sensor that best matches the output and characteristics of the referee analyzer according to:

- Non-Linearity
- Precision
- Lower Detectable Limit
- Concentration Resolution
- Lag Time and Rise Time

### Candidate Sensors, Referee Instruments, Data Acquisition Equipment

The sensors and referee instruments are shown in Figure A-1.

**Figure A-1: Equipment**

| Equipment | Type | Description | Quantity |
|---|---|---|---|
| Sensors | NTK Nox | NTK Sensor | 3 |
| | UniNOx | Continental Sensor | 3 |
| | NOxTrac | CoorsTek Sensor | 3 |
| Referee Instrument | PG-350 | Horiba CEMs Equipment | 1 |
| | PG-250 | Horiba CEMs Equipment -> for other calibration range | 1 |
| Engine | C-65 | Capstone Microturbine, 65 kW | 1 |


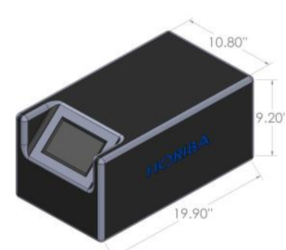


Source: UC Irvine

The primary referee analyzer (Horiba PG 350) has the following specifications and established measurement procedures incorporated (see Table A-1):

**Table A-1: Horiba PG-350 Specifications**

| Species | NOx | O2 |
|---|---|---|
| Measurement Range | 0 -25/50/100/250/500/1000/2500 ppm | 0-5/10/25 vol% |
| Accuracy | ± 0.5 % of full scale; ± 1.0 of full scale for NOx ≥ 100 ppm | ± 0.5 % of full scale |
| Measurement Principle | Cross-Flow Chemiluminescence Detection Method | Galvanic Method; Paramagnetic Method for EU only |
| Method | EPA Method 7E | EPA Method 3A |
| Response Time | 45 sec or less | 45 sec or less |
| Drift | ± 1.0 % of full scale/day | ± 1.0 % of full scale/day |

Source: UC Irvine

Each sensor can handle a maximum exhaust gas temperature of 800 °C (950 °C for 100 hours).

## Proposed Testbed Layout

Pictured in Figure A-2 is a proposed layout of the Test Bed. An exhaust duct will start out from the top of the C-65 Capstone casing and make its way down to a horizontal section. At this section, a sample line(s) will be installed which leads back to the referee instrument(s) in a designated data acquisition (DAQ) control room. The sensors installed in the horizontal section will send their signal along a CAN-Bus line back to the DAQ room.

Assuming a colder day (and at nights), the exhaust length of the Capstone engine will need to be a minimum length of 22 feet for fully developed flow.

A designated DAQ room will include equipment for both monitoring and storing data from the sensors as well as the referee instrument(s) that will be used. Figure A-3 shows a schematic of the sensor and the flow of communication from the sensor on the Controller Area Network (CAN-Bus). Each sensor provided from CoorsTek will include a power supply and device used for signal conditioning. A device that converts CAN-Bus to USB will be used to connect the CAN-Bus to a computer. Labview software and designated VI's will be used to monitor all the signals on a single graph. This data will subsequently be used later for analysis.

## Figure A-2: Test Bed Layout

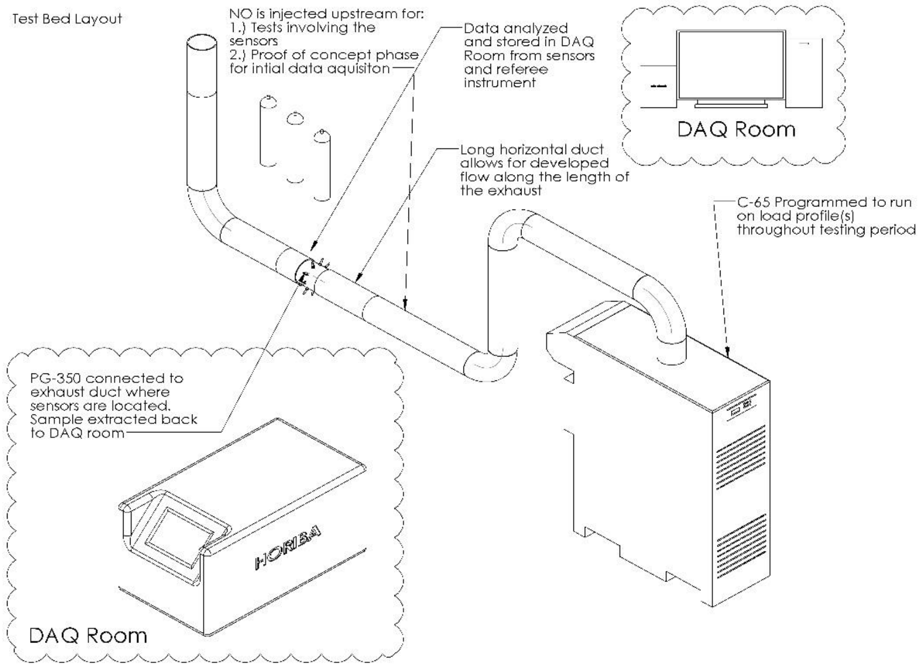


Source: UC Irvine

## Figure A-3: Data Acquisition Equipment Room

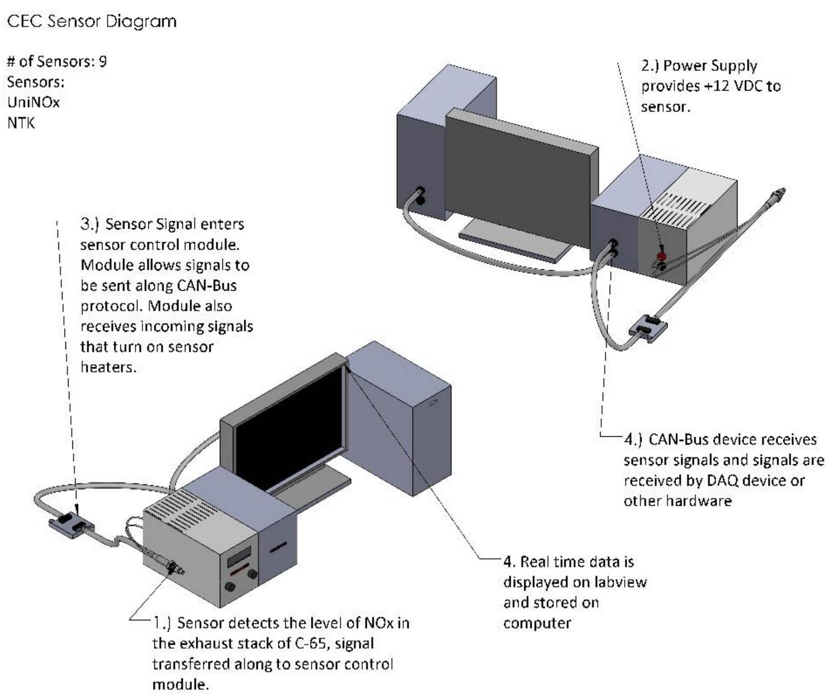


Source: UC Irvine

**Figure A-4: Horizontal Duct Arrangement**

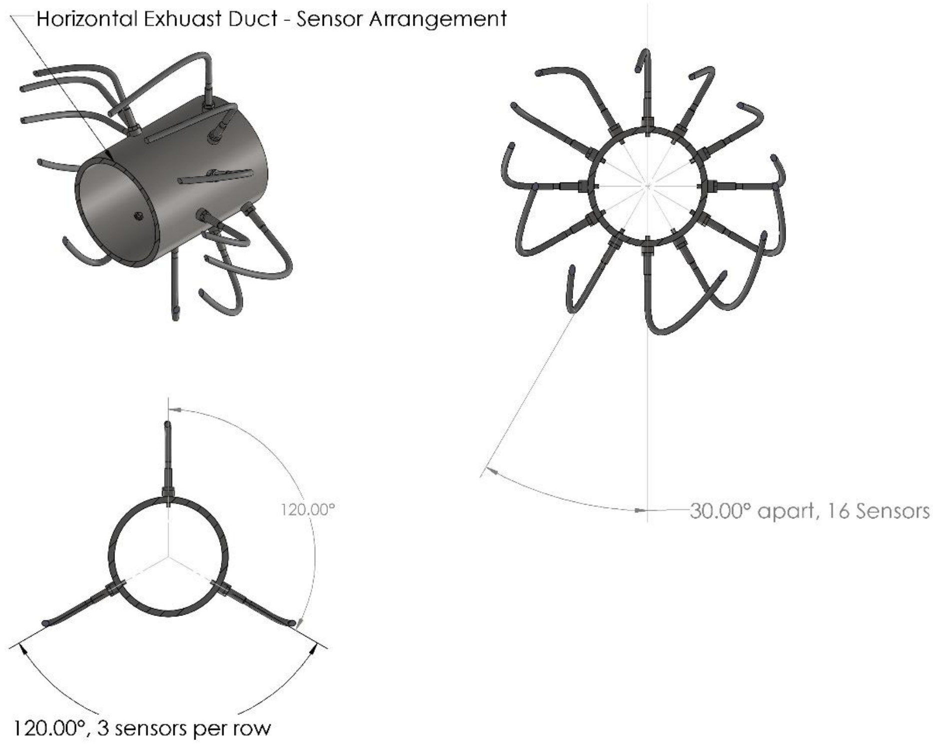


Source: UC Irvine

### Installation Configuration:

The solid-state electrochemical sensors will be installed in the exhaust stack of a Capstone C-65 Microturbine Engine. A total of 9 sensors will be installed (3 NTK sensors, 3 UniNOx sensors, 3 NOxTrac sensors), all along a horizontal section of the exhaust duct.

Sensors will installed in the following configuration.

- 3 sensors installed in each plane, 120° apart from one another
- Each plane will be equidistant from one another
- Adjacent sensors from each consecutive plane will be spread out 30° from one another
- Sensor configuration allows up to 16 sensors to be installed on exhaust duct without affecting the flow upstream of another sensor
- Hardware provided allows for up to 16 sensors on the same communication bus.

## Sensor Characteristics and Testing Approaches

Taken from ANSI/ISA–51.1–1979 (R1993) [7]:

- For each of the following static performance characteristics, the test equipment shall be allowed to stabilize under steady-state operating conditions. All testing shall be done under these conditions. The operating conditions which would influence the test shall be observed and recorded.
- The number of test points to determine the desired performance characteristic of each sensor should be distributed over the range. They should include points at or near (within 10%) the lower and upper-range values of each sensor. There should not be

less than 5 sampling points and preferably more. The number and location of these test points should be consistent with the degree of exactness desired and the characteristic being evaluated.

- Prior to recording observations the device under test shall be exercised by a number of full range traverses in each direction.
- At each point being observed the input shall be held steady until the device under test becomes stabilized at its apparent final value.
- Tapping or vibrating the device under test is not allowed unless the performance characteristic under study requires such action (*vibration due to engine running is unavoidable*).

**Figure A-5: Calibration Curve [7]**

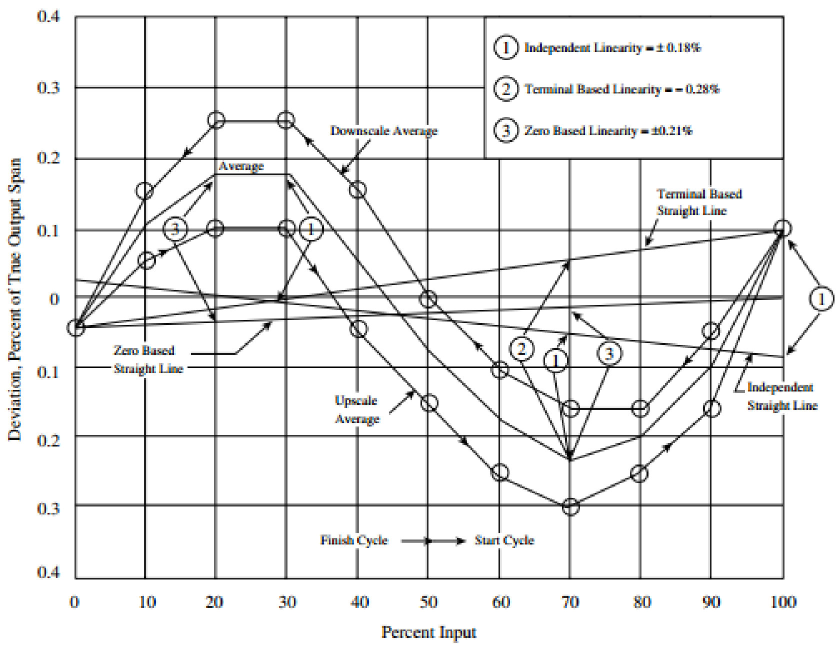


Source: UC Irvine

Calibration Cycle: First step for each sensor characteristic is to produce a calibration cycle:

- Maintain test conditions and precondition the test device as indicated above.
- Observe and record output values for each desired input value for one full-range traverse in each direction starting near mid-range value.
- Final input must be approached from the same direction as the initial input.
- Apply the input in such a way as to not overshoot each input value.

Calibration Curve: Then use the calibration cycle to produce a calibration curve:

- Determine the difference between each on served output value and its corresponding ideal output value.
- Present difference (deviation) as percent of ideal output span.
- Plot deviation vs. input

Linearity: The closeness to which the output approximates a straight line. This is usually measured as nonlinearity and expressed as linearity (the maximum deviation between an average curve and a straight line). Linearity can be expressed three ways: independent linearity, terminal based linearity, or zero-based linearity. We will use the independent based linearity in our definition and analysis [7].

We will measure the non-linearity of each sensor according to:

$$Nonlinearity_{Independent}(\%) = \frac{D_{in\,(Max)}}{IN_{f.s}} \cdot 100 \qquad [1]$$

$D_{in(Max)}$ *Is the maximum deviation (equal at several points)?*
$IN_{f.s.}$ *Is the maximum, full scale input*

**Figure A-6: Linearity**

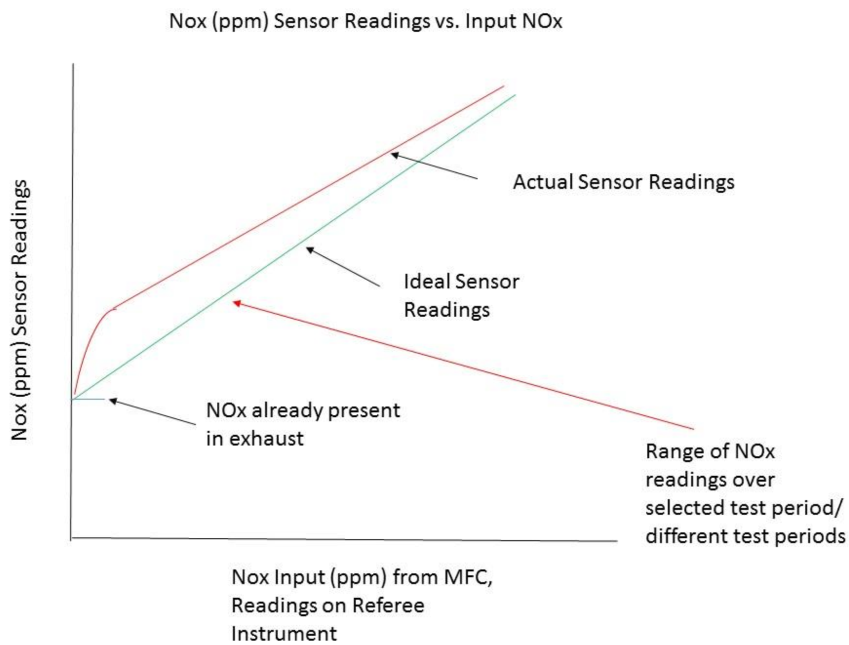


Source: UC Irvine

Proposed Test Approach: To best reflect the linearity from each of the sensors, the following steps should be performed [7]. The following are steps in accordance with procedures set forth by the ANSI in ANSI/ISA–51.1–1979 (R1993)

- Plot a deviation curve, which is the average of the corresponding upscale and downscale output readings.
- Draw a straight line through the average deviation curve so as to minimize the maximum deviation (independent linearity). It is not necessary that the straight line be horizontal or pass through the end points of the average deviation curve.
- Find the maximum deviation over the input span you have used.
- Find the nonlinearity percentage for each sensor.

Precision: According to ISO 5725, precision is the closeness of agreement among a set of results [8]. This refers to the degree of reproducibility in the output readings, and the stability of the instrument with regards to readings [1]. It is a measure of dispersion or scattering around the mean value and usually expressed in terms of standard deviation, standard error or a range (difference between the highest and the lowest result) [2].

Proposed Test Approach: To best reflect the precision characteristics of each sensor, we will follow the steps outlined in ANSI/ISA–51.1–1979 (R1993) for repeatability that will also help us determine precision. It may be determined directly from the deviation values of a number of calibration cycles [7].

- Perform a number of calibration cycles as described under "Calibration Cycle."
- Prepare a calibration curve based on the maximum difference between all upscale and downscale readings for each input observed. The deviation values are determined from the number of calibration cycles performed from step 1 above.
- Maintain the test device in its regular operating condition, energized and with an input test signal applied.
- At the end of the specified time, repeat steps 1 and 2.
- Find the maximum difference between recorded output values (both upscale and downscale) for a given input value
- Report precision as a percentage of output span (for both upscale and downscale). This will be the maximum deviation from ideal output in upscale and maximum deviation from ideal output in downscale (e.g. Precision in upscale direction is .05% of output span, precision in downscale direction is .06% of output span).

**Figure A-7: Precision**

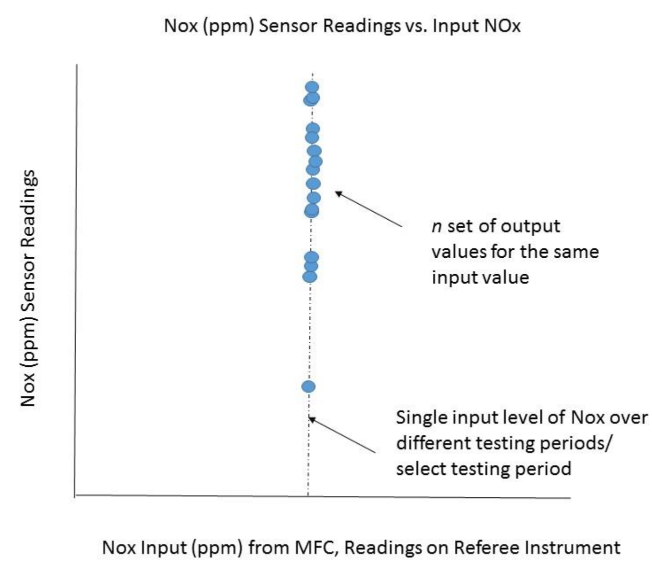


Source: UC Irvine

Lower Detectable Limit: This is the lowest concentration level that can be statistically differentiated from the zero value with 99% confidence [5].

Proposed Test Approach: To best quantify the LDL, we will do the following:

- Measure signal from n samples points (n > 7) when the engine is not running (~0 ppm NOx present in exhaust).

- Compute the standard deviation of the measurements for a set amount of time
- Compute the average of the data set for a set amount of time.
- Compute the signal detection limit: $\mathrm{D.L.} = \sigma_{\mathrm{zero}} + 3 \cdot \mathrm{S.D.}_{\mathrm{zero}}$
- Record the time of testing, the engine load condition, as well as the number of data points taken for the LDL.

**Figure A-8: Lower Detectable Limit**

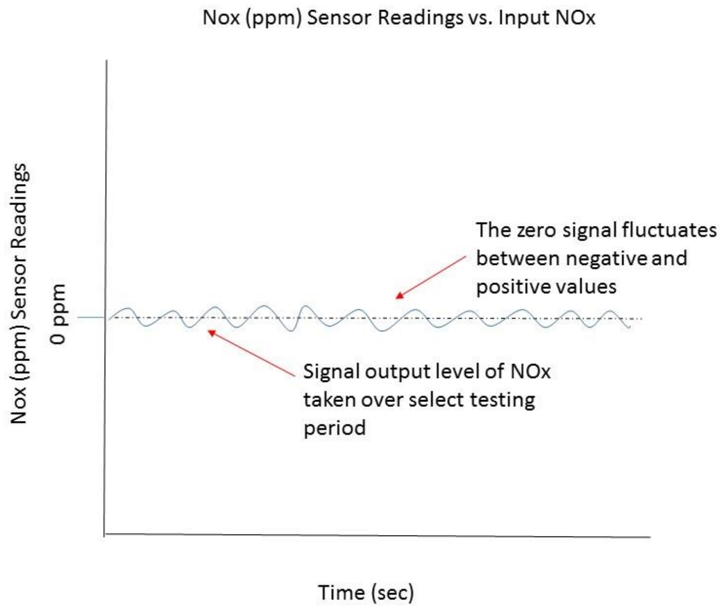


Source: UC Irvine

Concentration Resolution: The smallest detectable incremental change of input parameter that can be detected in the output signal. It is either a proportion of the full reading or reported in absolute terms [1].

Proposed Test Approach: To fully understand the resolution of the sensor, the following parameters must be identified for each sensor [9]:

- Resolution specification
- Bandwidth at which the resolution is obtained
- If any bandwidth filters are integral to the sensor
- Unit and type (P-P or RMS) of measure of the resolution specification

To calculate the P-P resolution:

- Record the output at any given input to the sensor over a given period of time. Make sure to record the input conditions as well as the duration of the test, as well as the number of samples taken.
- Determine the frequency and bandwidth at which the sampling data is being given.
- Analyze the data and determine the maximum peak-to-peak distance.

**Figure A-9: Concentration Resolution**

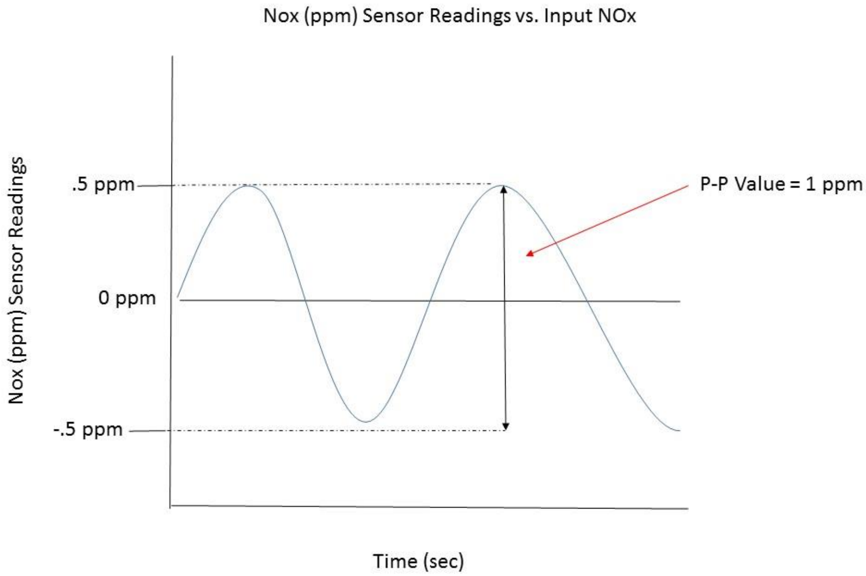


Source: UC Irvine

Lag Time and Rise Time: Rise time the time it takes to rise from 10% to 90% of the output signal step height. Lag time is the time taken to reach 10% of output signal step height [10].

In summary:

- $t_{Rise} = t_{.9 \cdot F.V.} - t_{.1 \cdot F.V.}$
- $t_{Lag} = t_{.1 \cdot F.V.}$

Where F.V. is the final value

Proposed Test Approach: In parallel with the proposed test approaches listed above, perform the following steps:

- Have designated Mass Flow Controller perform a step input increase in NO that produces a noticeable change in output signal on the sensor being tested. Make sure output signal on the sensor is able to reach a steady-state value before stepping down the input.
- Record testing duration and input conditions, as well as the step input value of the MFC.
- Analyze the data. Determine the rise time and lag time for the sensor at the specified step input value for the sensor.
- Determine an equation that relates change in step input to change in rise time and lag time (equation for time constant?).

**Figure A-10: Lag Time and Rise Time**

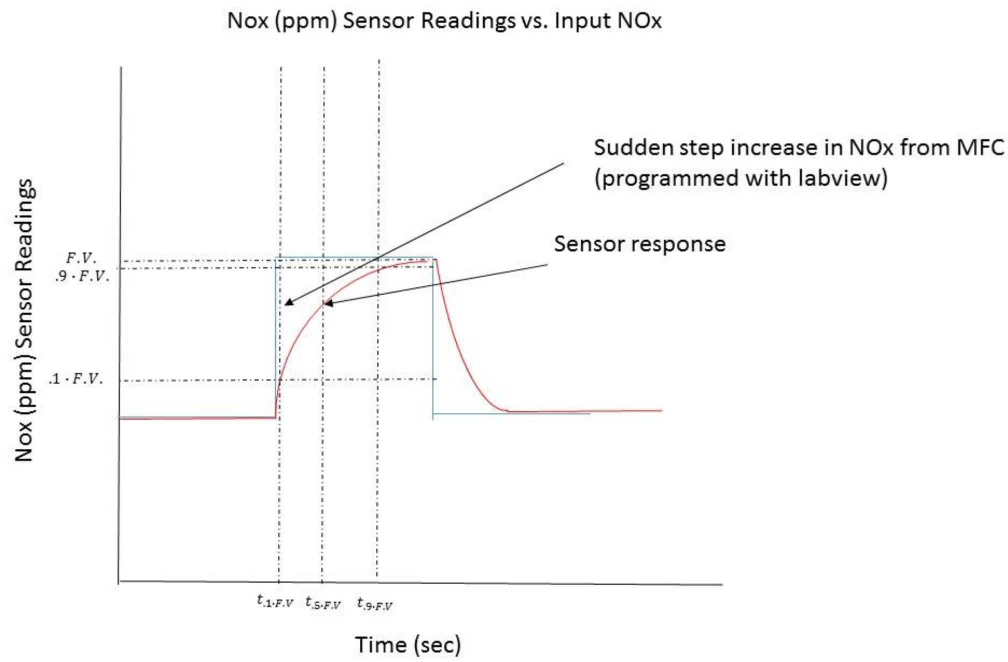


Source: UC Irvine

References:

- http://www.ni.com/white-paper/14860/en/
- http://www.fao.org/docrep/W7295E/w7295e08.htm
- http://www.ni.com/white-paper/4439/en/
- https://en.wikipedia.org/wiki/Transient_response
- https://en.wikipedia.org/wiki/Detection_limit
- http://www.lionprecision.com/definitions/resolution.html
- ftp://ftp.unicauca.edu.co/Facultades/FIET/DEIC/Materias/Instrumentacion%20Industrial/Instrument_Engineers__Handbook_-_Process_Measurement_and_Analysis/Instrument%20Engineers'%20Handbook%20-%20Process%20Measurement%20and%20Analysis/1083ch1_3.pdf
- https://en.wikipedia.org/wiki/Accuracy_and_precision#ISO_Definition_.28ISO_5725.29
- http://www.lionprecision.com/tech-library/technotes/article-0010-sensor-resolution.html
- https://www.iso.org/obp/ui/#iso:std:iso:10155:ed-1:v1:en:term:3.3.1.1

## Testing Procedure

An initial test will be conducted, followed by a test each week for the first month and followed by a test each month subsequent to the weekly tests. NOx injection test will be conducted in which NOx is introduced to the exhaust upstream of the sensors. Such a test will give greater control over input parameters that limit how we can test and quantify the characteristics of each sensor. We will:

- Inject while running the engine at steady state conditions (50 – 100% load). Record input conditions.
- Run injection tests at regularly scheduled intervals throughout testing period and determine if sensor characteristics change over time.
- CEMs equipment run during these scheduled tests. They will be calibrated before and after to account for drift. CEMS instruments will sample every 15 minutes during steady state operation and every 15 seconds during load profile testing.

This will allow us to test for the follow parameters listed:

- Linearity: Run the test approach as listed in section 1.4. Run in parallel with the CEMS instrument. Make sure NO is injected and diluted depending on which direction over the span you are trying to traverse. Make at least 7 measurements per input. Make sure incremental increases/decreases in input are as little as possible in each direction.
- Precision: Run the test approach as listed in section 1.4. Run in parallel with the CEMS instrument. Achieve data in parallel for linearity listed above.
- Lower Detectable Limit: Run the test approach as listed in section 1.4. Achieve data in parallel with Linearity and Precision listed above. Try to achieve as close to 0% of the full span as possible.
- Concentration Resolution: Run the test approach as listed in section 1.4. Achieve data in parallel with other characteristics listed above. Determine P-P distance at each input for at least 7 measurements per input.
- Lag Time and Rise Time: Run the test approach as listed in section 1.4. Designate mass flow controller to continually ramp NO injection up and down at a specified input span that is most easily achieved.

After these testing periods, the robustness test will be resumed and the load profile included below will be followed.

Load Profiles: The following load profile (Figure A-11 provided from Capstone will be used for our 6 months of testing.

## Figure A-11: Full Day Load Profile Data

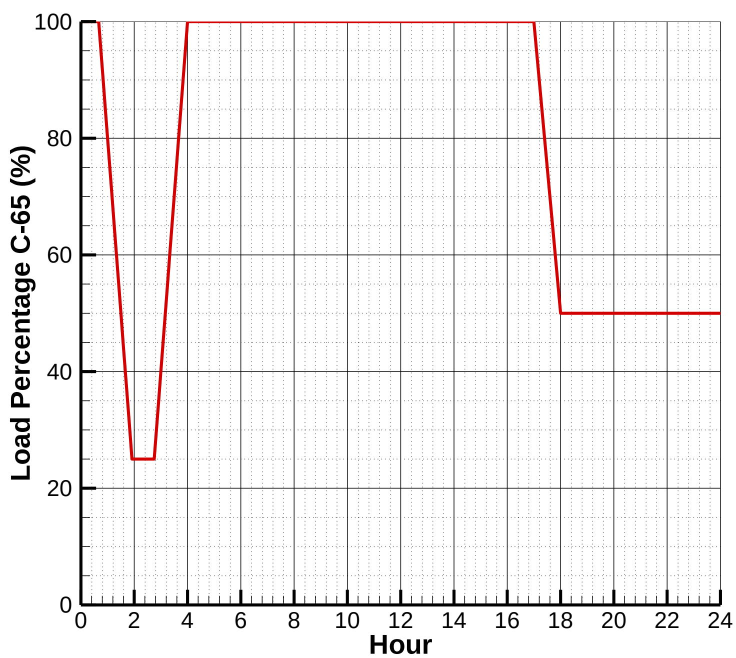


| Command | Load | Load | Dwell | Elapsed | Elapsed |
|---|---|---|---|---|---|
| | % | kW | min | min | hr |
| Start | | | | | |
| | 100% | | | | 0 |
| Load | 100% | 65 | 40 | 40 | 0.7 |
| Load | 95% | 62 | 5 | 45 | 0.8 |
| Load | 90% | 59 | 5 | 50 | 0.8 |
| Load | 85% | 55 | 5 | 55 | 0.9 |
| Load | 80% | 52 | 5 | 60 | 1.0 |
| Load | 75% | 49 | 5 | 65 | 1.1 |
| Load | 70% | 46 | 5 | 70 | 1.2 |
| Load | 65% | 42 | 5 | 75 | 1.3 |
| Load | 60% | 39 | 5 | 80 | 1.3 |
| Load | 55% | 36 | 5 | 85 | 1.4 |
| Load | 50% | 33 | 5 | 90 | 1.5 |
| Load | 45% | 29 | 5 | 95 | 1.6 |
| Load | 40% | 26 | 5 | 100 | 1.7 |
| Load | 35% | 23 | 5 | 105 | 1.8 |
| Load | 30% | 19 | 5 | 110 | 1.8 |
| Load | 25% | 16 | 5 | 115 | 1.9 |
| Load | 20% | 13 | 5 | 120 | 2.0 |
| Load | 15% | 10 | 5 | 125 | 2.1 |
| Load | 10% | 6 | 5 | 130 | 2.2 |
| Load | 5% | 3 | 5 | 135 | 2.3 |
| Load | 0% | 0 | 5 | 140 | 2.3 |
| Load | 5% | 3 | 5 | 145 | 2.4 |
| Load | 10% | 7 | 5 | 150 | 2.5 |
| Load | 15% | 10 | 5 | 155 | 2.6 |
| Load | 20% | 13 | 5 | 160 | 2.7 |
| Load | 25% | 16 | 5 | 165 | 2.8 |
| Load | 30% | 20 | 5 | 170 | 2.8 |
| Load | 35% | 23 | 5 | 175 | 2.9 |
| Load | 40% | 26 | 5 | 180 | 3.0 |
| Load | 45% | 29 | 5 | 185 | 3.1 |
| Load | 50% | 33 | 5 | 190 | 3.2 |
| Load | 55% | 36 | 5 | 195 | 3.3 |
| Load | 60% | 39 | 5 | 200 | 3.3 |
| Load | 65% | 42 | 5 | 205 | 3.4 |
| Load | 70% | 46 | 5 | 210 | 3.5 |
| Load | 75% | 49 | 5 | 215 | 3.6 |
| Load | 80% | 52 | 5 | 220 | 3.7 |
| Load | 85% | 55 | 5 | 225 | 3.8 |
| Load | 90% | 59 | 5 | 230 | 3.8 |
| Load | 95% | 62 | 5 | 235 | 3.9 |
| Load | 100% | 65 | 5 | 240 | 4.0 |
| Stop | | | | | |

### Testing Duration and Intervals:

- Each time the Capstone engine runs the load profile above it will run for the specified time
- The Capstone engine, once started, will be ramped up to 100% and then dwell there until steady-state conditions are achieved. Once in steady-state, the engine can now run the suggested load profile.
- Once the suggested load profile has been performed, the engine will run at 100% for the rest of the duration of the testing day.
- Engine will run testing profile once each day (excluding weekends), for 5 days a week.

- Engine will run at 100% load during the day, 50% load at night for 5 days a week, 24 hours a day.
- Testing will begin on the first startup of the Capstone C-65 and end 6 months later when the Capstone C-65 is brought to 0% load (shutoff).
- Testing with NOx injection will be scheduled at regular intervals throughout the testing period. A critical flow orifice will be used to control the injection.

**Data Acquisition, Test Data and Analysis:**

- Data will be taken for the duration of the testing period specified above, 24 hours per day for 5 days a week (excluding maintenance hours).
- Data will be taken from each sensor at a rate of 10 Hz
- Data will be taken from the referee sensor at a rate of 1 Hz
- Data taken before and after load profile is being performed will be stored as steady-state data.
- Data taken while load profile is being performed will be stored at transient data.
- Data will be analyzed using programs such as MATLAB and Excel
- Data will be stored on a DAQ designated computer and backed-up with an external hard drive.

**Sensors and Hardware, Referee Instrument Calibration:**

- A total of three sensors for each type of sensor (UniNOx, NTK, NOxTrac) will be provided to ensure statistically meaningful data is received.
- Two referee instruments will used during testing, one calibrated at low range and one calibrated at high range (ppm of NOx). During load profile testing, two sample lines will be running to both.
- Each referee instrument will be calibrated before and after the load profile is performed to help prevent calibration drift. They will also be calibrated at other select times throughout the day while the C-65 is at 100% load, once in the morning and once at night.

**Explanation**

The suggested load profile in Figure A-11 has several implications for our testing conditions. As the C-65 starts from 100% load percentage, ramping down to 25% load will allow for a full range of testing conditions for the sensor while left in situ.

As shown in, during the trial-run of the Uni-NOx sensor, a significant change in ppm of NOx can occur while the engine switches the number of injectors it is operating on. These types of change will give us the best conditions in which to perform the robustness test. Running the engine from 100% to 0% load will give us a better of idea of how the sensor performs over a wide range of different NOx levels and other conditions in the exhaust.

**Figure A-12: C-65 Data**

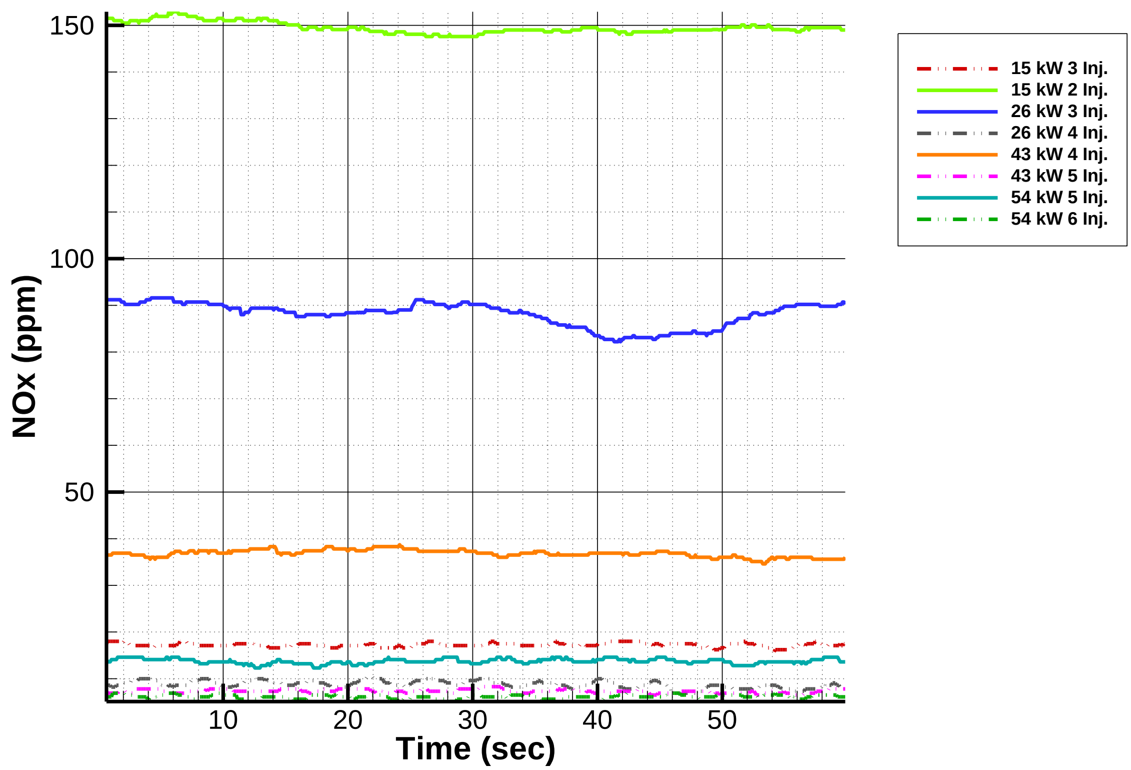


Source: UC Irvine

From the preliminary sensor data (UniNOx sensor), it becomes apparent that multiple referee instruments may be required for this test to ensure appropriate coverage of the expected NOx range. As more injectors are switched on, the need for a lower calibrated range NOx analyzer becomes our primary referee instrument, whereas for lower calibrated ranges both will be.

## Additional Comments and Questions

While this test plan incorporates some experiential results, some questions remain which will be addresses as testing commences. In some cases, assumptions/recommendations have been suggested.

1. Can CEMs instruments only be included in the NO injection phase? Will the data they provide during these stages give us enough information to make a well informed decision about which sensor is the best choice for integration in closed-loop control? Which sensor is the most robust?
2. How many Horiba CEMs equipment should we have calibrated? There are several ranges over which they can be calibrated.
3. Should the CEMs instrument be included in the whole test plan? Should they be extracting samples at all times?
4. How often should the referee instrument(s) be calibrated?
5. Will the NO injection test be the sole factor in determining the instrument characteristics? Other factors during the reliability test could be attributed to the decline in reliability and degradation of sensor measurement quality. Will these others factor remain unknown or should we try to determine their causes?

6. It is planned to exclude the CEMs instruments from the lag-time and rise-time test as they have internal delays that will inherently limit the response
7. How much data should be stored when the Capstone engine is running 100% load? How much data should be stored when the Capstone engine is running at 50% load? How well should we track input conditions during these times?

# APPENDIX B: Water Mole Fraction Calculation

Stoichiometric Balance

$$CH_4 + \alpha(O_2 + 3.76N_2) \rightarrow dCO_2 + bH_2O + cN_2$$

CHON:

C: $\mathbf{1 = d}$

H: $4 = 2b, \boldsymbol{b} = \mathbf{2}$

O: $2\alpha = 2d + b, 2\alpha = 2 + 2, \boldsymbol{\alpha} = \mathbf{2}$

Excess Air

$$CH_4 + 2\alpha(O_2 + 3.76N_2) \rightarrow CO_2 + 2H_2O + cN_2 + \boldsymbol{zO_2}$$

**O:** $\boldsymbol{4\alpha = 2 + 2 + 2z = 4 + 2z}$

$$2z = 4\alpha - 4, z = 2(\alpha - 1)$$

N: $\alpha(4)(3.76) = 2c$

$$c = 2(3.76)\alpha$$

- Mole fraction H20:

$$x_{H20} = \frac{2}{1 + 2 + c + z} = \frac{2}{1 + 2 + 2(3.76\alpha) + 2(\alpha - 1)}$$

- Find alpha from AFR values

$$AFR = \frac{2\alpha(MW_{air})}{1 * MW_{fuel}} = \frac{2\alpha\big(32 + 3.76(28)\big)}{1(12 + 4)} = \frac{2(137.28\alpha)}{16}$$

$$\alpha = \frac{8AFR}{137.28}$$

- Use C60 values for AFR

# APPENDIX C:
# Nitrogen Oxides Calculation

## 60 kW Emissions (Example):

### Lb of Air to mols Air

Estimates of air and fuel flowrates taken from real recorded data from Capstone C-60 (Air flowrate average of 1820 data points, S.D. = 13.25, Fuel flowrate average of 1820 data points, S.D. = 16.45)

AIR MW (g/mol) = 28.97

$$\mathbf{3905}\frac{\boldsymbol{lb}}{\boldsymbol{hr}}\cdot\frac{453.592\ g}{lb}\cdot\frac{mol}{28.97\ g}=6.114E4\frac{mol}{hr}$$

### Lb of Fuel to Mols of Fuel

CH4 MW (g/mol) = 16.04

$$\frac{3905\frac{lb}{hr}air}{AFR}=x\frac{lb}{hr}fuel,\boldsymbol{AFR}=\mathbf{218},x=17.9\frac{lb}{hr}$$

$$17.9\frac{lb}{hr}\cdot\frac{453.592\ g}{lb}\cdot\frac{mol}{16.04\ g}=506\frac{mol}{hr}$$

Equation

$$506CH_4+6.114E4(O_2+3.76N_2)\rightarrow aCO_2+bH_2O+cN_2+dO_2$$

CHON:

C: $506=a,a=506$

H:$2024=2b,b=1012$

O:$122{,}280=2a+b+2d,d=60128$

N:$459773=2c,c=229{,}886$

Moles of Exhaust Total: $291{,}532\frac{mols}{hr}$

NO Emissions at 60 kW for 1hr: 1 ppmvd

NO MW (g/mol) = 30.01

$$\frac{1\ mol\ NO}{1E6\ mols\ of\ exhaust}=\frac{x\ mol\ NO}{291{,}532\ mols\ of\ exhaust},x=.292\frac{mol\ NO}{hr},.292\frac{mol}{hr}\cdot\frac{30.01\ g}{mol}=8.76\frac{g}{hr}$$

$$8.76\frac{g}{hr}\cdot\frac{lb}{453.592\ g}\cdot\frac{1\ ton}{2000\ lb}=9.656E-6\frac{tons\ NO}{hr}$$

Assuming 8 hrs of operation at 60 kW:

$$7.725E-5\,\frac{tons\ NO}{8\ hrs}$$